

https://dspace.org/

The design and synthesis of antituberculosis peptidomimetics focusing on lassomycin derivatives

Ngqinayo, Ntombizanele

2019

https://hdl.handle.net/10539/29563

Ngqinayo, Ntombizanele. (2019). The design and synthesis of anti-tuberculosis peptidomimetics focusing on lassomycin derivatives. University of the Witwatersrand, https://hdl.handle.net/10539/29563

Downloaded from a DSpace repository. https://dspace.org/

THE DESIGN AND SYNTHESIS OF ANTI-TUBERCULOSIS PEPTIDOMIMETICS FOCUSING ON LASSOMYCIN DERIVATIVES



2019

NTOMBIZANELE NGQINAYO

Supervised by Dr. Maya Makatini

I declare that this dissertation is my own work and has not been submitted before for any degree or qualification in this or any other university. A dissertation submitted to the Faculty of Sciences at the University of the Witwatersrand, Johannesburg, for the Degree of Master of Sciences.



ABSTRACT

Tuberculosis (Tb) is a disease ranked among the top ten causes of death worldwide and is responsible for infecting around 10 million people each year. Tb is caused by the *Mycobacterium Tuberculosis* (*M. tb*) bacterial pathogen.

The mycobacterium has become resistant towards currently approved drugs which mostly target the cell wall and this has led to the development of the multidrug resistant (MDR) and extremely drug resistant (XDR) *M. tb* strains. The resistant strains are difficult to treat and require longer treatment duration with the use of combinatory drugs that result in a number of serious side effects. These limitations have led to the search for novel anti-Tb agents and the discovery of lassomycin, an antimicrobial peptide (AMP) that utilizes a different mode of action. The peptide targets the caseinolytic protease of *M. tb* which is essential for cell survival and causes uncontrolled protein unfolding which results in cell death. Lassomycin is a 16-amino acid long basic peptide isolated from a soil bacteria, *Lentzea kentuckyensis* sp. that been found to be highly selective and potent towards *M. tb* without affecting mammalian cells.[2]

The objectives of this project are **(i)** to modify lassomycin into drug-like derivatives by incorporating *N*-methylated amino acids to make the peptide more stable against enzymatic degradation; **(ii)** to shorten the synthetic route by replacing the lactam bridge with a disulfide bridge; **(iii)** to replace the arginine amino acids in the peptide sequence (difficult to couple) with lysine amino acids to investigate the role of arginine in the binding of the peptide to the acidic region of the caseinolytic enzyme; and **(iv)** to make the peptide more cationic to improve selectivity for the negatively charged bacterial membrane by adding lysine residues.

Peptides were synthesized via the fmoc solid phase peptide synthesis strategy; purified using a semi-preparative High Performance Liquid Chromatogram (prep-HPLC) and analyzed using High Performance Liquid Chromatography Mass Spectrometry (HPLC-MS) and nuclear magnetic resonance (NMR) spectroscopy.

The bactericidal activity of selected lassomycin derivatives against *M. tb* was determined using the Alarmar blue assay and one of the derivatives showed a bactericidal effect at a concentration of 9.87 µg/ml which is comparable to that of ethambutol. The derivatives were also found to be selective for pathogens that share a similar protease to that of the *M. tb* such as *Bacillus Subtilis* (*B. subtilis*) and inactive against other pathogens that do not contain the

protease. The 3-dimensional structure of the active derivatives will be determined in the future using NMR spectroscopy.

ACKNOWLEDGEMENTS

I would like to thank God for the blessings and opportunities He has granted me.

I would like to give thanks to my supervisor **Dr. Maya Makatini** for the opportunity. I am grateful for all the support including but not limited to financial, academic and emotional. I am grateful for the hope you have given me every time I had lost mine countless times, I am grateful for all the time, guidance and patience you have given on the project and me. I have learnt a great deal from this experience and I am confident the skills I have gained will be useful in my future.

I would like to thank Sinazo Cobongela for the constructive editions and my other teammates **Peptide group** for all the assistance: Khanani Machumele, Pious Shuro, Thabo Peme, Phathutshedzo Masithi, Refilwe Moepya, Thapelo Mbhele, Tebello Mofokeng and Lesotho.

I would also like to thank colleagues from the **Organic group**: Mudzuli Maphupha, Donald Seanago, Peter Juma, Charles Changuda and many more.

I would like to thank my family: My dad (Sabelo Bennedict Ngqinayo) and my sisters (Nombutho Ngqinayo, Thobeko Ngqinayo, Ntombizodwa Ngqinayo) for encouragement, support, love and everything else.

I would like to acknowledge the University of the Witwatersrand and the South African Medical Research Council (SAMRC) and National Research Fund (NRF) for financial assistance.

LIST OF ABBREVIATIONS

ADEP	Acyldepsipeptides
ATPase	Adenosine triphosphate enzyme
BCG	Bacille Calmette- Guérin
Clp	Caseinolytic proteolytic complex
ClpC1	Caseinolytic enzyme
ClpP	Caseinolytic protease
Dipea	Diisopropylethyl amine
EMB	Ethambutol
Fmoc-	Fluorenylmethyloxycarbonyl
HATU	2-(7-aza-1H-benzotriazole-1-yl)-1,1,3,3-tetramethyluronium hexafluorophosphate
HBTU	2-(1H-benzotriazole-1-yl)-1,1,3,3-tetramethyluronium hexafluorophosphate hexafluorophosphate
INH	Isoniazid

MDR-TB	Multi-drug resistant
PAS	Para-aminosalicyclic acid
Pbf	2,2,4,6,7-pentamethyldihydrobenzofuran-5-sulfonyl
PZA	Pyrazinamide
RIF	Rifampicin
Tb	Tuberculosis
TFA	Trifluoroacetic acid
Trt	Triphenylmethyl
XRD-TB	Extensively-drug resistant

LIST OF TABLES

Table 1 comparing the properties of Pep_1_NN and Pep_1_NNA derivatives to lassomycin35

Table 2 The yield and purity of Pep_1_NN and Pep_1_NNA derivatives.....36

Table 3 comparing the properties of Pep_2_NN and Pep_2_NNA derivatives to lassomycin40

Table 4 Predicting the difficulty of the sequence as predicted by the PTI peptide predictor ..41

Table 5 The LC-MS results for Pep_2_NNA short peptides.....42

Table 6 The LC-MS results of the impurities associated with synthesized Pep_2_NNA short peptides 43

Table 7 The purity of Pep_2_NN and Pep_2_NNA isomers.....44

Table 8 comparison of the yields of the synthesized derivatives.....45

Table 9 highlighting the difference in the sequences of the cationic derivatives synthesized 50

Table 10 LMS results for cationic peptides 51

Table 11 summarized data for *N*-methylated valine, alanine and leucine amino acids.....58

Table 12 Selected NMR data for *N*-methylated amino acids. 59

Table 13 The HPLC-MS data results for *N*-methylated Pep_2_NN and *N*-methylated Pep_2_NNA.....60

Table 14 Comparing the activities obtained with regards to lassomycin and some of its derivatives, to date 62

Table 15 The relationship between the concentration of Pep_2_NN and toxicity 63

Table 16 The biological activity results of Pep_2_NN and the Pep_2_NNA conformers. RIF (rifampicin), INH (isoniazid) and EMB (ethambutol) were used as control. 64

Table 17 Minimum Inhibition Concentration of Pep_Lys_NN against different organisms ..66

Table 18 Absorbances used to determine loading test of Pep_2_NNA.....72

Table 19 with characterization data, found mass, yield and colour for lassomycin derivatives 74

Table 20 LCMS results for Pep_1_NN and Pep_1_NNA lassomycin derivatives.....74

Table 21 LCMS results for Pep_2_NN and Pep_2_NNA derivatives.....75

Table 22 LCMS results for cationic lassomycin derivatives 76

Table 23 LCMS results for N-methylated lassomycin derivatives.....77

LIST OF SCHEMES

Scheme 1 Irreversible Fmoc cleavage using 20% piperidine solution 27

Scheme 2 The activation of an Fmoc protected amino acid using HBTU as a coupling reagent to form easily replaced active esters 28

Scheme 3 The synthetic method for the synthesis of derivatives using the automated peptide synthesizer, the peptide chain represents Pep_2_NN 29

Scheme 4 The final improved synthetic route (methods 5 - 6) used to synthesize the lassomycin amide derivatives 32

Scheme 5 The mechanism of HATU 33

Scheme 6 A mechanism of the cyclization of Trt-protected Cys to form a disulfide bridge ..34

Scheme 7 Synthesis of the 5-oxazolidinones from Fmoc protected amino acids. R is the side chain of the amino acid 56

Scheme 8 The synthesis of *N*-methylated Fmoc- protected amino acids from the 5-oxazolidinone precursors 57

LIST OF FIGURES

Figure 1 The Mycobacterium tuberculosis cell wall.....2

Figure 2 Flow chart illustrating the cause, spread and recovery of Tb.....3

Figure 3 Tb incidence cases per 100,000 people in South Africa (2004 – 2016).....6

Figure 4 Tb incidence rates per 100,000 people for each province in South Africa (2007 – 2015) 6

Figure 5 The Bactec-320 instrument used for Tb-culture diagnosis.....8

Figure 6 The BCG vaccine and administration.....9

Figure 7 An image of an infant that has developed a BCG- induced lymphadenitis in the armpit 9

Figure 8 Structure of streptomycin 10

Figure 9 The mode of action of currently approved drugs 11

Figure 10 Structure of isoniazid.....12

Figure 11 Structure of ethambutol 13

Figure 12 Structure of pyrazinamide 13

Figure 13 The structure of rifampicin.....14

Figure 14 Structure of para-aminosalicylic acid.....15

Figure 15 A model representing a compressed state of the Clp protease 16

Figure 16 Structure of the caseinolytic protease with the serine catalytic site 17

Figure 17 The proteolysis of protein resulting from the interaction of ClpC1 and the caseinolytic protease 17

Figure 18 The structure of the acyldepsipeptides, ADEP1 and the more potent ADEP4 from the modification of the natural ADEP1 18

Figure 19 A simplified structure of the lassomycin peptide 20

Figure 20 The structures of (a) Cyclomarin A and (b) Ecumicin which are both found to target the ClpC1 of the *M. tb* 20

Figure 21 Mode of action of lassomycin where it decouples the ClpC1 from the ClpP inhibiting proteolysis 21

Figure 22 (a) A threaded lassomycin structure (b) A non-threaded three-dimensional lassomycin structure 22

Figure 23 The structures of the lassomycin natural peptide and one of its derivatives, Pep_1_NNA, highlighting the differences as a result of structure modification. 24

Figure 24 Structures of lassomycin, the Pep_1_NN and Pep_1_NNA derivatives 25

Figure 25 Picture of the automated peptide synthesizer. 26

Figure 26 The structures of lassomycin and its derivatives 35

Figure 27 The hand-notation and molecular structures of Pep_1_NNA 38

Figure 28 The hand-notation and molecular structures of Pep_1_NN 39

Figure 29 The structures of Pep_2_NN and Pep_2_NNA derivatives with the C- terminal amide ending 41

Figure 30 The molecular and hand notation structures of Pep_2_NNA. 47

Figure 31 The The molecular and hand notation structures of Pep_2_NN 48

Figure 32 The structures of Pep_1_NNA_Lys, Pep_1_NN_Lys, Pep_Lys_NNA and Pep_Lys_NN cationic derivatives 49

Figure 33 The structure of Pep_1_NN_Lys 53

Figure 34 The structure of Pep_1_NNA_Lys 54

Figure 35 General structure of amino acids where R represents the organic side chain unique to each amino acid 58

Figure 36 General structure of amino acids where R represents the organic side chain unique to each amino acid 59

Figure 37 The Alarmar blue assays done on the peptide derivatives 67

Figure 38 The structure of *N*-methylated Leucine 78

Figure 39 The structure of *N*-methylated Valine 79

Figure 40 The structure of *N*-methylated Alanine 79

Figure 41 LC-MS of Pep_2_NNA_Conf1 91

Figure 42 LC-MS of Pep_2_NNA_Conf2 92

Figure 43 LC-MS of Pep_2_NN 93

Figure 44 LC-MS of Pep_1_NN 94

Figure 45 LC-MS Pep_1_NNA 95

Figure 46 LC-MS of Pep_Lys_NNA 96

Figure 47 LC-MS of Pep_Lys_NN 97

Figure 48 LC-MS of Pep_1_NN_Lys 98

Figure 49 ^{1}H NMR of *N*-methylated Fmoc-alanine 99

Figure 50 ^{13}C NMR of *N*-methylated Fmoc-alanine 100

Figure 51 ^{1}H NMR spectrum of N-methylated Fmoc-Leucine 101

Figure 52 ^{13}C NMR spectrum of N-methylated Fmoc-Leucine 102

Figure 53 ^{1}H NMR spectrum of *N*-methylated Fmoc- Valine 103

Figure 54 ^{13}C NMR spectrum of N-methylated Fmoc-Valine 104

Figure 55 LC-MS of *N*-methylated Pep_2_NN 105

Figure 56 LC-MS of *N*-Methylated Pep_2_NN.....106

Figure 57 Experimental procedure for Pep_Lys_NN cytotoxicity studies against Human T cell (MT4) obtained from Mintek-Advance Material Division.....107

TABLE OF CONTENTS

Contents

ABSTRACT.....i

ACKNOWLEDGEMENTS..... iii

LIST OF ABBREVIATIONS.....iv

LIST OF TABLES.....vi

LIST OF SCHEMES..... viii

LIST OF FIGURES ix

TABLE OF CONTENTS..... xiii

CHAPTER 1 1

1. Introduction.....1

1.1. Mycobacteria.....1

1.1.1. Physiology 1

1.2. Tuberculosis 2

1.2.1. Latent and Active Tuberculosis.....2

1.2.2. Tuberculosis and Human Immunodeficiency Virus (HIV) 3

1.2.3 The History and Origins of Tuberculosis 4

1.2.4. Tuberculosis: A Global Challenge 4

1.2.5. Tuberculosis in South Africa.....5

1.2.6. Statistics.....5

1.3. Diagnosis and treatment 7

1.3.1. Diagnosis 7

1.3.2. Vaccination 8

1.3.3. Treatment Using Anti-Tb Drugs 10

1.3.4. The Mechanism of Action of Anti-Tb Drugs 11

1.4. Caseinolytic Protease complex (Clp) 15

1.4.1. Compounds that Target the Caseinolytic Protease Complex (ClpP) 18

1.4.2. Lassomycin 21

1.5. Aims and objectives 23

1.5.1. Aim 23

1.5.2. Objectives 23

CHAPTER 2 24

2.1. General information: 24

2.1.1 C-terminal amidation and addition of a disulfide bridge 24

2.1.2. The analogues synthesized 24

2.1.3. Synthesis and method modification 25

2.1.4. Purification using semi-preparatory HPLC 33

2.1.5. Analysis of results 33

2.2. Lassomycin-amide derivatives 34

2.2.1. Insertion of the disulfide bridge 34

2.2.2. Peptide synthesis 35

2.2.3. Results and discussion 35

2.3. Substitution of Arginine with Lysine 40

2.3.1. Challenges with Arginine 40

2.3.2. Synthesis of Pep_2_NN and Pep_2_NNA: 41

2.3.4. Pep_2_NN and Pep_2_NNA lassomycin derivative 44

2.3.5. Conclusion: 46

2.4 Cationic lassomycin-amide peptide derivatives 49

2.4.1. Results and discussion 50

2.4.2. Conclusion 52

CHAPTER 3 55

3.1 Synthesis of *N*-methylated amino acids 55

3.1.1. Synthesis of 5-oxazolidinones 56

3.1.2. Synthesis of *N*-methylated amino acids from 5-oxazolidinones 57

3.1.3. Results 57

3.2 Synthesis of *N*-methylated Peptide derivatives 59

3.2.1. Synthesis: 59

3.2.2. Results 59

CHAPTER 4 62

4.1. Toxicity and Biological Testing 62

4.1.1. Pep_2_NN, Pep_2_NNA_conf1 and Pep_2_NNA_conf2 63

4.1.2. Pep_Lys_NN 65

CHAPTER 5 68

5.1 CONCLUSION AND FUTURE WORK 68

CHAPTER 6 70

6.1 Materials and Instrumentation 70

6.2 Instrumentation 70

6.3. Synthesis of the peptide derivatives 71

6.3.1 Synthesis of Pep_2_NNA 71

6.3.2 Synthesis of other peptide derivatives 73

References 81

Appendix: 90

CHAPTER 1

1. Introduction

Mycobacterium tuberculosis (*M. tb*) is a bacterial pathogen that belongs to the *Mycobacterium tuberculosis* complex group (MTC) which causes the tuberculosis (Tb) disease in humans and animals. Other members of the MTC group include *Mycobacterium Africanum* (*M. Africanum*), *Mycobacterium bovis* (*M. bovis*), *Mycobacterium pinnipedii* and *Mycobacterium microti*.[3,4] Members of the MTC share a genetic similarity of about 99.9% and this allows them to be able to infect and cause diseases in different mammals even though they have their own preferred hosts.[5]

1.1. Mycobacteria

M. tb is a mycobacterium species that belongs to the Mycobacteriaceae family.[6,7] Members of the Mycobacteriaceae family are characterized by a cell wall containing long-chain lipids attached to carbohydrates through covalent bonding known as glycolipids and mycolic-acid (long fatty acids).[8] These lipid substances are found within the cell wall and they resist ordinary staining methods such as Gram staining resulting in the classification of Mycobacteria to be neither Gram-positive nor Gram-negative.[9,10] Mycobacteria are divided into fast and slow growing species. The slow growing mycobacterial species may take longer than a week for populations to generate and appear on solid media while the fast growing species may take 3-5 days to appear. *M. tb* is a slow-growing Mycobacterium.[11]

1.1.1. Physiology

The mycobacteria have an irregular rod shape and their cell wall is made of inner and outer sections. The inner section consists of the arabinogalactan and peptidoglycan layers.[9] The arabinogalactan layer is a polymer of arabinose and galactose carbohydrates bound with mycolic acids and the peptidoglycan layer is a polymer of sugars and amino acids.[6,12] The outer section of the bacterial cell wall consists of the glycolipids and together with the inner segment result in a lipid-rich cell wall which enables the mycobacteria to limit drug permeability. A segment of the mycobacterial cell wall is shown in Figure 1.[10] *M. tb* is classified as an obligate

aerobe as it requires oxygen to grow, however, it can survive in anaerobic environments by down-regulating its metabolism.[13–15]

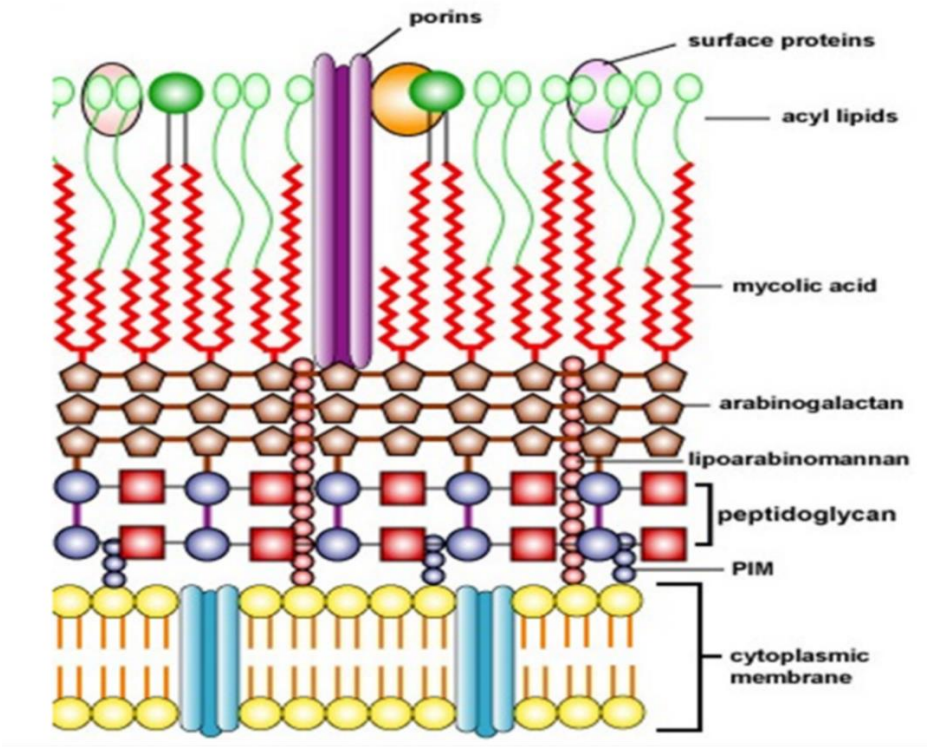


Figure 1 The Mycobacterium tuberculosis cell wall[8]

1.2. Tuberculosis

1.2.1. Latent and Active Tuberculosis

M. tb is normally transmitted into a human host via the inhalation of droplets filled with the Mycobacterium (bacilli) into the lungs.[16] Upon transmittance, the bacilli are then enclosed by a wall called 'tubercles' made from cells of a strong human immune system that prevents the bacilli from spreading in the body. When the bacilli is trapped in the "tubercles" it results in Latent Tb (also known as inactive Tb) which has no symptoms.[17]

Tuberculosis is caused when the bacilli are activated in the lungs (pulmonary Tb) and it can spread to other parts of the body such as gastrointestinal, bones and the nervous systems (extra-pulmonary-Tb).[18] The immune system of the human body is not equipped to stop the growth and spread of the Mycobacterium into other parts of the body after infection. *M. tb* is a tough

and resilient pathogen that can survive in a host for a long time.[19–22] When Tb is left untreated it can cause death in infected persons.[20,23]

People with active Tb can spread the disease through coughing or sneezing. Poverty, overcrowded settings and malnutrition are some of the major factors that increase the risk of spreading Tb.[24] The common symptoms of Tb include coughing, fever, coughing up blood, breathing that is associated with pain, fatigue and weight loss.[19,1,22] People with a low body weight and those with compromised immune systems such as those infected with chronic illnesses including HIV, cancer and diabetes have an increased risk of developing Tb.[20,23,25–29] A flow chart illustrating the transmission of the bacilli to the spread and recovery of Tb is shown in Figure 2.

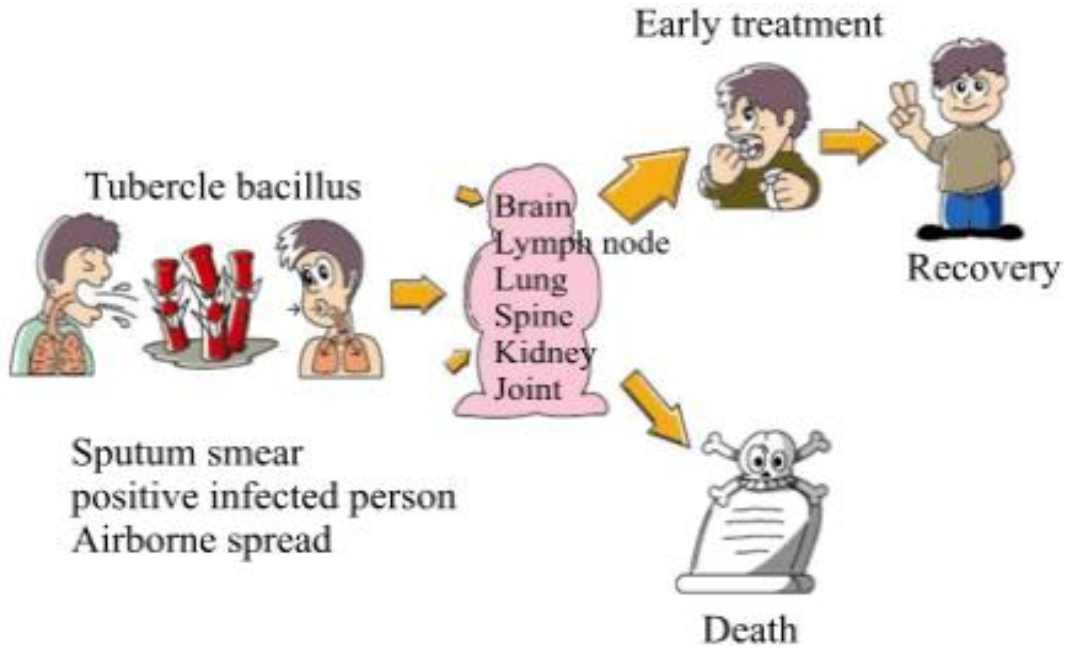


Figure 2 Flow chart illustrating the cause, spread and recovery of Tb[30]

1.2.2. Tuberculosis and Human Immunodeficiency Virus (HIV)

The Human Immunodeficiency Virus (HIV) poses a major challenge against successful Tb treatment and eradication because it weakens the immune system and increases the risk of infection with the opportunistic Tb disease.[23,28] HIV also increases the risk of relapse in resistant Tb.[31] HIV infection is thus regarded as the most powerful risk factor that enhances the progression of latent Tb to active Tb.[22] Tuberculosis also poses challenges for HIV-positive patients as it is the major cause of death. In order to contain both diseases in an infected person, antiretroviral therapy (ART) is used. In previous studies, it was found that ART lowered the

Tb infection rate by 80% which decreased the death rate amongst HIV-positive people.[1,23,28] Tb is considered to be the oldest infectious disease.

1.2.3 The History and Origins of Tuberculosis

The *Mycobacterium* genus has been around for more than 150 million years and *M. tb* was discovered in 1882, however, it has been around for 70,000 years.[32] Although the origin of Tb is not really known, some speculate that *M. bovis*, which causes Tb in cattle, was the probable ancestor of the disease and was transmitted to humans during domestication. Others suggest that *M. tb* and *M. bovis* developed around the same time while *M. Africanun* was the probable ancestor .[6,32,33]

A number of studies have been done to determine how long Tb has been affecting humans. One such study was done on mummies dating back to 2400 BC in which some skeletal deformities associated with Tb were found.[34] Nonetheless, the first written documentation describing Tb dates back to about 2300 and 3300 years ago in China and India, respectively.[32] Despite the limitations in information with regards to the origin of Tb, the first recorded Tb outbreak was observed around the 1880s where it caused around 900 deaths per 100,000 people.[35] Tb has long been regarded as one of the leading causes of death and to this day, Tb continues to kill millions of people yearly worldwide.

1.2.4. Tuberculosis: A Global Challenge

Tb affects everyone directly or indirectly and *M. tb* can infect anyone indiscriminately. The effect of Tb has become a global concern such that the World Health Organization had declared Tb a global health emergency around 1993.[1] Studies show many countries have to work together in order to successfully combat Tb. Participating countries can play a role through scientific research and by providing data through entities such as the United Nations (UN) and World Health Organization (WHO). Upgrading certain factors such as income, living arrangements and the use of effective anti-Tb drugs can lead to decreased incidence (new and relapse) and death rates.[1] Due to factors such as economic disadvantages, developing countries such as South Africa are more affected by Tb than high-income countries.[20]

1.2.5. Tuberculosis in South Africa

As a developing country, it is not surprising that South Africa (SA) is struggling more than some countries with Tb. It has been classified in the recent 2018 WHO report as one of the countries with a high Tb burden counted in all 3 categories (Tb, Tb/HIV and MDR-Tb)[1]. This trend is also observed on other members of the Southern African Development Community (SADC) including Zimbabwe, Mozambique, Democratic Republic of Congo, and Angola. SA is faced with the HIV epidemic[36] that also contributes to accelerating the Tb problem as HIV increases the risk of Tb infection.[28]

1.2.6. Statistics

1.2.6.1. Global and General statistics:

Tb is one of the leading causes of death worldwide[37] and almost one third of the world's population are carriers of *M. tb.*[32] Tb incidence cases have always been high and this was noticed in a study where new cases of Tb had increased from 8.0 million cases in 1997 to 8.3 million cases in 2005. About 10 years later (2016), the Tb incidence cases have increased to about 10.4 million with around 1.7 million Tb-associated deaths.[22] In the most recent WHO report (2018), approximately 1.7 billion people of the estimated global population of 7.7 billion have been infected with *M. tb.*[1,38]

1.2.6.2. South African Tb Statistics:

South Africa has always been one of the countries most affected by the Tb disease and it was ranked the 9th out of 22 countries that were hardest hit by Tb (WHO, 2005). In a recent WHO report (2018), SA is now listed as one of the 14 countries that fall in all three high burden Tb categories (Tb, Tb/HIV and TB-Multi-drug resistant (MDR)).[1,19] In 2017, SA had an estimated population of 57 million people of which around 56,000 HIV-positive people died of Tb (more than twice the number of the HIV-negative deaths, 22,000).[1] Tb incidence cases in SA had reached the highest at 832 cases in 2009 and decreased to 520 cases per 100,000 people in 2016.[39] A graph illustrating a decreasing trend of Tb incidence cases in SA is shown in Figure 3.

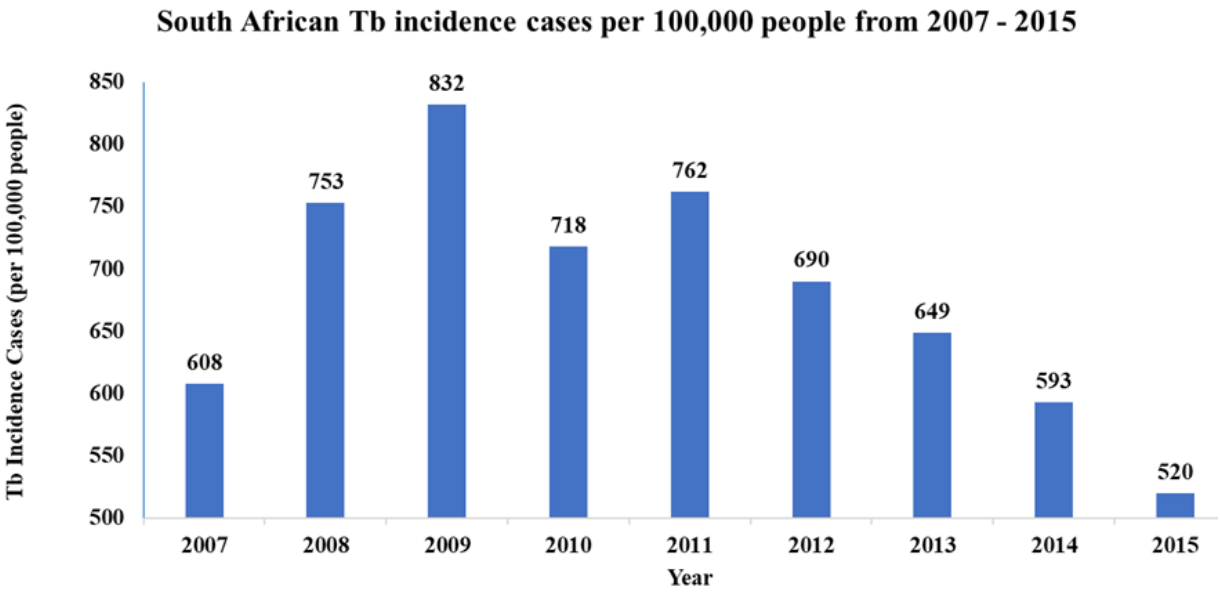


Figure 3 Tb incidence cases per 100,000 people in South Africa (2004 – 2016)**

****Data from the TB Facts website**[39]

The trend for incident cases for each SA province is illustrated in Figure 4.

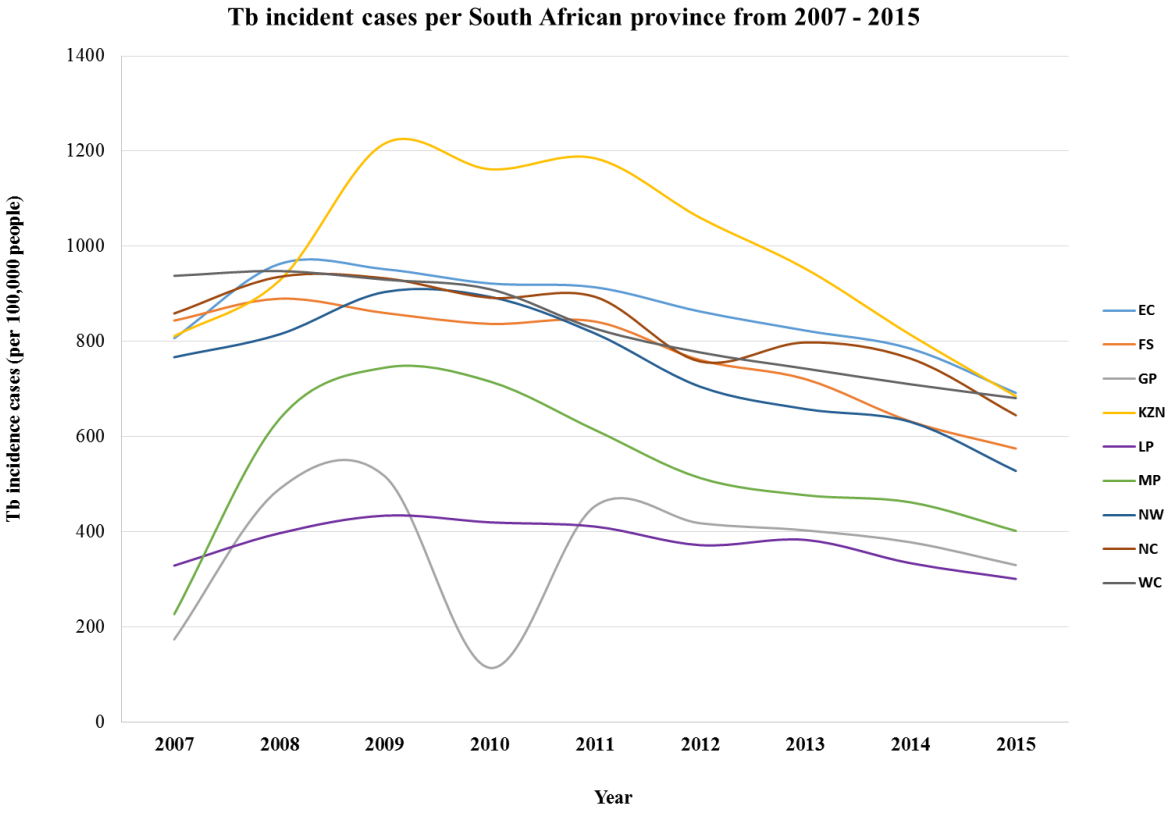


Figure 4 Tb incidence rates per 100,000 people for each province in South Africa (2007 – 2015)**

****Data from the TB Facts website[39] (EC = Eastern Cape, FS = Free State, GP = Gauteng Province, KZN = Kwa-Zulu Natal, LP = Limpopo Province, MP = Mpumalanga, NW = North West, NC = Northern Cape and WC = Western Cape.**

Kwa-Zulu Natal reached the highest incidence rate in the country at 1216 per 100,000 in 2009 and Gauteng had the lowest at 114 per 100,000 in 2010.[39] Based on the information presented in sections 1.2.4 to 1.2.6 above, it is evident that the effect of Tb globally and locally has been studied profusely over the years in order to understand the trends of Tb.[24,40] Tb is therefore a serious disease and requires effective strategies to control and manage it.[19]

1.3. Diagnosis and treatment

1.3.1. Diagnosis

It is important to detect the Mycobacterium and its resistant genetic variants (strains) in the early stages of infection for effective Tb treatment. Diagnosis can be achieved through the use of accurate, rapid and cost-effective screening tests.[41] The currently approved diagnostic techniques include rapid molecular tests, sputum smear microscopy and culture-based methods.[1] A positive Tb diagnosis is obtained when the presence of Mycobacterium is detected. In the absence of these techniques, diagnosis is often done by monitoring symptoms associated with Tb such as blood in the sputum and constant coughing with chest pains.[19,42]

The rapid molecular test is a more accurate diagnostic technique that can also detect resistant Tb and it can provide results as early as 2 hours[43]. Culture-based methods require more developed laboratory equipment such as the Bactec-320[44] (Figure 5) and results may take up to 3 months. Many countries are increasing their use of rapid molecular tests while phasing out the sputum smear microscopy tests. Xpert MTB/RIF is an example of a rapid molecular test that is currently used.[20] Line probe assays (LPAs) are techniques that can also be used to detect resistant Tb in an infected person.[1]



Figure 5 The Bactec-320 instrument used for Tb-culture diagnosis[44]

Challenges are faced with the diagnosis of Tb in children, people living with HIV and pregnant women. It is difficult to diagnose Tb in children as most of the currently used techniques require sputum and children below the age of five are unable to cough up phlegm from their lungs.[45] Drastic measures are therefore used to diagnose children such as swallowing a nylon string which will be removed to check for mycobacterial culture.[46,47] Tb diagnosis in pregnant women is difficult due to body changes that are similar to the early symptoms of Tb such as night sweats and fatigue and therefore diagnosis is done during the third trimester for accurate results.[48] HIV is found to decrease the presence of bacilli in the sputum which results in inaccurate diagnosis.[46]

Appropriate measures can be applied such as the use of effective drugs and healthy living to treat Tb. Protective approaches such as the use of vaccine in non-infected persons can also be exercised to prevent or reduce the risk of infection.

1.3.2. Vaccination

Vaccination is an approach that is used to prevent infection and is usually not effective on persons who have been infected.[22,49] A number of effective vaccines are available to prevent infection against diseases such as those caused by bacteria (e.g. Cholera) and viruses (Chicken pox and polio). The mode of action of viral and bacterial vaccination is similar. The bacterial vaccine functions by introducing a non-infectious or attenuated (alive with decreased virulence effect) bacilli into the body to activate the immune system. The immune system is activated by

producing antibodies against the bacteria to prevent infection in the future. Inactive or attenuated viruses are introduced into the body for viral vaccination.

The Bacille Calmette- Guérin (BCG) is a Tb vaccine (Figure 6) invented in 1919 by Albert Calmette and Camille Guérin to prevent infection in humans.[20] BCG was created using attenuated *M. bovis* bacilli and currently there are many varieties available which include those with *M. tb* strains.[50] The BCG is administered via injection and has minor side-effects such as formation of ulcers along the site of injection.



Figure 6 The BCG vaccine and administration[51,52]

The use of the BCG in HIV-infected infants has limitations due to the increase in the risk of developing complications such as the inflammation of lymph nodes known as lymphadenitis (Figure 7). The lymphadenitis usually ruptures if left untreated and may also result in death. Lymphadenitis is treated by using antibiotics and can also be removed surgically.[46]



Figure 7 An image of an infant that has developed a BCG- induced lymphadenitis in the armpit[46]

Tb can be treated using anti-Tb drugs since vaccination is not an effective approach for infected people.

1.3.3. Treatment Using Anti-Tb Drugs

Before the discovery of modern anti-Tb drugs, people relied on ancient remedies such as the use of sanatoriums where people believed rest and healthy eating could treat Tb.[6,28] Furthermore, people in most African countries relied on medicine made from roots and plants which were provided by traditional healers to treat Tb.[19]

Streptomycin (Figure 8) was the first successful anti-Tb drug discovered in 1945 by Schatz.[53] Limitations of streptomycin such as nerve toxicity side-effects and resistance led to the search for more effective drugs with reduced side-effects.

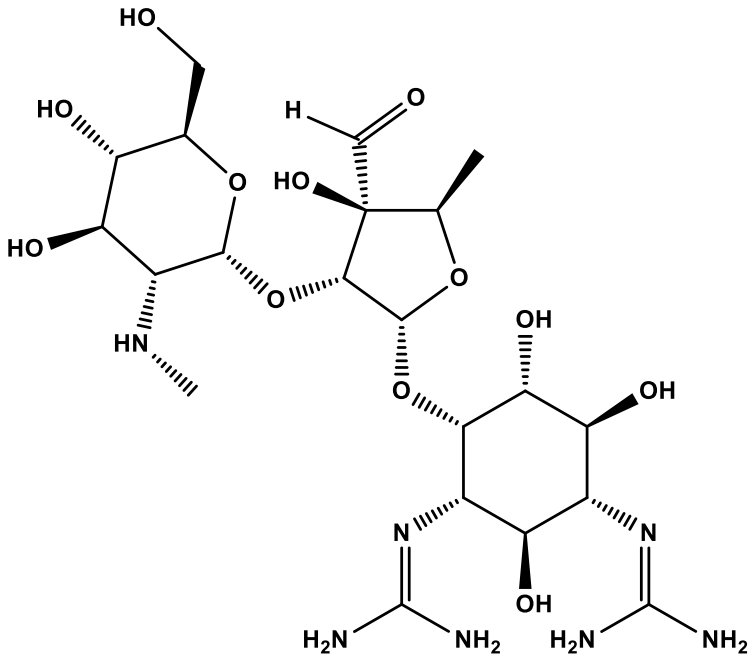


Figure 8 Structure of streptomycin[54]

The currently approved treatment includes the first-line and second-line anti-Tb drugs. First-line drugs are used in new Tb cases and second-line drugs are used when Tb has become resistant to the first-line drugs. Resistant Tb occurs when the Mycobacterium becomes non-responsive towards treatment.

The first-line anti-Tb drugs include isoniazid (INH), rifampicin (RIF), pyrazinamide (PZA) and ethambutol (EMB) and are used for a duration of 6 months.[55,56] Second-line anti-Tb drugs

include fluoroquinolones (such as ciprofloxacin and levofloxacin), ethionamide, cycloserine, capreomycin and para-aminosalicylic acid (PAS). Treatment with second-line drugs usually takes up to 20 months with a global success rate less than 50%.[31] Second-line drugs are expensive and more toxic than first-line drugs.[37] The toxic effects which can be fatal include cardio-toxicity caused by fluoroquinolones and gastrointestinal toxicity caused by para-aminosaliyclic acid.

The challenge that the world is currently facing is Tb resistance towards currently approved drugs as a result of multidrug resistant (MDR-Tb) and extensively-drug resistant (XDR-Tb) strains.[57] MDR-Tb develops when the Mycobacterium becomes resistant to rifampicin or isoniazid first-line drugs and XDR-Tb develops when the Mycobacterium has become resistant towards the second-line anti-Tb drugs. Treatment of XDR-Tb remains difficult because there are only a few available active drugs.[20,28,31,58] The use of effective anti-Tb drugs has prevented about 45 million deaths between 2000 and 2017 (WHO, 2018). [6,28]

1.3.4. The Mechanism of Action of Anti-Tb Drugs

Most approved anti-Tb drugs employ a similar mode of action which target the cell wall of the Mycobacterium, illustrated in Figure 9 below.

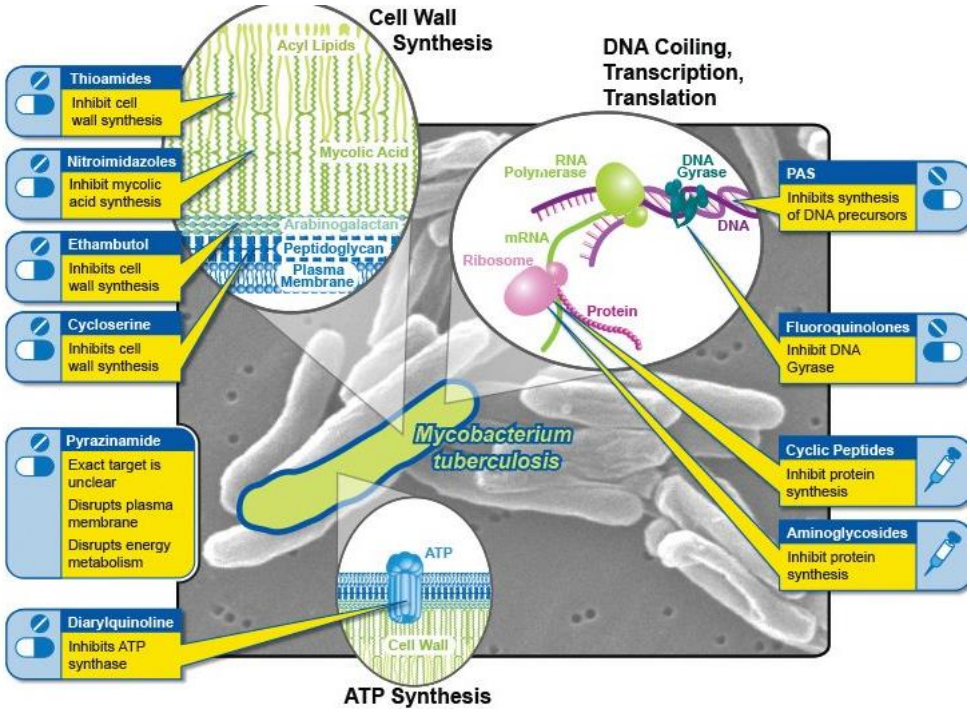


Figure 9 The mode of action of currently approved drugs[59]

1.3.4.1. Drugs that target the Mycobacterium cell wall

Isoniazid:

The bacilli in the lungs utilize a catalase-peroxidase enzyme (katG) in order to survive the hydrogen peroxide produced during respiration. KatG also activates isoniazid (INH, Figure 10) to produce a number of compounds that interact with different enzymes in the Mycobacterium.

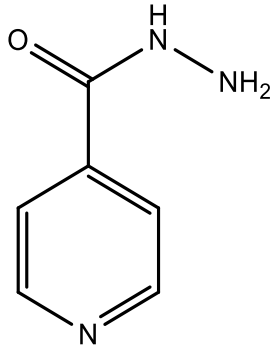


Figure 10 Structure of isoniazid

The activated INH interacts with nicotinamide adenine dinucleotide (NAD^+) and nicotinamide adenine dinucleotide phosphate ($NADP^+$) to form the INH-NAD(P) adducts. These adducts bind to a number of proteins in the Mycobacterium with high affinity. The INH-NAD adduct (4-isonicotinoylnicotinamide) inhibits the synthesis of mycolic acid by binding to a reductase enzyme (InhA) of the *M. tb*.[33] Isoniazid is not active against non-replicating bacteria. The isoniazid side effects can be fatal and include hepatic toxicity and neurotoxicity.[57] Tb resistance against INH occurs due to genetic mutations in the katG and InhA enzymes.

Ethambutol:

Ethambutol (EMB, Figure 11) targets the arabynosyl transferase enzyme responsible for the synthesis of the arabinogalactan which is the main constituent of the cell wall. The inhibition of the synthesis of the arabinogalactan by EMB increases cell wall permeability.[57,60] Therefore, when EMB is used in combination with other drugs it increases their potency. The arabynosyl transferase is encoded in the ribosome by the *emb* gene and mutation in the gene results in resistance against EMB. The major side-effect of EMB is visual loss resulting from a toxic reaction occurring in the optic nerve.[61] Other side-effects include dizziness, headache and itching.[57]

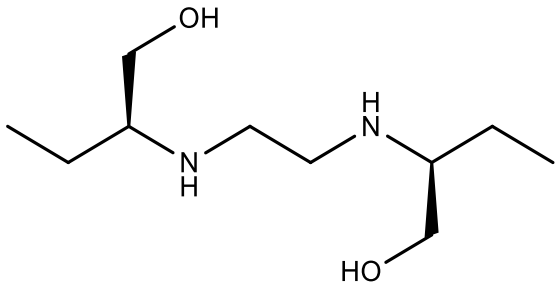


Figure 11 Structure of ethambutol

Pyrazinamide:

Pyrazinamide (PZA, Figure 12) is a pro-drug activated by the pyrazinamidase (PZase) enzyme at acidic pH in the *M. tb* cell to form the pyrazinoic acid active compound. When the pyrazoinic acid is transported to the bacterial cells it decreases pH to highly acidic levels which are detrimental to some vital enzymes. The pyrazinoic acid inhibits the process that regulates passage of solutes through membranes.[62] Genetic mutation in the enzyme responsible for coding PZAse, *pncA*, may cause reduction in PZAse activity[57] which may affect the production of pyrazinoic acid and thus result in Tb resistance. The addition of PZA to a drug regimen with isoniazid and rifampicin was found to increase treatment success rates to 95% in six months.[62] Side effects of PZA include an upset gastrointestinal tract.

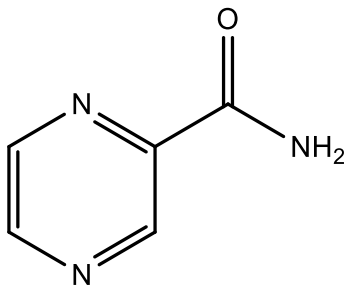


Figure 12 Structure of pyrazinamide

1.3.4.2. Drugs that target DNA processes in the Mycobacterium cell

Rifampicin:

Rifampicin (RIF) is a semisynthetic drug from the rifamycin group which is orally administered.[56] After absorbance in the gastrointestinal tract, RIF (Figure 13) diffuses into tissue cells until it reaches the Mycobacterium cells. RIF binds to the ribonucleic acid (RNA) polymerase enzyme. RNA polymerase enzyme is responsible for separating the deoxyribonucleic acid (DNA) strands during transcription where a segment of DNA is copied into RNA.

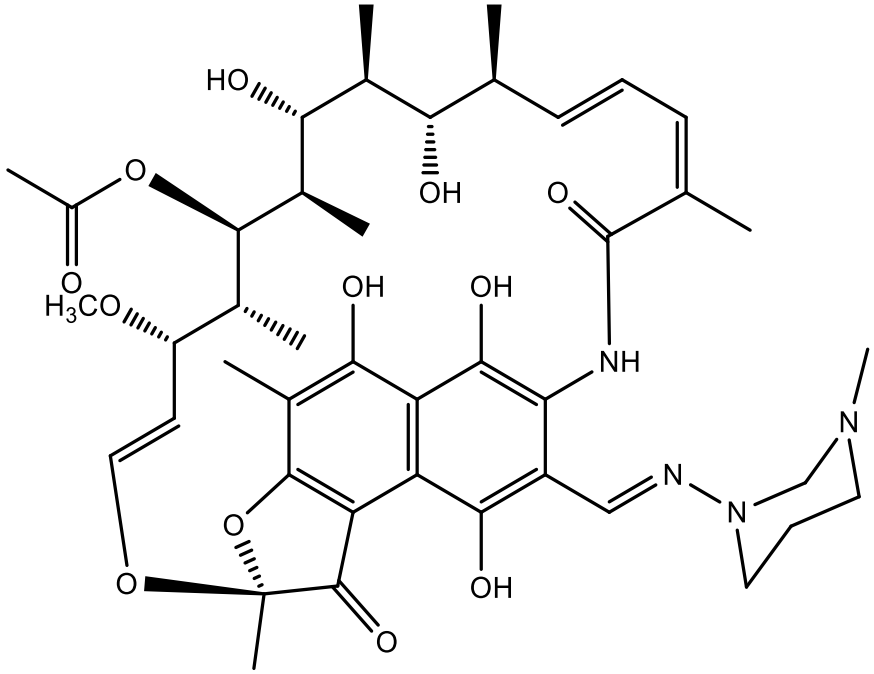


Figure 13 The structure of rifampicin

When RIF binds to the RNA polymerase it inhibits DNA-transcription which prevents the Mycobacterium from synthesizing messenger RNA (mRNA) and proteins resulting in cell death.[56,60] Messenger RNA is responsible for transferring genetic information from DNA to the ribosome, where proteins are synthesized. Gene mutations in the RNA-polymerase result in Tb resistance. The side-effects of RIF include loss of appetite and fever. RIF has lower hepatic toxicity than isoniazid.

1.4.3.3. Drugs that target folate biosynthesis

Para-aminosalicylic acid:

The Mycobacterium uses folate to synthesize nucleic acids required to make DNA and when Para-aminosalicylic (PAS, Figure 14) is used, the Mycobacterium is unable to distinguish it from the vital salicylic acid required for cell nourishment. PAS inhibits the folate biosynthesis resulting in cell death. PAS is prone to bacterial resistance, however, the risk of resistance is reduced when used in combination with streptomycin. The use of streptomycin has been stopped due to hepatic toxicity.[22] The common side-effect of PAS is gastrointestinal tract disturbance.

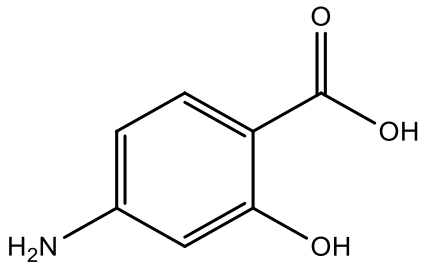


Figure 14 Structure of para-aminosalicylic acid[54]

The problem with currently approved drugs is their susceptibility to resistance resulting in the drugs being used as combinatory regimens in order to minimize resistance and improve potency. Most of the currently approved drugs are not active against the non-replicating persister cells of the Mycobacterium. Persister cells are drug-tolerant and lack resistant genes, thereby enabling them to survive Tb treatments.[25] They were discovered in 1944 by Joseph Bigger when he noticed that some cells of a *Staphylococcus aureus* (*S. aureus*) culture survived treatment with penicillin and yet they were not resistant.[25] The fraction of persisters in a population affects the growth rate of the bacteria inversely.[31]

Failure to contain the Tb disease due to limitations such as the development of drug resistant Tb and life-threatening side-effects has led to the search of new novel anti-Tb agents. This has resulted in the discovery of drugs that target the protease of the Mycobacterium to cause cell death. The basic function of proteases is the cleavage of substrates into shorter peptides.

1.4. Caseinolytic Protease complex (Clp)

The protease found in *M. tb* is known as the caseinolytic protease (ClpP) and plays a crucial role in cell viability.[63] Clp is important in maintaining the bacterial cell during infection by managing the stress pertaining cell survival inside a host (such as phagocytosis) as well as protein quality control. Phagocytosis occurs when *M. tb* cells are ingested by host macrophages

which leads to the Mycobacterium adopting a dormant state (non-replicating) facilitated by Clp protease to survive.[31,64] Other bacteria that share a similar protease include *Bacillus subtilis* (*B. subtilis*) and *Listeria monocytogenes* (*L. monocytogenes*).

ClpP is made of two heptameric rings of ClpP1 and ClpP2 subunits stacked together to form a tetradecamer that creates a channel housing serine catalytic sites. The catalytic sites are made up of a triad of serine (Ser), histidine (His) and aspartic acid (Asp) residues which are accessed via the axial openings. The Ser residue is responsible for substrate cleavage and the aspartic acid stabilizes the complex.[65,26] A compressed state (Figure 15) is formed when the Ser and His residues are further apart resulting in no substrate degradation.

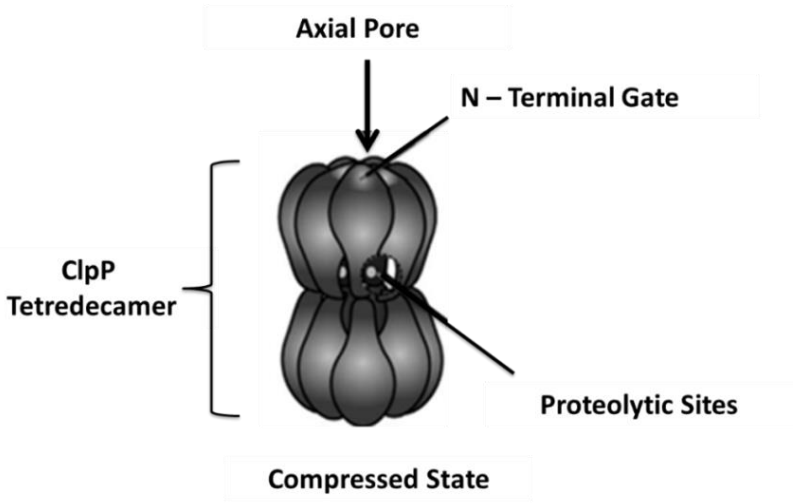


Figure 15 A model representing a compressed state of the Clp protease[65]

To activate proteolysis, an adenosine triphosphate enzyme (ATPase) binds to the ClpP to form the proteolytic complex (Clp) with the extended conformation. ATPase stores and provides the energy needed for substrate degradation. The caseinolytic enzyme (ClpC1) is an ATPase that belong to the AAA+ super family of chaperons in *M. tb*. ClpC1 binds to the N-terminal region of the ClpP through hydrophobic pockets. The Ser and His residues in the extended state are closer and activated for substrate degradation (Figure 16).

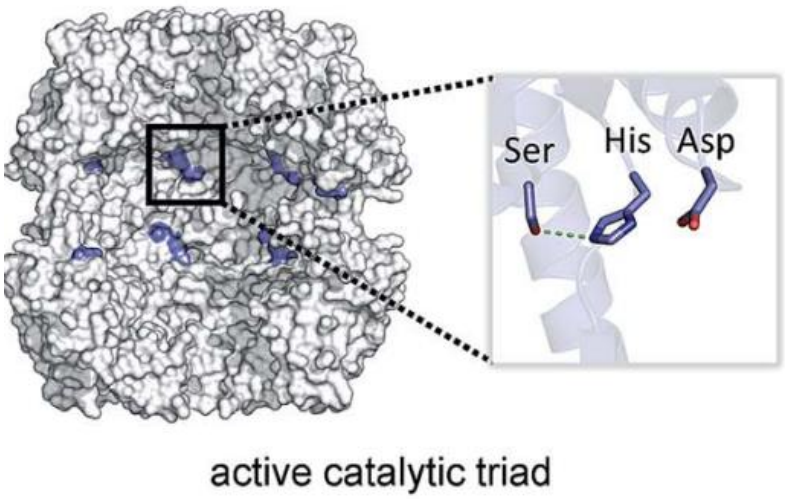


Figure 16 Structure of the caseinolytic protease with the serine catalytic site[63]

The ClpC1 unfolds the folded, damaged and misfolded protein substrates that are tagged with a degradation signal. Furthermore, the ClpC1 translocates the unfolded substrates to the ClpP catalytic sites for degradation in an ATPase dependent-fashion where they are cleaved into smaller peptides (Figure 17).[26,63,65,66] ClpP that is not bound to ClpC1 is unable to degrade protein substrates, however it can degrade peptides.[26,63,65]

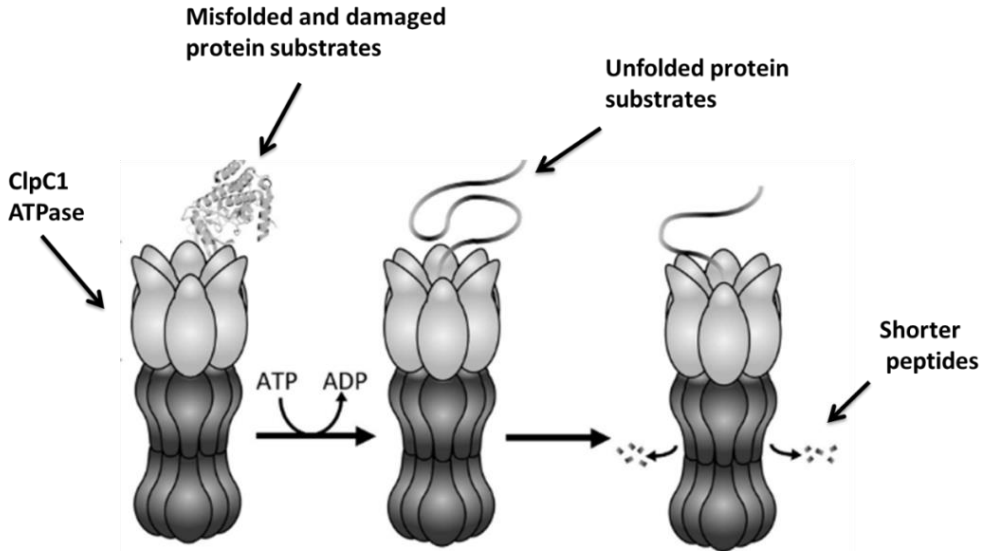


Figure 17 The proteolysis of protein resulting from the interaction of ClpC1 and the caseinolytic protease[65]

The Clp plays an important role in the survival of the Mycobacterium such that it has been targeted as a means for new anti-Tb agents that use a different mode of action. These agents include anti-microbial peptides (AMPs) such as the acyldepsipeptides (ADEPs).

1.4.1. Compounds that Target the Caseinolytic Protease Complex (ClpP)

1.4.1.2. Caseinolytic protease activators

The increase in drug-resistant Tb cases has led to the search and discovery of new anti-Tb agents that target the caseinolytic protease such as acyldepsipeptides (ADEPs, (Figure 18). ADEPs are compounds that are produced by a soil bacterium known as *Streptomyces hawaiiensis* NRRL15010.[65] ADEPs bind to the active site of ClpP by mimicking the ClpC1 which activates the protease for proteolysis. The resulting unregulated and non-selective proteolysis causes cell death.[65,67] ADEPs are also active against the ClpP present in *Escherichia coli* (*E. coli*), *B. subtilis* and *Neisseria meningitides* bacterial pathogens. ADEPs are also active against persister cells and have a very low risk of the development of Tb resistance.[65]

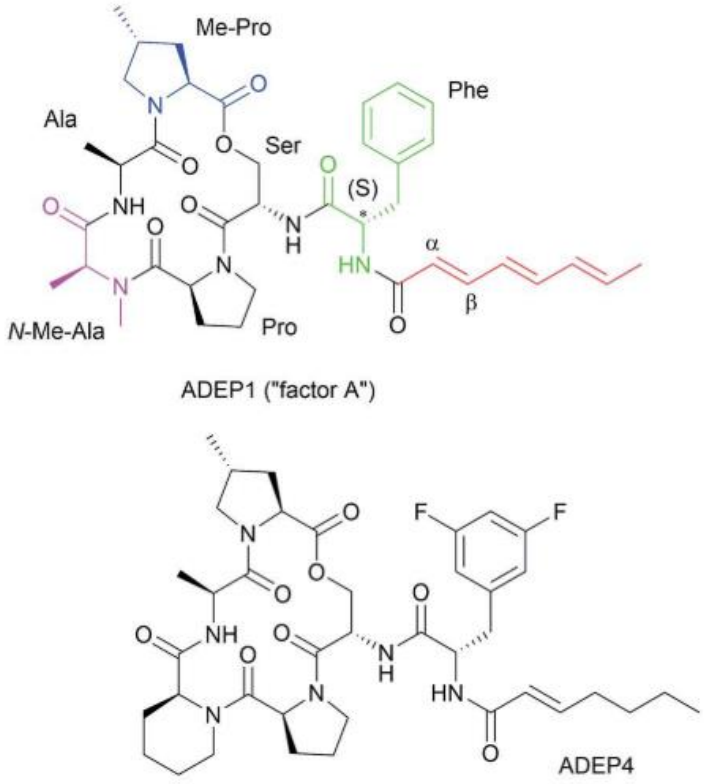


Figure 18 The structure of the acyldepsipeptides, ADEP1 and the more potent ADEP4 from the modification of the natural ADEP1[63]

ADEPs are extremely potent towards the Tb mycobacterium; however, they are associated with some limitations such as poor water solubility, rapid enzymatic degradation and chemical instability. Modifications to improve ADEPs led to the development of the ADEP4 derivative (Figure 18) which is more potent than ADEP1. The increase in the activity of ADEP4 is mostly

due to increased structural rigidity. ADEPs remain chemically unstable despite numerous efforts to improve their activity through structural modifications.

The limitations of ADEPs led to the discovery of other compounds that target and activate the ClpP known as Activators of Self-Compartmentalizing Proteases (ACPs) and sclerotiamide. However, the ACPs and sclerotiamide were found to be less effective than the ADEPs and this led to the discovery of natural peptides that target the caseinolytic enzyme (ClpC1) selectively.

1.4.1.2. Compounds that target the caseinolytic enzyme

Lassomycin (Figure 20), Cyclomarin A (CymA) and, ecumicin (Figure 19) are peptides that were discovered through natural screening tests as potential anti-Tb agents and they share similar structural and chemical properties. They are cyclic lasso peptides that contain a macrolactam ring and are usually threaded. They target the acidic region of the ClpC1 with high affinity; however, they bind at slightly different sites. Lassomycin is more basic than ecumicin and CymA and binds to a highly acidic site of ClpC1. All three peptides were found to be active against growing, dormant and resistant *M. tb* cells and are not active against mammalian cells.

CymA causes cell death by activating uncontrolled protein degradation while lassomycin and ecumicin cause cell death by inhibiting it.[68] Ecumicin and lassomycin both increase the ATPase activity (unfolding) while decoupling the ClpC1 resulting in the accumulation of substrates that cause cell death due to toxicity. CymA was also found to be a potent anti-inflammatory agent with cytotoxicity against cancer cells.

Ecumicin, CymA and lassomycin have the potential to make effective anti-Tb drugs due to their selectivity against the ClpC1. However structural modifications are needed to improve their pharmacodynamics properties. The limitations of ecumicin include poor solubility and poor intestinal absorption and CymA is susceptible to enzymatic degradation.[65]

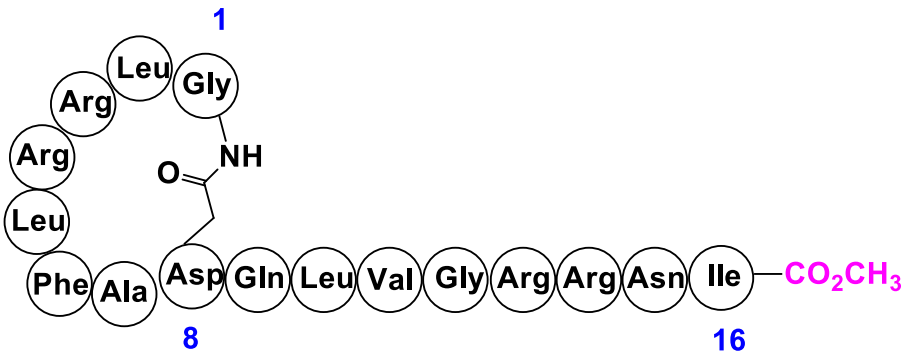


Figure 19 A simplified structure of the lassomycin peptide

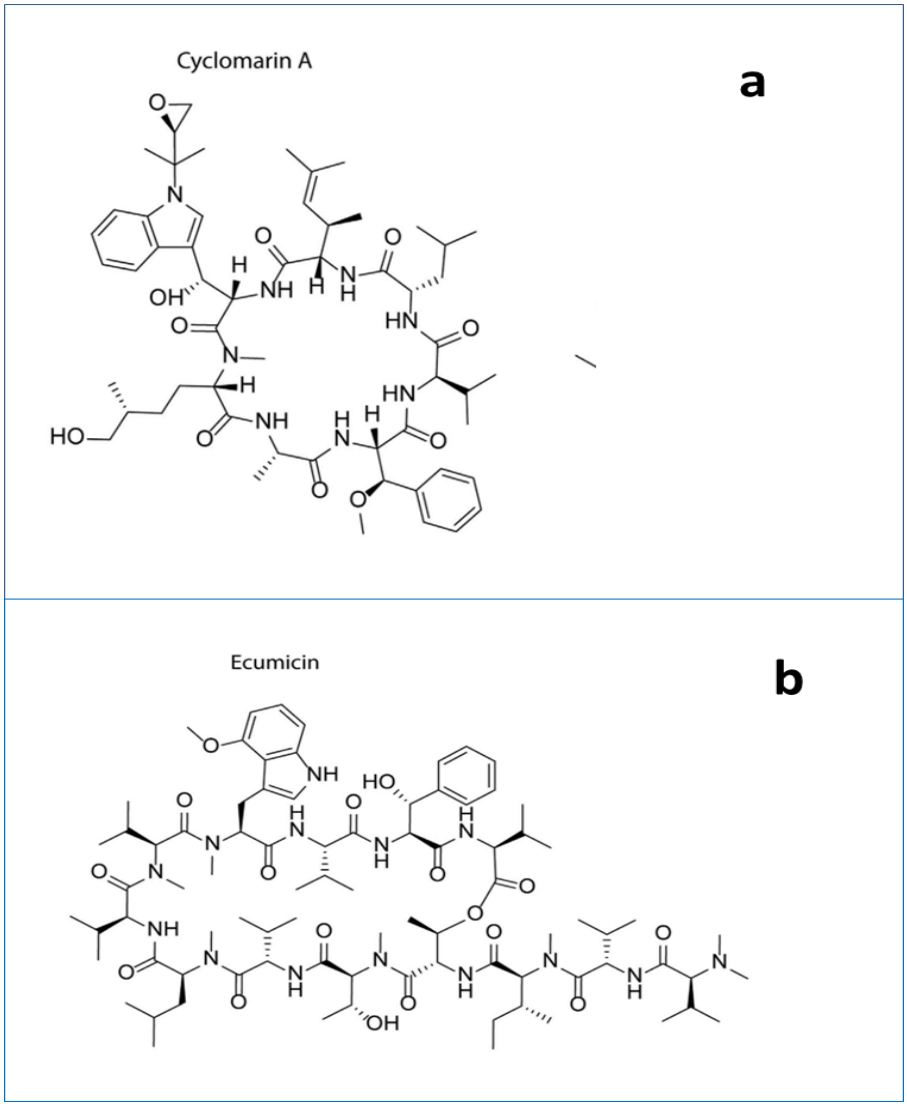


Figure 20 The structures of (a) Cyclomarin A and (b) Ecumicin which are both found to target the ClpC1 of the *M. tb*[63]

1.4.2. Lassomycin

Lassomycin is a 16- amino acid long cyclic peptide that was discovered and isolated from a soil bacterium, *Lentzea kentuckyensis* sp.[2] The peptide, which is synthesized in the ribosome, contains a macrolactam bond between the N-terminus (Gly1) and the carboxyl side chain of the aspartic acid (Asp8), illustrated in Figure 19 above. Lassomycin has poor penetration to mammalian cells which may contribute to its low cytotoxicity against mammalian cells and it also does not cause red blood cells to rupture.[2,21] The activity of lassomycin is comparable to that of rifampicin which is currently the most effective anti-Tb drug.

Lassomycin was reported to be active against a variety of *M. tb* strains including the MDR and XDR-Tb strains with a minimum inhibitory concentration (MIC) range of 0.8 – 3 μg/ml.[2] Lassomycin is also active against *Mycobacterium avium* and *Mycobacterium smegmatis*.

1.4.2.1. Mode of action

X-ray studies showed that lassomycin binds to the highly acidic region of ClpC1 with the highly basic arginine (Arg) residues.[2] Docking studies showed that ClpC1 binds to the lassomycin using a glutamine residue at position 17 (Gln17) in the sequence through hydrogen bonding. Both the lassomycin and protein substrates bind to the ClpC1 at different sites as the ClpC1 is able to unfold the substrates in the presence of lassomycin (Figure 21).

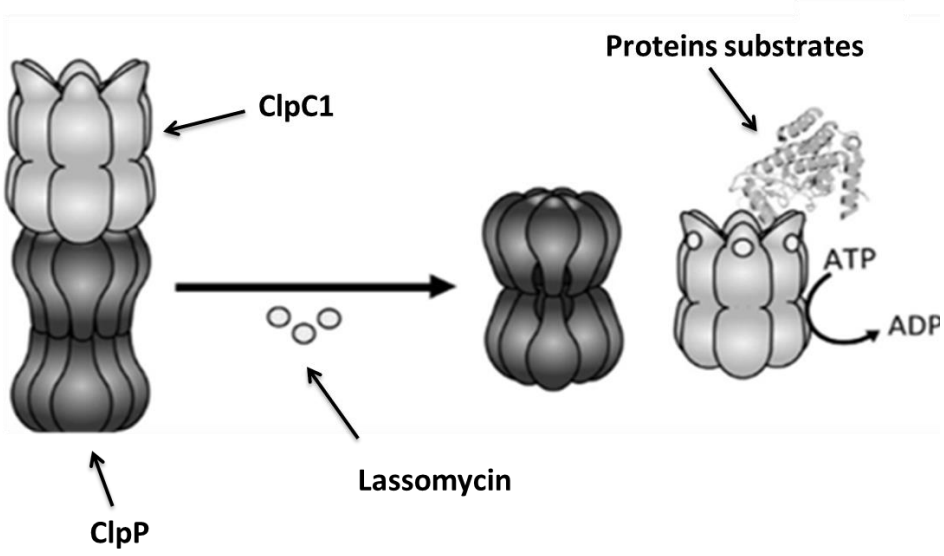


Figure 21 Mode of action of lassomycin where it decouples the ClpC1 from the ClpP inhibiting proteolysis [65]

The exact cause of death of the *M. tb* cell is not known, however, there are two reasons that could result in cell death and are explained below.[2,69]

(i) Cell death could result from toxicity due to accumulation of protein substrate when lassomycin binds and decouples ClpC1 from the ClpP, rendering the protease non-functional (Figure 21).

(ii) Cell death could also result from the uncontrolled and non-selective unfolding of proteins due to the increased unfolding activity by 10-fold.

Currently, the actual conformation of lassomycin when bound to the ClpC1 ATPase is not known, however, it can be determined using X-ray studies.[2]

1.4.2.2. Lassomycin active structure

Structure elucidation with nuclear magnetic resonance (NMR) and mass spectrometry predicted lassomycin to be non-threaded with the C-terminal end packed tightly against the N-terminal ring instead of passing through the ring.[2] However, the synthesized lassomycin reported by Lear *et al* was found to be inactive against the Mycobacterium with an unthreaded structure (Figure 22).[69] The lassomycin structure reported by Harris *et al* was also found to be unthreaded with low activity.[21] The structure of the natural lassomycin was then concluded to be threaded based on NMR studies done on synthesized lassomycin and that the synthesized peptides (with low activity) could not be threaded due to the nature of their synthesis.[8]

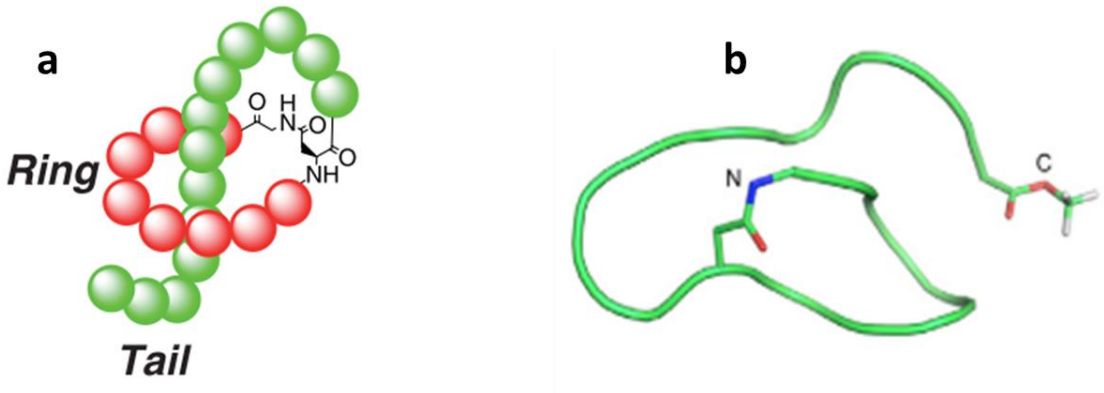


Figure 22 (a) A threaded lassomycin structure (b) A non-threaded three-dimensional lassomycin structure.[2,21]

The threaded lassomycin peptide is formed when the C-terminal tail passes through the cyclic ring and is held in place by sterically demanding residues above and below the ring, resulting in a distinctive topology comparable to a lariat knot.

Lassomycin shows great promise, thus we have decided to synthesize derivatives that use a simpler synthetic route, incorporate *N*-methylated amino acids to improve peptide stability and incorporate cationic amino acids to improve bacterial cell penetration and binding.

1.5. Aims and objectives

1.5.1. Aim

The aim of the project is to design and synthesize novel peptidomimetic inhibitors of the *Mycobacterium tuberculosis* caseinolytic protease.

1.5.2. Objectives

The objectives of the project include:

- To synthesize lassomycin derivatives with improved bioavailability and decreased toxicity
- To synthesize peptides with *N*-methylated amino acids to prevent enzymatic degradation.
- To investigate the effect of enlarging the cyclic ring of lassomycin on the activity
- To investigate the importance of the lactam bond by replacing it with a new disulfide bridge
- To study the binding mechanism of lassomycin by replacing the arginine amino acid groups with the less basic lysine groups

CHAPTER 2

THE DESIGN AND SYNTHESIS OF LASSOMYCIN-AMIDE DERIVATIVES TARGETING THE MYCOBACTERIUM CASEINOLYTIC PROTEASE

2.1. General information:

2.1.1 C-terminal amidation and addition of a disulfide bridge

The ester C- terminal ending of lassomycin was substituted with an amide for all derivatives synthesized to increase biological activity and improve secondary structure. Amidation also increases resistance towards the attack and breakdown by exopeptidases that target and cleave peptides from the endings.[70–72] The lactam bond on the natural peptide was replaced with a disulfide ring afforded by incorporating 2 cysteine (Cys) residues. Figure 23 below illustrates the modifications.

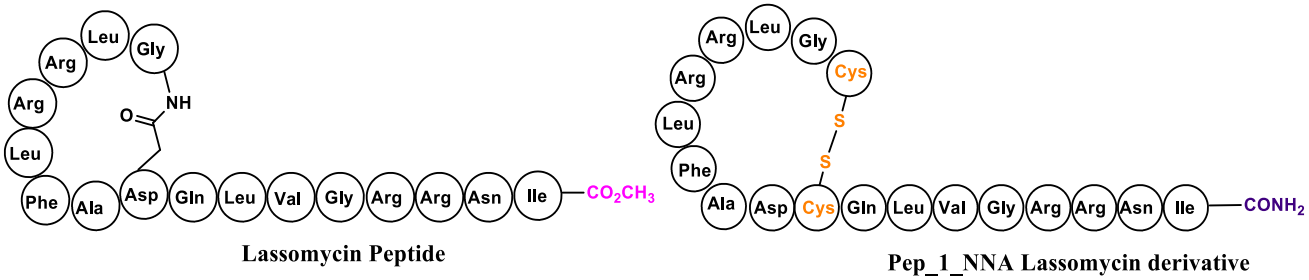


Figure 23 The structures of the lassomycin natural peptide and one of its derivatives, Pep_1_NNA, highlighting the differences as a result of structure modification.

2.1.2. The analogues synthesized

The peptide derivatives are divided into 2 groups which include those that contain the –NNA and –NN ending in their name such as Pep_1_NNA and Pep_1_NN, respectively, illustrated in Figure 24. The two groups of derivatives consist of similar residues in their peptide tail

sequence, but the –NN were mistakenly synthesized to contain a sequence that is a reverse of the natural peptide sequence in the cyclic ring and asparagine (Asn) was used in the position of aspartic acid (Asp). After the mistake was noted, we still proceeded and tested the derivatives and to our amazement one of –NN group was highly active and therefore throughout we have synthesized both the –NN and –NNA derivatives.

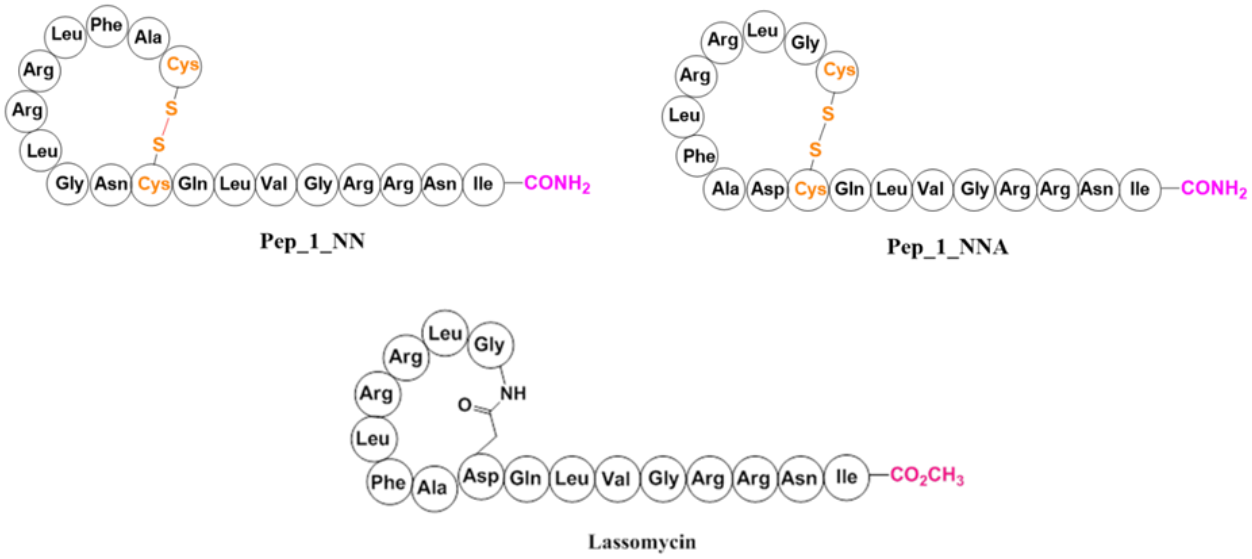


Figure 24 Structures of lassomycin, the Pep_1_NN and Pep_1_NNA derivatives

2.1.3. Synthesis and method modification

All the derivatives were synthesized via Fluorenylmethyloxycarbonyl (Fmoc-) solid phase peptide synthesis (SPPS) strategy using a Rink Amide 4-methylbenzhydrylamine (MBHA) resin to afford the derivatives an amide C- terminal ending. The rink amide resin is acid-labile and can be cleaved from a peptide using a strong concentration of an acid solution such as 94% Trifluoroacetic acid (TFA) solution.

In the SPPS, the peptide is attached to an insoluble resin bead and remains when the waste dissolved in solvent is filtered off; however, the peptides in solution phase are suspended together with the waste and by-products. Therefore, the SPPS is chosen to improve yields.

Method 1:

Peptides synthesized: Pep_2_NN, Pep_2_NNA, Pep_1_NN and Pep_1_NNA

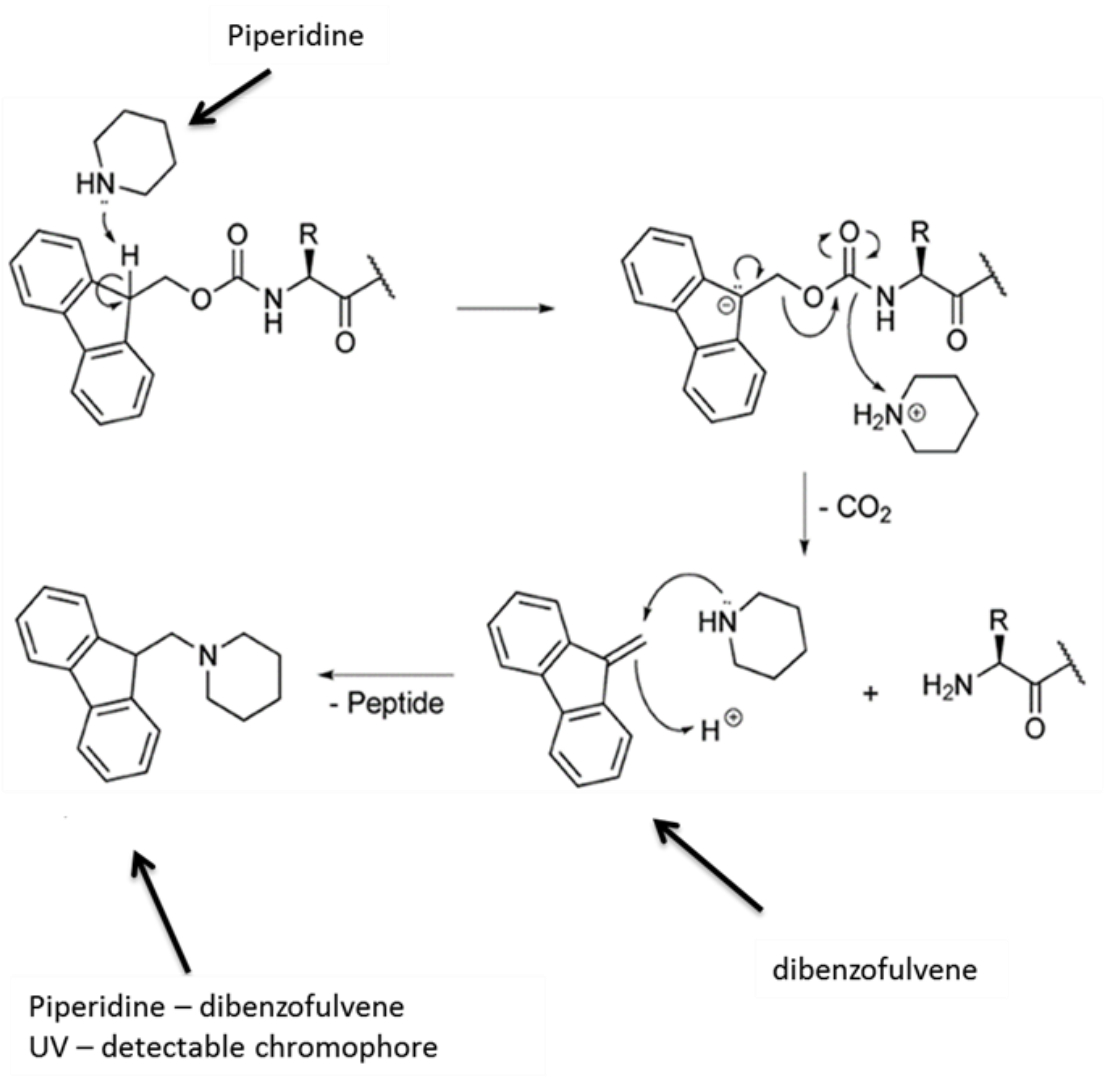
The peptides were synthesized automatically using a peptide synthesizer (Figure 25).



Figure 25 Picture of the automated peptide synthesizer.

2.1.3.1. Rink amide swelling and Fmoc- removal

The Fmoc- protected Rink Amide MBHA resin was swelled in dimethylformamide (DMF) to expose the active sites as the peptide synthesis occurs on the inside of the beads.[73] The piperidine solution was used to irreversibly cleave the base-labile Fmoc- group and expose the free amino group (NH_2). The mechanism is shown in Scheme 1. Washing with DMF is done in between steps to remove contaminants.

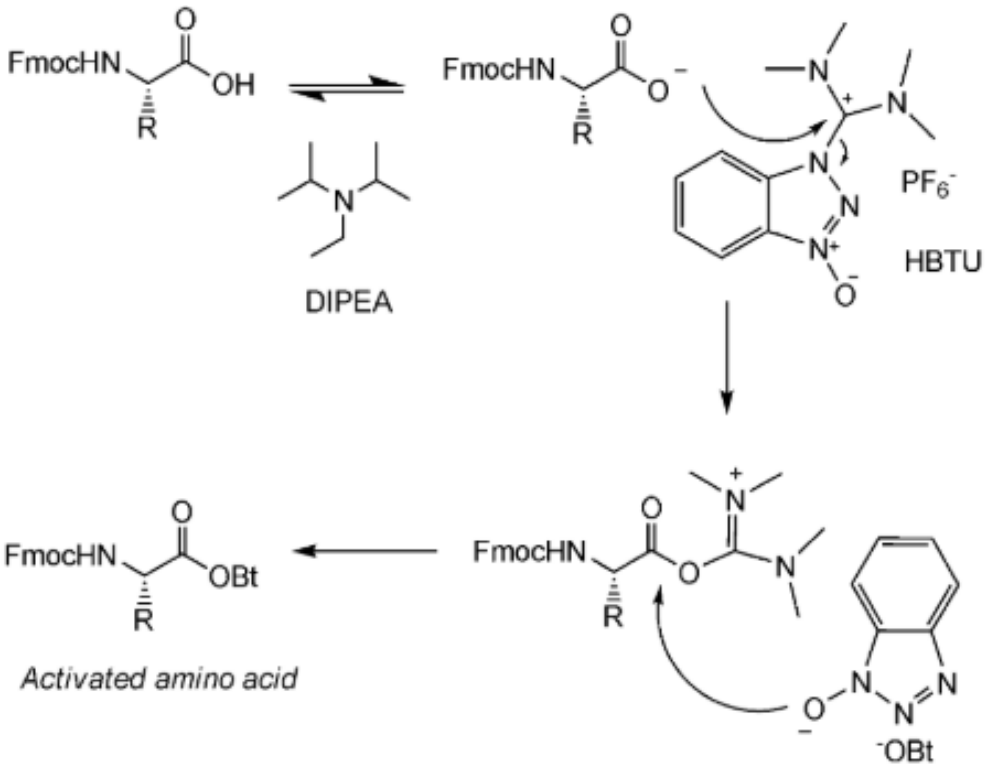


Scheme 1 Irreversible Fmoc cleavage using 20% piperidine solution[74]

All the amino acids used were Fmoc-protected on the amino site as unprotected amino acids have poor solubility leading to slow reaction rates. Protected amino acids minimize the risk of contamination.[75]

2.1.3.2. Amino Acid Activation

The amino acids were activated into active esters using 2-(1H-benzotriazole-1-yl)-1,1,3,3-tetramethyluronium hexafluorophosphate hexafluorophosphate (HBTU/Dipea) (Scheme 2) and coupled to the N-terminus of the peptide chain for 40 min.



Scheme 2 The activation of an Fmoc protected amino acid using HBTU as a coupling reagent to form easily replaced active esters[76]

Dipea was chosen because of its bulky nature to deprotonate the amino acids and HBTU was chosen over 2-(7-aza-1H-benzotriazole-1-yl)-1,1,3,3-tetramethyluronium hexafluoro-phosphate (HATU) as it is less expensive.

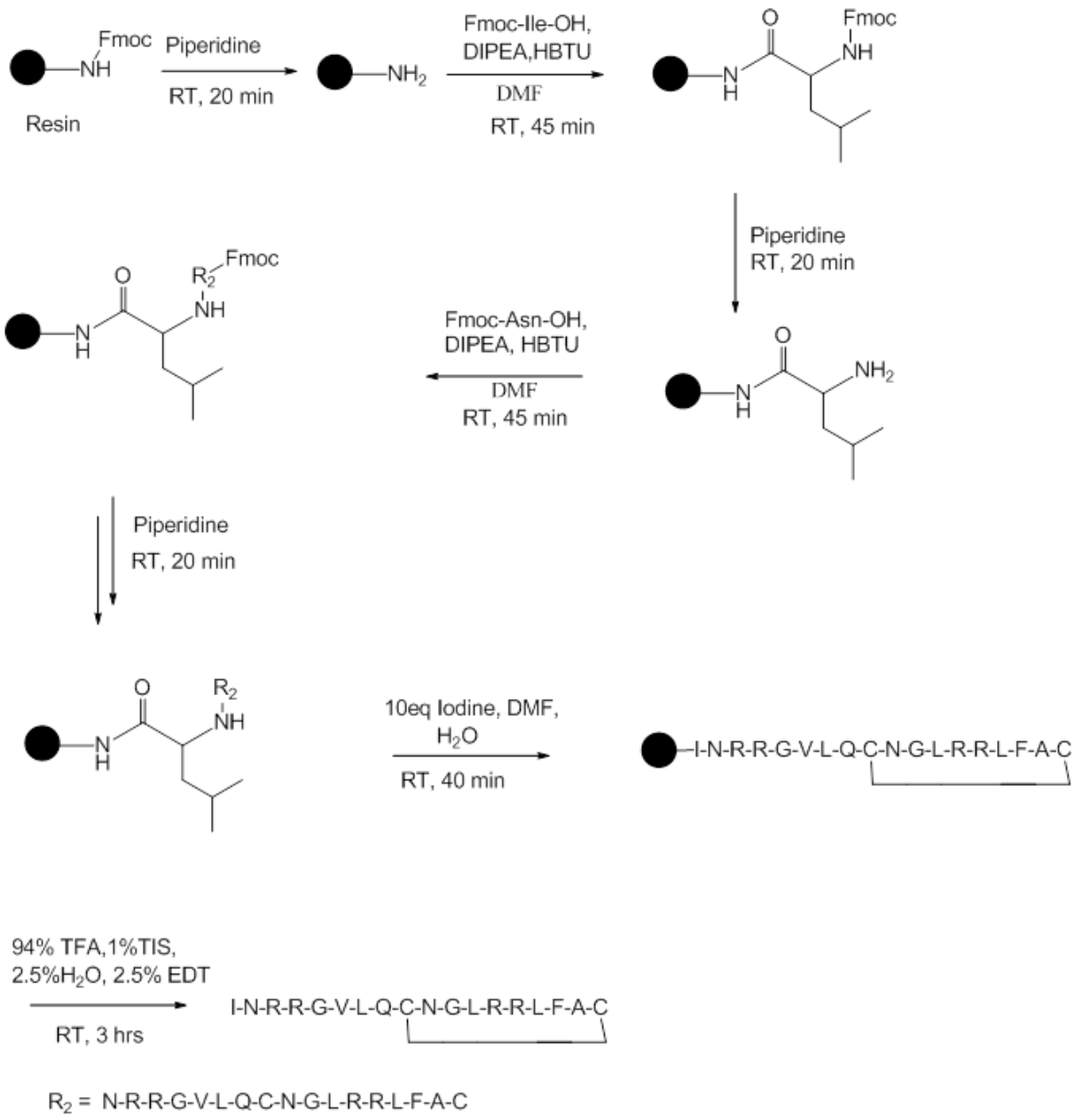
2.1.3.3 Cyclization using iodine

After all the amino acids were coupled, a disulfide bridge was formed between two cysteine (Cys) residues in each derivative using a solution of iodine in DMF/water (4:1). Iodine simultaneously cleaves the cysteine triphenylmethyl (Trt) protecting group and also oxidizes Cys to form a cyclic ring. The iodine also acts as a scavenger for the Trt carbocation. The cyclization reaction time was 40 min. A dilute iodine solution was used to ensure that the disulfide bridges formed are intra-molecular (taking place within a molecule) and not intermolecular (taking place between molecules).

2.1.3.4. The TFA-cleavage of the permanent protecting groups

Peptides were cleaved from the resin linker and permanent protecting groups by acidolysis with 94% trifluoroacetic acid (TFA) with 1% triisopropylsilane (TIS), 2.5% 1,2-ethanedithiol

(EDT) and 2.5% water. The peptide was precipitated using diethyl ether and the solution was decanted after centrifuging. The process was repeated four times. TIS, water and EDT function as scavengers for the cleaved protecting groups as they can irreversibly attack the peptide backbone and alkylate it resulting in the formation of impurities and low yields. The peptide cleavage time from the resin was 3 hours. Scheme 3 summarizes the synthetic route used to synthesize the peptide derivative represented by Pep_2_NN. Pep_2_NNA, Pep_1_NN and Pep_1_NNA also used a similar route. The structures of the derivatives are explained in detail from section 2.1.



Scheme 3 The synthetic method for the synthesis of derivatives using the automated peptide synthesizer, the peptide chain represents Pep_2_NN

2.1.3.5. Determination of the resin loading capacity

Loading capacity was determined after coupling the first amino acid of the sequence by analyzing the piperidine-dibenzofulvene by-product (Scheme 1) using the UV spectrophotometer. The average loading capacity of the derivatives was approximately 0.4 mmol/g.

All the peptide derivatives were synthesized at room temperature.

2.1.3.6. Results and discussion

The peptides were analyzed using high performance liquid chromatography coupled to mass spectrometry (HPLC-MS). All the derivatives (Pep_2_NN, Pep_2_NNA, Pep_1_NN and Pep_1_NNA) were not successfully synthesized. The choice of coupling reagent may have led to the poor results. HBTU is inferior to other coupling reagents such HATU.

The use of the automated synthesizer has advantages such as the ability to couple all the 18 amino acids of the peptide consistently without stopping. Mechanical errors such as skipping amino acids and stopping synthesis in the middle of a reaction also contributed to the poor results obtained. The synthetic method was modified by changing some conditions to obtain better yields.

2.1.3.6.1. Modifications of the synthetic method

The derivatives were synthesized manually to monitor the reactions and the conditions were also modified. For each modified method (**methods 2** – **6**) presented below only the conditions changed will be stated.

Method 2

The coupling reaction time was increased to 3 hours to allow the in-coming amino acid sufficient time to interact and couple to the peptide chain. The synthesis was not successful.

Method 3

The coupling reaction time was decreased to 2.5 h and the HBTU/Dipea set was substituted with HATU/Dipea. The synthesis was not successful.

Method 4

The reaction time was decreased to 1.5 h and HATU/Dipea was used. The synthesis was not successful.

Methods 5

The coupling reaction time was reduced to 30 minutes and the amino acids were double coupled (adding the activated amino acid twice, before removing Fmoc), HATU/Dipea was used as a coupling reagent, the results improved significantly and the peptides were successfully synthesized.

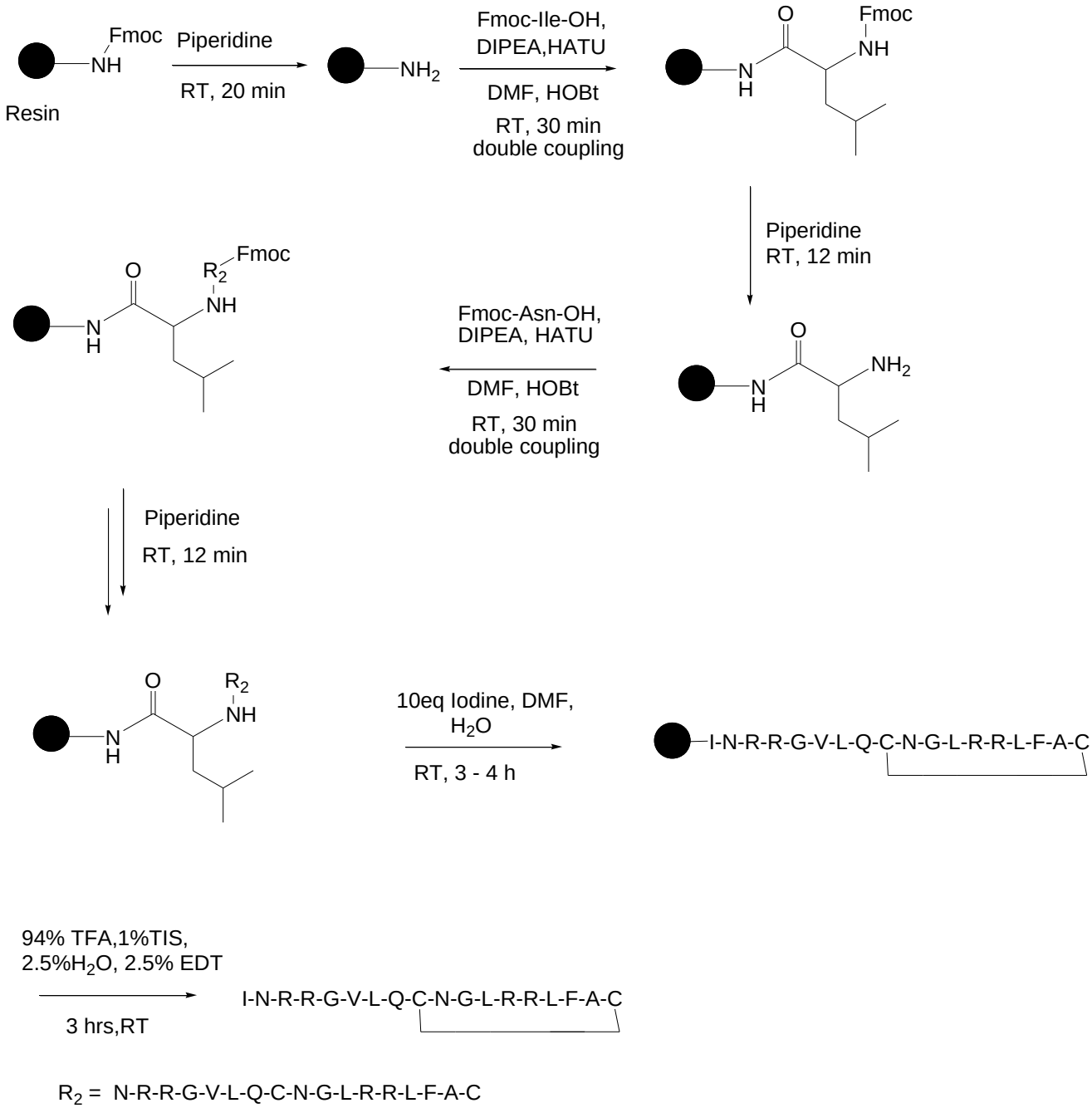
Method 6

Method 5 was used and 1-hydroxy-1*H*-benzotriazole (HOBt) was used an additive. The results were also improved. The additives catalyze the reaction by decreasing coupling reaction times.

2.1.3.7. Conclusion

The peptide derivatives were successfully synthesized at lower reactions times (30 minutes) with double coupling. The longer reactions times may have resulted in some side reactions, probably formed by-products, resulting in poor results. Derivatives synthesized when HOBt was used as an additive showed better results. Replacing HBTU with HATU also resulted in better outcomes. A general method was thus obtained from method 5 and was used to synthesize other derivatives. Scheme 4 shows the summarized synthetic method.

Final method for synthesis:

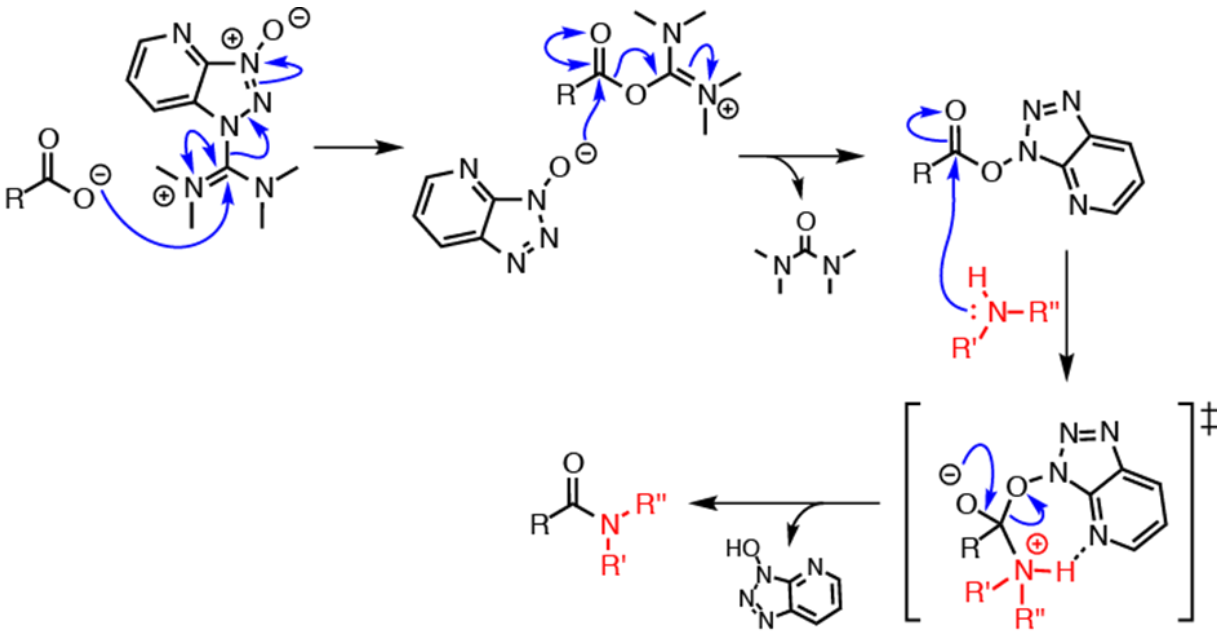


Scheme 4 The final improved synthetic route (methods 5 - 6) used to synthesize the lassomycin amide derivatives

2.1.3.8. HATU and HBTU mechanism

HATU and HBTU use the same mechanism to activate amino acids; however, the presence of the pyridine ring on HATU makes it more reactive. HATU increases reaction rates and reduces epimerization which result in a low contamination risk and an increased aminoacylation

efficiency. HATU is therefore superior to HBTU. The activation mechanism of HATU is shown in Scheme 5.



Scheme 5 The mechanism of HATU

2.1.3.9. HOBt

The use of HOBt as an additive has advantages such as minimizing the occurrence of side reactions, which leads to less peptide contamination, better results and improved yields by increasing reaction rates.

2.1.4. Purification using semi-preparatory HPLC

All the derivatives synthesized were purified using a semi-preparative HPLC instrument via reversed phase chromatography. The samples were eluted using a flow rate of 15 ml/min and collected using a fraction collector. An acetonitrile/water mobile phase solvent system was used. Each solvent had 0.1% formic acid (v/v) used as an ion pairing agent.

2.1.5. Analysis of results

The peptides were analyzed using Liquid Chromatography Mass Spectrometry (LC-MS) and eluted with a gradient from 5 – 95 % ACN in 10 min with a flow rate of 0.3 ml/min. A two-buffer system was employed, Buffer A consisted of 0.1 % formic acid/H_2O (v/v) and buffer B consisted of 0.1 % formic acid/acetonitrile (v/v). A Phenomenex Kinetex XB-C18 column (5

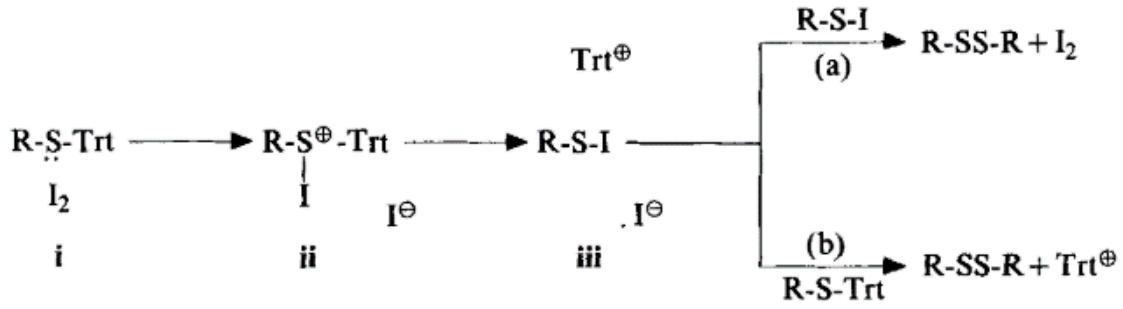
μm, 100 Å, 250 mm × 21.2 mm) was used to separate the compounds with a flow rate of 15 ml/min.

2.2. Lassomycin-amide derivatives

2.2.1. Insertion of the disulfide bridge

Lassomycin is a basic peptide that contains a macro-lactam bridge which was replaced with a disulfide bridge using cysteine amino acids. The lactam is replaced to increase the ring size and therefore the role of the ring size on the activity of lassomycin against *M. tb* can be investigated. The formation of a disulfide bridge via oxidation using a dilute iodine solution has fewer synthetic steps when compared with the macro-lactamization. The reduced number of steps results in a reduction in risk of contamination and reaction time. In a previous study, the lactamization step required a total reaction time of 20 hours and the yield of the final product was poor at 14%.[21]

Two cysteine amino acids were inserted into the lassomycin sequence and a disulfide bond was formed between the cysteine residues by shaking the peptides in a solution of iodine in DMF/water (1:4) for 6 hours. The iodine solution was diluted in order to form intra-molecular disulfide bonds as a concentrated solution results in inter-molecular bonds. A cationic complex ion (**ii** in Scheme 6) is formed via an electron transfer reaction to make a bond between sulfur and iodine. Cyclization is achieved when an iodine-bound Cys reacts with another Cys upon Trt cleavage (**iii**). Excess iodine is reduced and removed using ascorbic acid.[77]



Scheme 6 A mechanism of the cyclization of Trt-protected Cys to form a disulfide bridge[51]

The sequences of the synthesized Pep_1_NN and Pep_1_NNA lassomycin-amide derivatives are compared to that of natural lassomycin in Table 1 and Figure 26.

Table 1 comparing the properties of Pep_1_NN and Pep_1_NNA derivatives to lassomycin

Compound	Sequence	Comment
Lassomycin	INRRGVLQDAFLRRLG	Natural peptide, ester C- terminal end
Pep_1_NN	INRRGVLQCNGLRRLFAC	Disulfide bond addition, reversed sequence, amide C-terminal end
Pep_1_NNA	INRRGVLQCDAFLRRLGC	Disulfide bond addition, amide C- terminal end

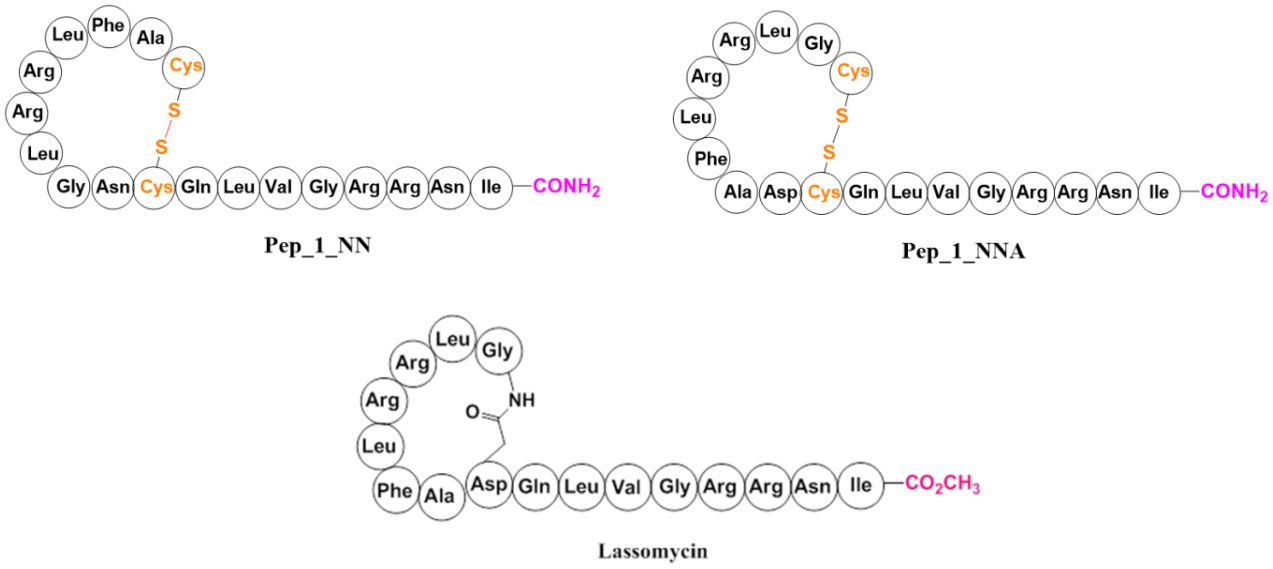


Figure 26 The structures of lassomycin and its derivatives

2.2.2. Peptide synthesis

The peptides were synthesized as described in Scheme 4 using methods 5 and 6.

2.2.3. Results and discussion

Pep_1_NN and Pep_1_NNA derivatives both contain 4 arginine (Arg) residues in their respective sequences. The Arg groups are known to be “difficult” amino acids because of the challenges they pose during synthesis such as formation of incomplete sequences. The Arg used has bulky side-chains and bulky 2,2,4,6,7-pentamethyldihydrobenzofuran-5-sulfonyl (pbf) protecting groups which may result in incomplete aminoacylation due to steric hindrance.

In addition to Arg, the derivatives also contained asparagine (Asn) and glutamine (Gln) residues which were both protected with the bulky Trt known to cause steric hindrance. HOBt was therefore used to aid the reaction in order to improve coupling efficiency.

2.2.3.1. Challenges during TFA-cleavage

During the cleavage step using TFA, both Pep_1_NN and Pep_1_NNA derivatives formed salts observed as white precipitates on the resin. This is caused by the interaction between the guanidinyl side chains of Arg with the concentrated TFA. The guanidinyl side chains are basic with a pKa of $\approx$ 12.5 and behave like organic bases and react with a deprotonated anionic TFA. Due to the formation of salt, the peptides were left in the TFA solution overnight to ensure sufficient reaction time was provided to achieve complete deprotection. When a small portion of uncyclized Pep_1_NNA was cleaved in a relatively small volume of the TFA solution (using an Eppendorf), it dissolved better in the TFA solution. A crude white powder was obtained for Pep_1_NN and Pep_1_NNA after the cleavage step. The powder obtained for both derivatives was soluble in water because the derivatives are basic and have a charge of +4 due to the presence of the Arg groups.

2.2.3.2. LC-MS Analysis

Pep_1_NN and Pep_1_NNA were both successfully synthesized and cyclized despite the salt formation during cyclization (Table 2). A small amount of Pep_1_NNA (7%) remained uncyclized. Even though Pep_1_NN has a reversed sequence to the parent lassomycin, it showed better results. The molecular structures of Pep_1_NN and Pep_1_NNA are illustrated below in Figure 27 and Figure 28.

Table 2 The yield and purity of Pep_1_NN and Pep_1_NNA derivatives

Derivative	**% Purity**	**Mass (mg)**	**% Yield**	**Calculated Mass**	**Found Mass**
Pep_1_NN	> 95	12.3	15	2086.1346	1044.0720 $[M+2H]^{2+}$
Pep_1_NNA	92	119.6	28	2087.1186	1044.5733 $[M+2H]^{2+}$

The Cysteine amino acids were successfully inserted in the lassomycin peptide.

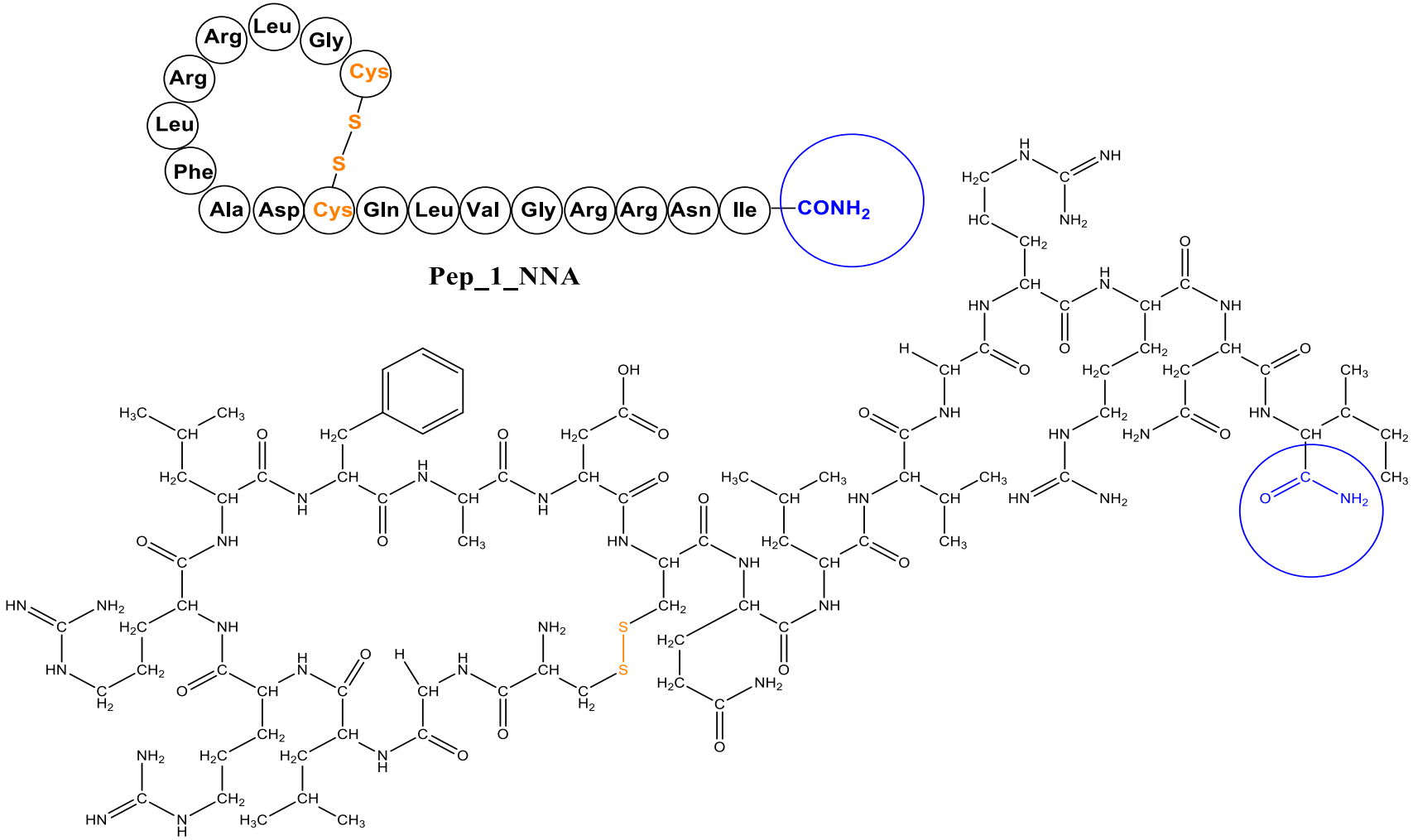


Figure 27 The hand-notation and molecular structures of Pep_1_NNA

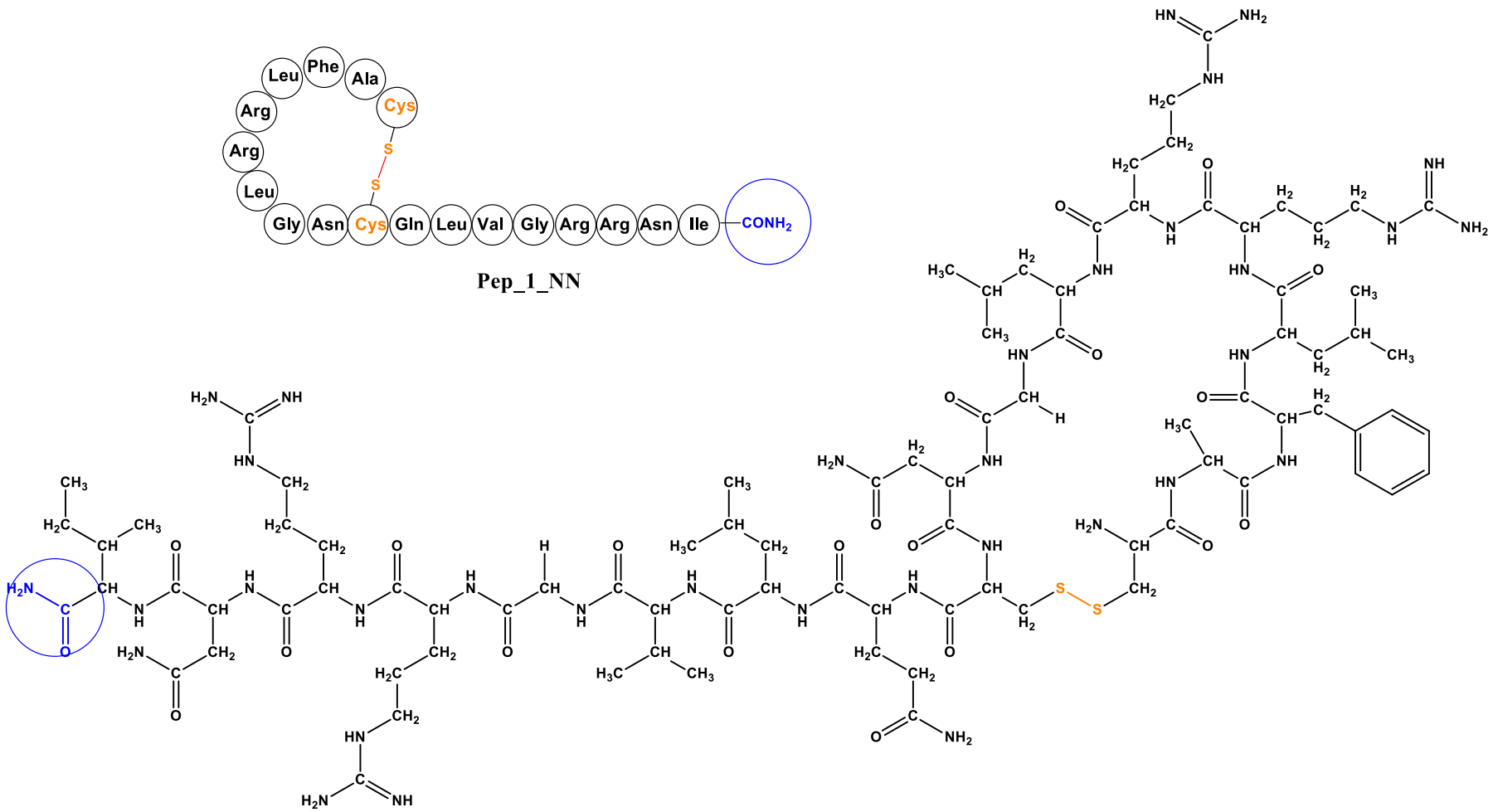


Figure 28 The hand-notation and molecular structures of Pep_1_NN

2.3. Substitution of Arginine with Lysine

2.3.1. Challenges with Arginine

The addition of Arg residues is found to increase the charge of peptides which increases the probability of binding or penetrating the negatively charged membrane of the bacterial cell. The challenges associated with coupling Arg during peptide synthesis include steric hindrance caused by the bulky side-chain (pbf) that result in incomplete coupling. Steric hindrance also results in using longer reaction times to ensure completion of reaction.[78]

The lysine (Lys) amino acids are slightly less basic and are used to replace the Arg while still maintaining the basicity of the peptide. Substitution with Lys also decreases the overall molecular mass which may improve bioavailability (absorption) in the human body. Furthermore, Lys increases the probability of rupture within the bacterial cell which causes slow leakage from the cell. This is likely due to the interactions with the anionic proteins found in the bacterial membrane.[79] The substitution of Arg with Lys was mainly done to investigate the importance of Arg in the binding of lassomycin to the caseinolytic enzyme. The difference between the synthesized Pep_2_NNA and Pep_2_NN derivatives are highlighted in Table 3 and Figure 29 below. The residues in the sequences are highlighted to show changes from the natural peptide.

Table 3 comparing the properties of Pep_2_NN and Pep_2_NNA derivatives to lassomycin

Compound	**Sequence**	**Comment**
Lassomycin	INRRGVLQDAFLRRLG	Natural peptide, ester C- terminal end
Pep_2_NN	INKKGVLQCNGLKKLFAC	Disulfide bond addition, Reversed sequence, amide C-terminal end, Arg (R) Substituted with Lys (K)
Pep_2_NNA	INKKGVLQCDAFLKKLGC	Disulfide bond addition, amide C- terminal end, Arg (R) Substituted with Lys (K)

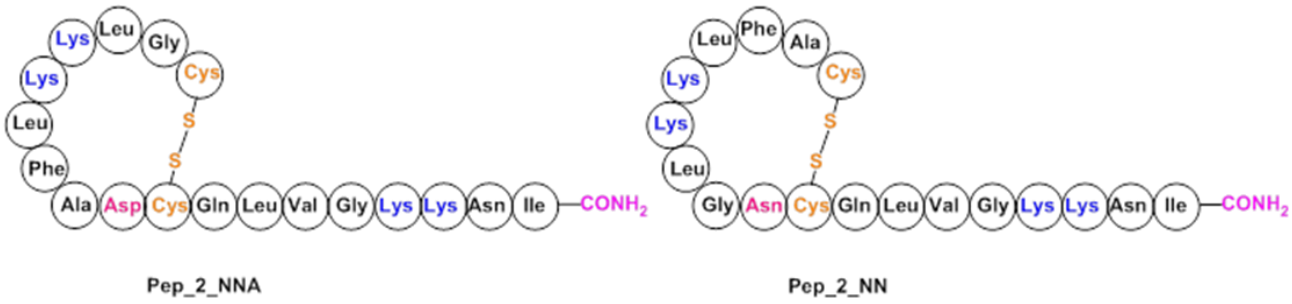


Figure 29 The structures of Pep_2_NN and Pep_2_NNA derivatives with the C- terminal amide ending

2.3.2. Synthesis of Pep_2_NN and Pep_2_NNA:

The synthesis of Pep_2_NN and Pep_2_NNA was similar to that of Pep_1_NN and Pep_1_NNA. A rink amide resin was used to synthesize Pep_2_NN (100 mg) and Pep_2_NNA (100 mg). A loading capacity of 0.4 mmol/g was obtained for Pep_2_NNA. HOBt was not used during the coupling step for both derivatives. Pep_2_NNA was cyclized using iodine for 6 hours and Pep_2_NN was cyclized for 4 hours. Cleavage of the peptides from the resin linker and permanent protective groups was achieved using a cocktail of 94% TFA for 4 - 6 hours.

2.3.2.1. Peptide difficulty:

The coupling efficiency decreases with increasing chain length and both Pep_2_NN and Pep_2_NNA are 18- amino acid long chains which were anticipated to be “difficult” peptides to synthesize. The derivatives were also confirmed to be difficult peptides by the Protein Technologies, Inc. (PTI) peptide difficulty predictor. Difficult peptides generally result in poor results due to the length and nature of their sequences. The predicted Pep_2_NNA sequence is given in Table 4 below.

Table 4 Predicting the difficulty of the sequence as predicted by the PTI peptide predictor

Amino acid	I	N	K	K	G	V	L	Q	C	D	A	F	L	K	K	L	G	C
Color code	R	Y	R	R	Y	R	R	Y	R	G	R	R	R	R	R	R	Y	R

The color codes in Table 4 above represent the difficulty of each amino acid during the synthesis of Pep_2_NNA. The amino acids with the red (R) code are the most difficult to couple and those with green (G) are the least difficult to couple. Isoleucine (Ile) is coupled to the linker

of the resin and is used to determine the loading capacity, however, it is predicted to have difficulty coupling to the resin which my result in decreased yields. The peptide difficulty predictions were done to study the behavior of the amino acids during synthesis in order to improve yields. Short peptides of Pep_2_NNA were synthesized and analyzed to monitor the synthesis.

2.3.2.2. Pep_2_NN short peptides:

Short Pep_2_NNA peptides were synthesized and analyzed using LC-MS. The short peptides were successfully synthesized and the results are summarized in Table 5.

Table 5 The LC-MS results for Pep_2_NNA short peptides

Sequence peptide sequence	**Calculated mass**	**Found mass**	**Molecular ion**	**Retention time/ min**
INKKG	557.3649 $C_{24}H_{47}N_9O_6$	558.3708	[M + H]	3.71
INKKGV	656.4333 $C_{29}H_{56}N_{10}O_7$	657.4403	[M + H]	3.94
INKKGVL	769.5174 $C_{35}H_{67}N_{11}O_8$	770.5238	[M + H]	5.77
INKKGVLQ	897.5760 $C_{40}H_{75}N_{13}O_{10}$	898.5835	[M + H]	5.78
INKKGVLQC	1000.5852 $C_{43}H_{80}N_{14}O_{11}S$	501.2972	$[M + H]^{2+}$	6.62

The synthesized short peptides were, however, contaminated with deletion sequence impurities and are summarized in Table 6. Deletion impurities are observed when at least one amino acid is missing in the sequence. Other impurities associated with peptide synthesis include mismatched sequences and incomplete sequences resulting from sequence termination.

Table 6 The LC-MS results of the impurities associated with synthesized Pep_2_NNA short peptides

Expected short peptide sequences	Calculated Mass (of short peptide)	Found Mass (of impurity)	Suggested Sequence of impurities corresponding to found mass	Retention time/ min
INKKGV	656.4333	529.3433 $[M + H]^+$	INKGV	5.79
INKKGVL	769.5174	642.4259 $[M + H]^+$	INKGVL	6.64
INKKGVLQ	897.5760	406.7705 $[M + 2Na]^{2+}$	INKGVLQ	7.03
INKKGVLQC	1000.5852	898.5785 $[M + H]^+$	INKKGVLQ	6.50
		406.7687 $[M + 2Na]^{2+}$	INKGVLQ	7.02

2.3.2.3 Lysine and cysteine deletion impurities

The impurities observed on the short peptides were the Lys and Cys deletion sequences, summarized in Table 6. The Lys and Cys amino acids are coupled to the *N*-terminal asparagine (Asp) and glutamine (Gln) respectively. The side-chains of Asn and Gln are both protected with a Trt group. The presence of the bulky Trt protecting group causes steric hindrance and results in incomplete aminoacylations.[80,81] The Trt protection group is also associated with low reactivity and incomplete Fmoc removal thus resulting in truncated and deletion sequences. The impurities were co-eluted with the short peptides. The deletion observed for the peptides may not have resulted due to aggregation as the peptides synthesized were not hydrophobic.[82]

It was also noticed that the amount of contamination increased with the growing chain. Longer peptide chains require longer reaction times which result in side-reactions.

The short peptides were all soluble in water due to the presence of the Lys amino acids as they are known to improve the solubility of peptides. This phenomenon was noticed when the INKKGV peptide was observed to be more polar than its INKGV impurity which is missing a Lys residue. Solubility of peptidomimetic compounds in water is very important as it increases the chances of oral absorption.[49]

The success of the synthesis of the short peptide led us to proceed with the synthesis of full chain derivatives.

2.3.4. Pep_2_NN and Pep_2_NNA lassomycin derivative

Pep_2_NNA (Figure 30) and Pep_2_NN (Figure 31) were cleaved using TFA and crude products were obtained as white powders that were soluble in water.

During the purification of Pep_2_NNA using HPLC, 2 peaks that contained the desired mass were separated and eluted at different retention times. The column used for separation was non-chiral and therefore the fractions collected were conformational isomers. Shorter coupling-reaction times (30 min) and a good coupling reagent (HATU) were used to ensure that the derivatives synthesized were protected against racemization.[83] The isomers were named Pep_2_NNA_conf1 (RT = 7.3 min) and Pep_2_NNA_conf2 (RT = 7.7 min) and both contained a mixture of cyclized and uncyclized peptides. A small fraction of Pep_2_NNA_conf1 (28%) and Pep_2_NNA_conf2 (40%) was cyclized and the majority remained uncyclized Pep_2_NN was cyclized and purified (> 95%) successfully. The chromatogram of Pep_2_NN had less contamination than the chromatograms obtained for both Pep_2_NNA isomers. The results are summarized in Table **7**.below.

Table 7 The purity of Pep_2_NN and Pep_2_NNA isomers

Compound	Calculated mass	Observed mass [Molecular Ion]	Retention time/ min	Purity (%)
Pep_2_NNA_ conf1	1975.0947 $C_{88}H_{150}N_{24}O_{23}S_2$ Cyclized	495.0276 $[M + 4H]^{4+}$	8.99	28
	1977.0904 $C_{88}H_{152}N_{24}O_{23}S_2$ Uncyclized	660.0388 $[M + 3H]^{3+}$	7.38	72
Pep_2_NNA_ conf2	1975.0947 $C_{88}H_{150}N_{24}O_{23}S_2$ Cyclized	659.7071 $[M + 3H]^{3+}$	9.04	40
	1977.0904 $C_{88}H_{152}N_{24}O_{23}S_2$ Uncyclized	989.5577 $[M + 2H]^{2+}$	7.53 & 8.57	60
Pep_2_NN	1974.1100 $C_{88}H_{152}N_{26}O_{21}S_2$ Cyclized	988.0602 $[M + 2H]^{2+}$	7.86	> 95

Pep_2_NN also had better yields (13.8 mg, 18.20%) than Pep_2_NNA (5% for Pep_2_NNA_conf1 and 8.6% for Pep_2_NNA_conf2). The yields were determined using the loading capacity of the derivatives and are summarized in Table 8 below. The lower yields may have been caused by peptide impurities as a result of "difficult" synthesis. The lower yields can also be attributed to loss of peptide during purification.

Table 8 comparison of the yields of the synthesized derivatives

Purified compound	Mass obtained/ mg	% Yield
Pep_2_NN	13.8	18.28
Pep_2_NNA_conf1	3.9	5.16
Pep_2_NNA_conf2	6.5	8.61

Pep_2_NN and Pep_2_NNA isomers were tested and found to be potent against *M. tb*. The Pep_2_NNA isomers were active despite the presence of uncyclized peptides. The activities of the derivatives are explained in detail in Chapter 4.

2.3.5. Conclusion:

The uncyclized structures of Pep_2_NNA and Pep_2_NN were successfully synthesized. Pep_2_NN was successfully cyclized with iodine; however, a small fraction of Pep_2_NNA isomers was cyclized. Since a similar synthetic route was applied for both derivatives, the incomplete cyclization of Pep_2_NNA isomers may have been as a result of structural conformation (arrangement of residues). The Arg amino acids were also successfully replaced with Lys. The peptide was predicted to be a difficult peptide, as a result, deletions and truncated chain impurities were observed.

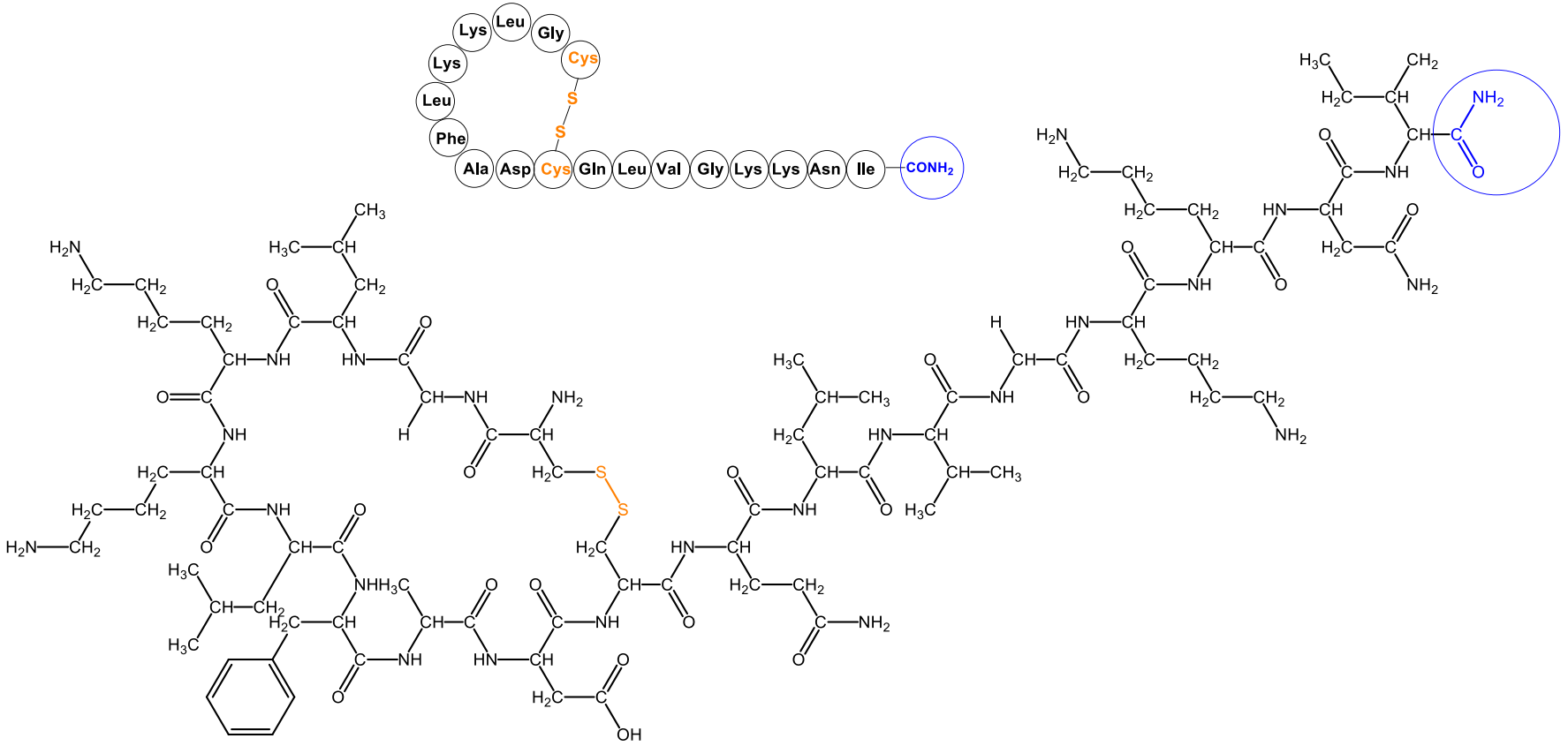


Figure 30 The molecular and hand notation structures of Pep_2_NNA.

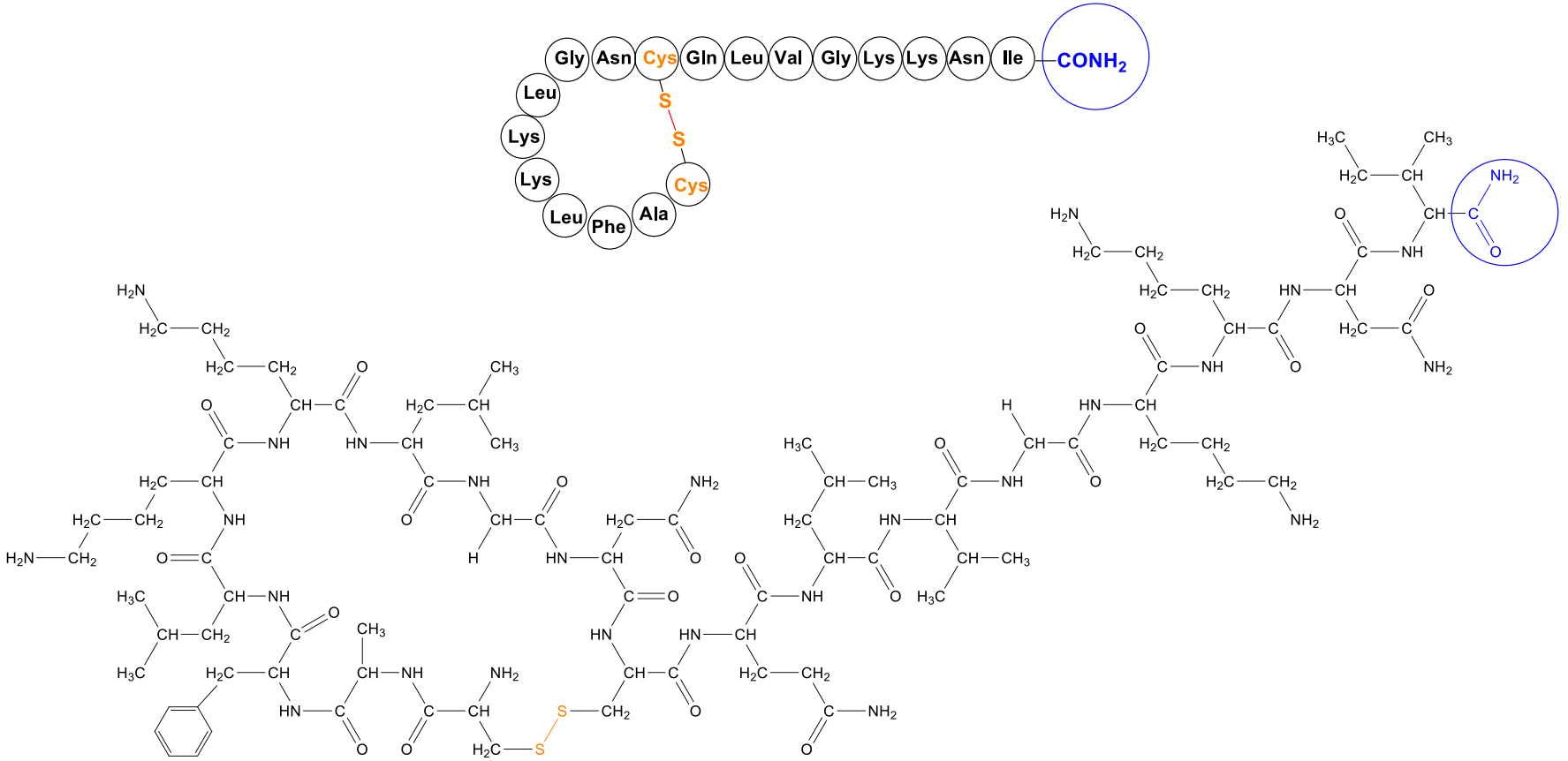


Figure 31 The molecular and hand notation structures of Pep_2_NN

2.4 Cationic Lassomycin-Amide Peptide Derivatives

Cationic peptides contain a number of basic amino acids including lysine and arginine and are found to interact with and penetrate the bacterial cell wall more easily. The arginine cationic peptides are more potent than those of lysine. Addition of Lys groups to peptide sequences improve their bacterial cell wall penetration and increases their ability to cause cell rupture once inside the cell.

The cationic derivatives synthesized were chosen to be lysine cationic peptides due to the difficulties associated with arginine during synthesis. The derivatives synthesized are Pep_Lys_NN, Pep_Lys_NNA, Pep_1_NN_Lys and Pep_1_NNA_Lys. The structures of the derivatives are shown in Figure 32 and the differences are highlighted in Table 9 below. The synthesis of the derivatives was achieved using the method mentioned previously except that of the cyclization of Pep_1_Lys_NN and Pep_1_Lys_NNA which was done overnight.

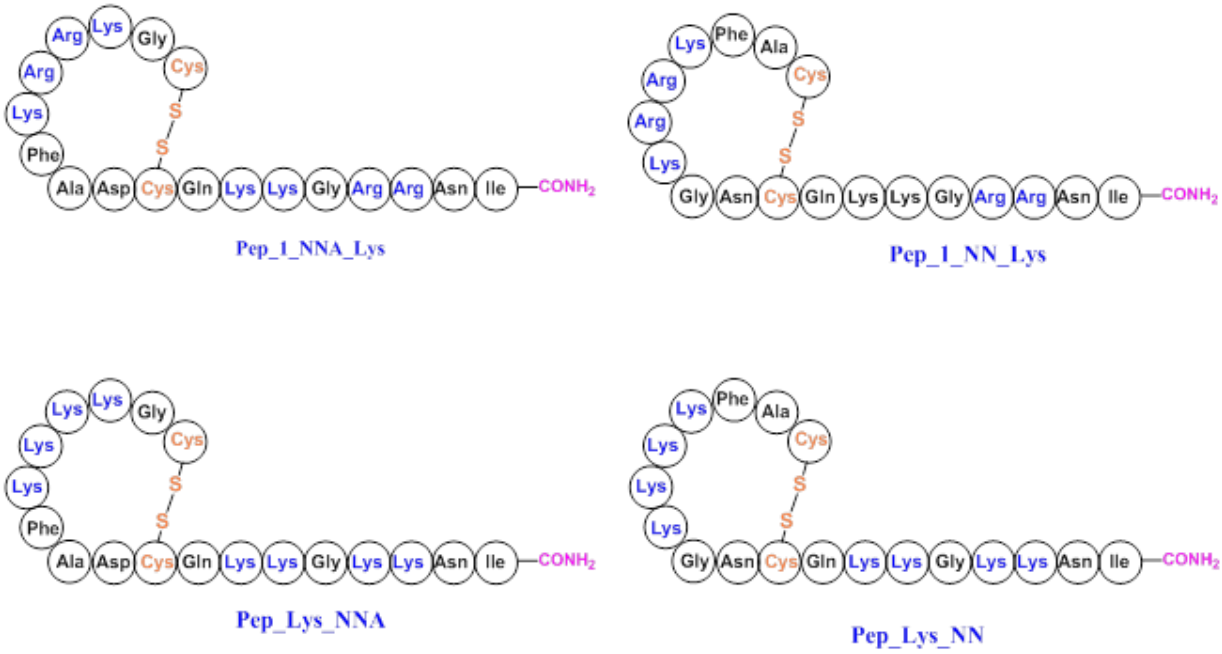


Figure 32 The structures of Pep_1_NNA_Lys, Pep_1_NN_Lys, Pep_Lys_NNA and Pep_Lys_NN cationic derivatives

Table 9 highlighting the difference in the sequences of the cationic derivatives synthesized

Compound	Sequence	Comment
Lassomycin	INRRGVLQDAFLRRLG	Natural peptide
Pep_Lys_NN	INKKGKKQCNGKKKLFAC	Reversed sequence; Arg (R), Leu (L) and Val (V) replaced with Lys (K)
Pep_Lys_NNA	INKKGKKQCDAFLKKLGC	Arg (R), Leu (L) and Val (V) replaced with Lys (K)
Pep_1_Lys_NN	INRRGKKQCNGKRRKFAC	Reversed sequence; only Leu (L) and Val (V) are replaced with Lys (K)
Pep_1_Lys_NNA	INRRGKKQCDAFKRRKGC	Only Leu (L) and Val (V) replaced with Lys (K)

2.4.1. Results and discussion

The linear peptides were cyclized using iodine. The purified Pep_Lys_NN was successfully cyclized and the mass obtained was 29.5 mg (38% yield) with 90% purity. Pep_Lys_NNA was not successfully cyclized and a mass of 54.1 mg (69.1%) uncyclized sample was obtained after purification. Pep_1_NN_Lys (7.9 mg) was obtained as a mixture of cyclized (56%) and uncyclized (43%) peptide. The results are summarized in Table 10 below.

The –NN groups (Pep_Lys_NN and Pep_1_Lys_NN) seemed to cyclize better than the –NNA group. This trend was also noticed for the previously discussed derivatives. Pep_1_NN_Lys and Pep_1_NNA_Lys formed a salt with TFA during cleavage which was observed as a white precipitate on the resin. The amount of salt formed was more for Pep_1_Lys_NNA than Pep_1_Lys_NN. Pep_1_NN_Lys and Pep_1_NNA_Lys formed the TFA-salts faster than Pep_1_NN and Pep_1_NNA (which were discussed in Section 2.2) and this may be due to the increased basicity. Pep_1_NNA_Lys was not purified. Pep_1_NN_Lys and Pep_1_NNA_Lys derivatives were contaminated with similar impurities.

Table 10 LMS results for cationic peptides

Compound	Calculated mass	Observed mass [Molecular ion]	Retention time (min)	Purity (%)
Pep_Lys_NN	2048.1693 $C_{89}H_{158}N_{30}O_{21}S_2$ Cyclized	1025.0980, $[M + 2H]^{2+}$	3.49	90
Pep_Lys_NNA	2049.1533 $C_{89}H_{157}N_{29}O_{22}S_2$ Cyclized	684.0569, $[M + 3H]^{3+}$	3.92	**
	2051.1689 $C_{89}H_{159}N_{29}O_{22}S_2$ Uncyclized	1026.5924 $[M + 2H]^{2+}$	3.40	**
Pep_1_NN_Lys	2159.1905 $C_{89}H_{158}N_{38}O_{21}S_2$ Cyclized	730.4135, $[3M + Methanol]^{+}$	4.70	56
	2161.2062 $C_{89}H_{160}N_{38}O_{21}S_2$ Uncyclized	1081.6120, $[M + 2H]^{2+}$	3.60	43

**** Problems were encounted with UV data**

2.4.1.1. Impurities associated with the derivatives

Pep_Lys_NN and Pep_Lys_NNA had similar truncated peptide impurities (INKKGVLQ and INKKGVLQC) which co-eluted with the peptides. Pep_1_NN_Lys contained the INRRGVLQC impurity that was also co-eluted with the peptide. The incomplete sequences

may be due to the presence of the bulky Trt protecting group. However, with these cationic derivatives, the incomplete sequences do not grow with the growing peptide, they remain incomplete as terminated sequences. The presence of the charged Lys residues may have also resulted in the incomplete sequences due to aggregation.

Pep_Lys_NN was tested against a number of pathogens (discussed more in Chapter. 4) and was found to be selectively active against *B. subtilis*, a pathogen sharing a similar protease to *M. tb*.

2.4.2. Conclusion

The synthesis of the cationic derivatives highlighted a trend in the behavior of the peptide derivatives, with the –NN groups giving better results than the –NNA groups. The substitution of non-polar residues with Lys to make cationic peptides was successful for all derivatives, however, the cyclization of the derivatives was problematic. The Trt protecting group was found to result in a number of terminated sequences. The Arg-based derivatives (Pep_1_NN, Pep_1_NNA, Pep_1_NN_Lys and Pep_1_NNA_Lys) seem to be more challenging to synthesize especially during cleavage with strong TFA solutions. The molecular structures of Pep_1_NN_Lys and Pep_1_NNA_Lys are shown in Figure 33 and Figure 34, respectively.

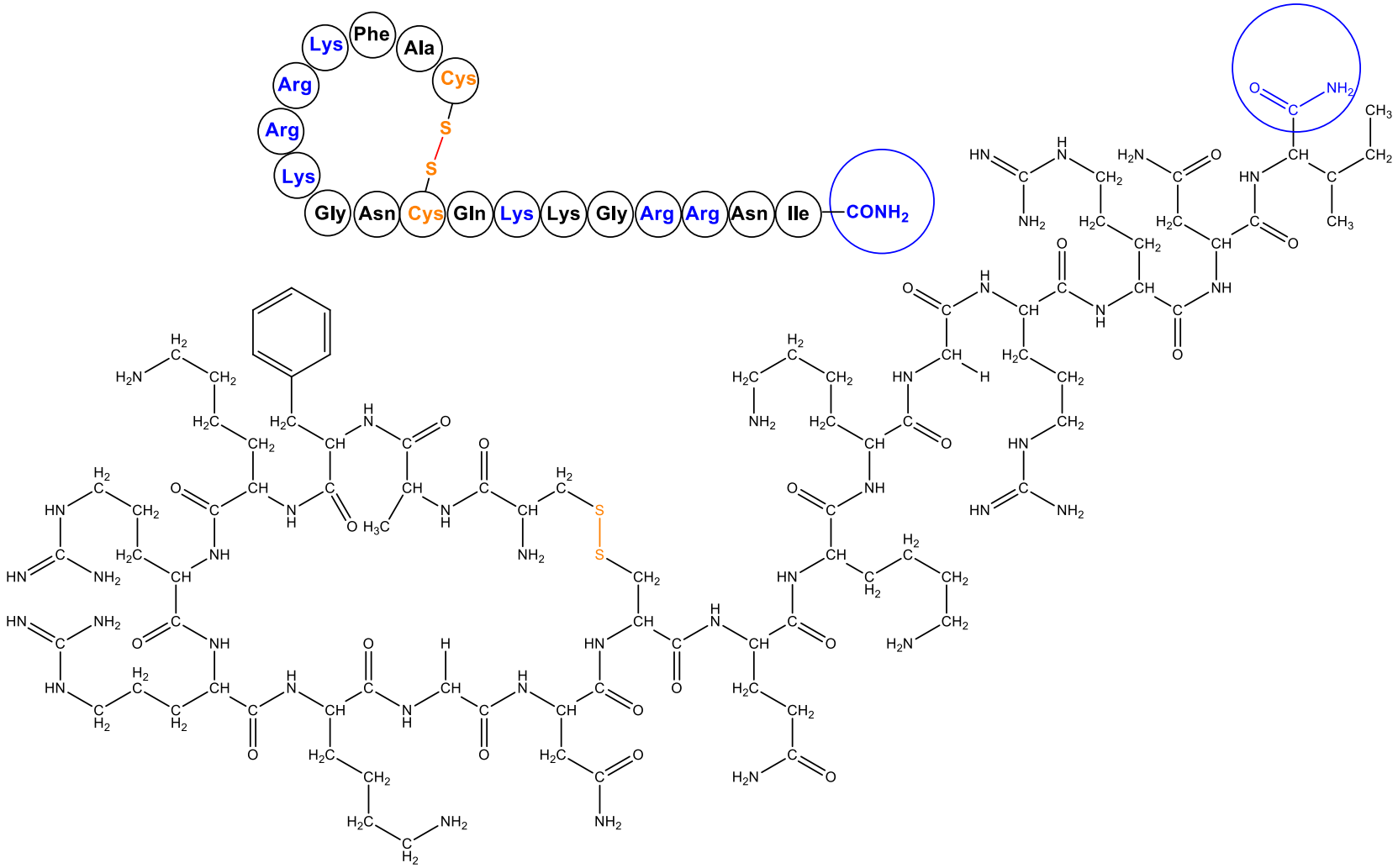


Figure 33 The structure of Pep_1_NN_Lys

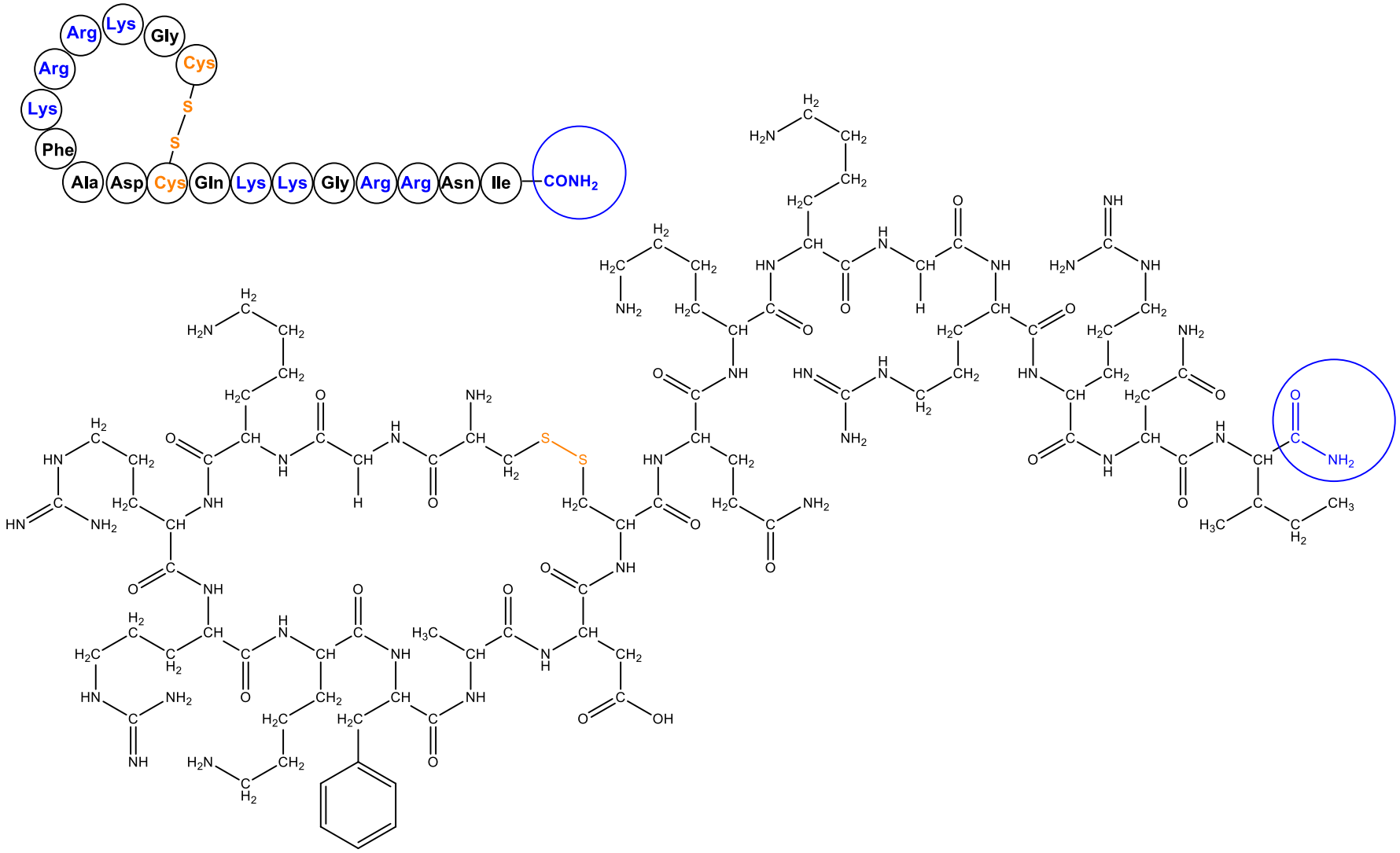


Figure 34 The structure of Pep_1_NNA_Lys

CHAPTER 3

THE SYNTHESIS OF *N*-METHYLATED FMOC-PROTECTED LEUCINE, VALINE AND ALANINE; AND THEIR INCORPORATION INTO THE PEP_2_NN AND PEP_2_NNA DERIVATIVES

Currently, there is no available information about the stability of lassomycin under physiological conditions, however, peptides (e.g. Cyclomarin A[65]) are generally known to be prone to enzymatic degradation due to the nature of their structures. Lassomycin was therefore modified by *N*-methylating selected amide bonds. This was done to improve stability and hydrophobicity, thereby increasing bioavailability. The length of the peptide and the number of *N*-methylated amino acids present in the chain inversely affect the purity of the final peptide product. This phenomenon was observed and better demonstrated during a study done by F. Albericio and colleagues (2005).[84] The long 18- amino acid Pep_2_NN chain and the incorporation of 5 *N*-methylated amino acids may result in the presence of peptide impurities, thus decreasing the purity.

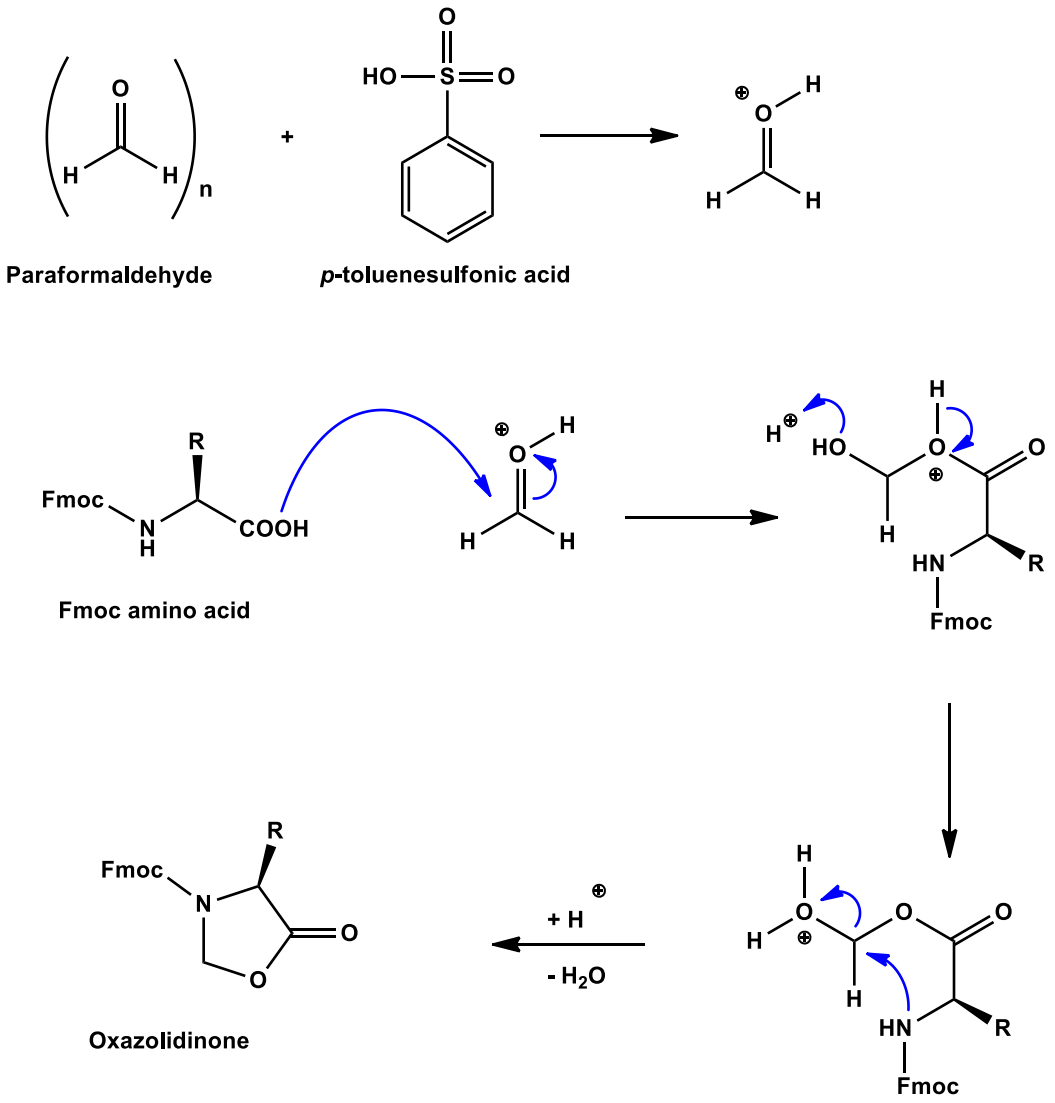
3.1 Synthesis of *N*-methylated amino acids

Commercial *N*-methylated Fmoc protected amino acids are expensive and were therefore synthesized in-house. The Freidinger synthetic route was chosen from a wide range of available α-*N*-methylation methods as it results in racemization-free reaction and any Fmoc- protected amino can be used.[85]

The first part of the synthesis converts the Fmoc- amino acids to 5-oxazolidinone precursors which are used to make the final α-*N*-methyl amino acid products. All the *N*-methylated amino acids were synthesized using the same route unless otherwise stated.

3.1.1. Synthesis of 5-oxazolidinones

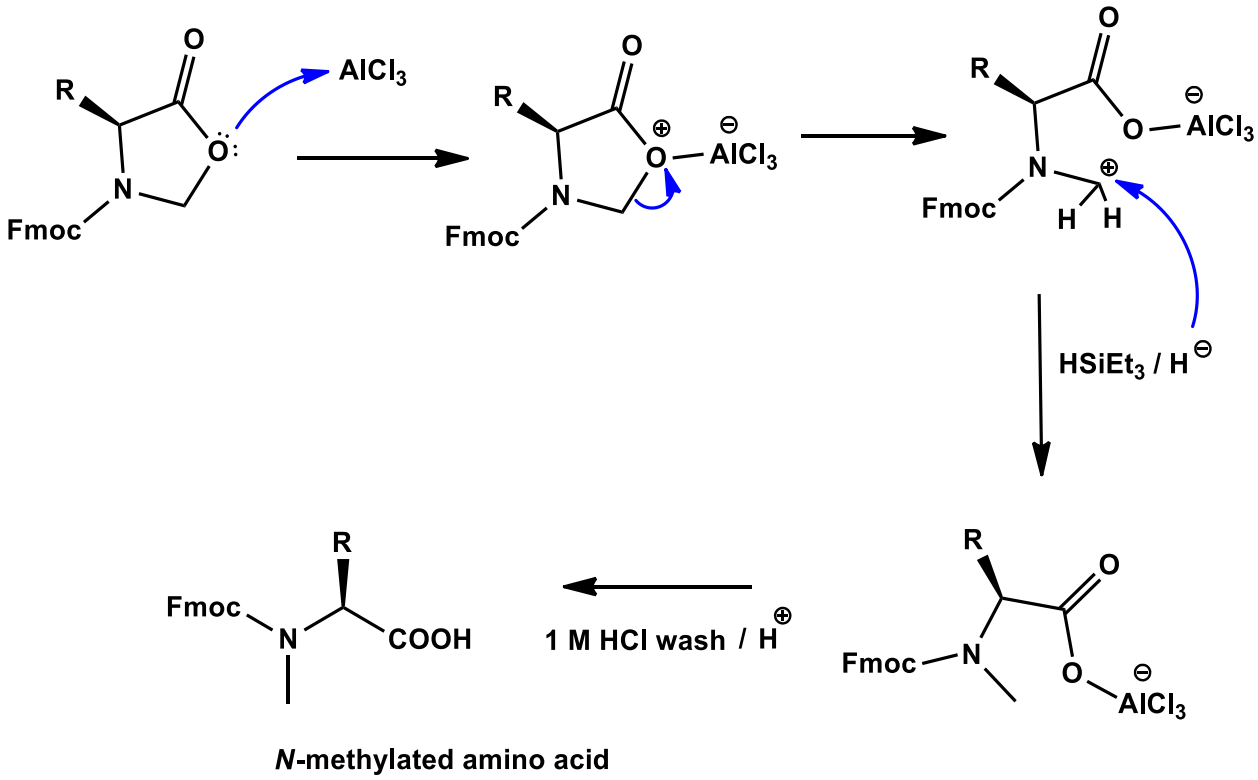
5-Oxazolidinones are 5- membered heterocyclic rings that are synthesized by reacting Fmoc amino acids with paraformaldehyde and are catalyzed by *p*-toluenesulfonic acid. The reaction is heated under reflux in toluene as solvent. The *p*-toluenesulfonic acid activates the paraformaldehyde to become more electrophilic so it can better react with the Fmoc- amino acid to form an oxazolidinone. Scheme 7 illustrates the synthetic route utilized to make the 5-oxazolidinones. The products were successfully synthesized and purified using recrystallization. The valine (Val), leucine (Leu) and alanine (Ala) 5-oxazolidinones were obtained as crystalline substances and were used to synthesize *N*-methylated amino acids.



Scheme 7 Synthesis of the 5-oxazolidinones from Fmoc protected amino acids. R is the side chain of the amino acid

3.1.2. Synthesis of *N*-methylated amino acids from 5-oxazolidinones

The 5-oxazolidinones were reduced with triethyl silane (TES) in an acid-catalyzed reaction to open the ring and form the *N*-methylated amino acids. A CO bond is not easily broken and therefore aluminum trichloride ($AlCl_3$) was used as a Lewis acid to activate the oxygen of the CO bond. Scheme 8 illustrates the synthetic route utilized to make the *N*-methylated products. The final products were washed with a hydrochloric acid solution (1M) to remove non-acidic contaminants and acidify the methylamino acid product. The final products were purified by recrystallization using acetonitrile.



Scheme 8 The synthesis of *N*-methylated Fmoc- protected amino acids from the 5- oxazolidinone precursors

3.1.3. Results

The *N*-methylated amino acid products were pre-concentrated *in vacuo* after purification and a gel-like substance which crystallized upon cooling was obtained. The *N*-methylated Leu (*N*-Me-Leu) and *N*-methylated Ala (*N*-Me-Val) products were obtained as slightly yellow crystals while the Val product was a white amorphous mixture. Analysis was done using HPLC-MS

and Nuclear Magnetic Resonance Spectroscopy (NMR). The *N*-methylation of amino acids was successful, with purity > 95% for all amino acids. The melting points of *N*-Me-Leu and *N*-Me_Ala were similar to those commercially purchased from Sigma-Aldrich. The melting point of *N*-Me-Val was slightly greater which may be due to the presence of minor impurities. *N*-Me-Leu was obtained in good yield (4.63 g, 84%) and *N*-Me-Ala yield was lower (1.53 g, 31%). Table 11 below summarizes the results obtained. The general structure for the amino acids is shown in Figure 35 where R represents the organic side chain group unique to each amino acid.

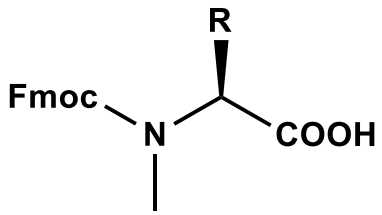


Figure 35 General structure of amino acids where R represents the organic side chain unique to each amino acid

Table 11 summarized data for *N*-methylated valine, alanine and leucine amino acids

***N*- methylated amino acid**	**R group**	**% Yield**	**% Purity**	**Theoretical M.P (°C)**	**Actual M.P (°C)**
N-Me-Ala	$-CH_3$	31	> 95	140	145
N-Me-Leu	$-CH_3CH(CH_3)_2$	84	> 95	113 -116	114
N-Me-Val	$-CH(CH_3)_2$	70	> 95	140 -145	> 150

The synthesized *N*-methylamino acids were analyzed by NMR spectroscopy and the signals corresponding to the *N*-methylated amino were observed in the proton and carbon NMR spectra. Selected NMR data is summarized in Table 12. The general structure for the amino acids is shown in Figure 36 where R represents an organic side chain group unique to each amino acid.

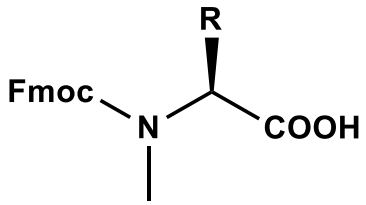


Figure 36 General structure of amino acids where R represents the organic side chain unique to each amino acid

Table 12 Selected NMR data for *N*-methylated amino acids.

***N*- methylated amino acid**	**R group**	**$^{\alpha}$*N*-C<u>H</u>$_3$ (ppm) ^{1}H NMR**	**$^{\alpha}$*N*-<u>C</u>H$_3$ (ppm) ^{13}C NMR**
N-Me-Ala	-CH_3	2.91 (3H, s, N-CH_3)	30.50 (C, s, N-CH_3)
N-Me-Leu	-$CH_3CH(CH_3)_2$	2.86 (3H, s, N-CH_3)	30.33 (C, s, N-CH_3)
N-Me-Val	-$CH(CH_3)_2$	2.90 (3H, s, N-CH_3)	27.43 (C, s, N-CH_3)

The *N*-methylated amino acids were incorporated into Pep_2_NN and Pep_2_NNA sequences to synthesize the *N*-methylated derivatives. Pep_2_NN and Pep_2_NNA were selected because they gave better synthetic and activity outcomes.

3.2 Synthesis of *N*-methylated Peptide derivatives

3.2.1. Synthesis:

The *N*-methylated peptides were synthesized using a synthetic route similar to that used for the previously discussed peptides. Ethyl (hydroxyimino)cyanoacetate (Oxyma Pure) and HOBt were used as additives when coupling the *N*-methylated amino acids and adjacent amino acids. The reaction time for coupling *N*-methylated amino acids was 1 hour using double coupling.

3.2.2. Results

The *N*-methylated Pep_2_NN and Pep_2_NNA derivatives were successfully synthesized. The peptides were purified using semi-prep HPLC and analyzed with HPLC-MS. The *N*-methylated

Pep_2_NN and Pep_2_NNA were both successfully synthesized and cyclized (Table 13), however they were not successfully separated and purified.

Table 13 The HPLC-MS data results for *N*-methylated Pep_2_NN and *N*-methylated Pep_2_NNA

Compound	**Calculated Mass**	**Observed Mass [Molecular ion]**	**Retention Time (min)**
N-methylated Pep_2_NN	2044.1889 $C_{93}H_{161}N_{25}O_{22}S_2$ Cyclized	1023.1012, $[M + 2H]^{2+}$	10.11
N-methylated Pep_2_NNA	2003.1060 $C_{90}H_{154}N_{24}O_{23}S_2$ Cyclized	1002.5714, $[M + 2H]^{2+}$	9.97

3.2.2.1. *N*-methylated Pep_2_NN

N-methylated Pep_2_NN was successfully cyclized; however, it was co-eluted with some impurities during purification. It is not uncommon for some peptidic impurities to be co-eluted with the parent peptide and this has been observed for most of the previously discussed peptides.

Due to the poor separation of *N*-methylated Pep_2_NN from impurities, the peptide was not successfully purified and the yield was not determined. Poor separation may have resulted from using a short purification time (9 min with an elution gradient of 30 – 95% ACN). In future, separation and purification could be improved by changing the column used to a Jupiter column as well as increasing the purification run-time. Jupiter peptide columns are equipped to handle larger compounds, their pore size is around 300 Å, however, they are more expensive.

N-methyl-rich peptides are mostly associated with deletion problems that may result from coupling *N*-methylated amino acids consecutive to each other. Most of the impurities observed

for *N*-methylated Pep_2_NN were incomplete sequences terminated after the addition of an *N*-methylated amino acid at the *N*-terminus. The terminated impurities included INKKGV(Me), INKKGV(Me)L(Me)QCNGL(Me) and INKKGV(Me)L(Me). Termination at the *N*-methylated amino acids may have resulted from the *N*-methyl groups blocking access to the carboxyl group of the incoming amino acid and thus resulting in incomplete aminoacylation. Fmoc deprotection of *N*-methylated amino acids may have been slow and incomplete, resulting in incomplete sequences. For future purposes, the deprotection solution or method may be modified by adding the non-nucleophilic 1,8-Diazabicyclo[5.4.0]undec-7-ene (DBU) to ensure complete Fmoc deprotection and improve yields. DBU is more sterically hindered than piperidine and in lower concentrations it has been found to result in fewer impurities and this may be attributed to its bulky nature.[86]

Other impurities included INKKGV(Me)L(Me)Q and INKKGVLQCN terminated sequences which may have resulted due to steric hindrance caused by the presence of the bulky Trt protecting groups. The trityl protecting group may result in slow or incomplete removal of the Fmoc group which may then result in incomplete aminoacylation with an incoming amino acid as a result of minimized access. Despite the presence of the above-mentioned impurities, the peptide was synthesized and successfully cyclized (Table 13).

CHAPTER 4

4.1. Toxicity and Biological Testing

Lassomycin and its derivatives have been synthesized before and the bactericidal concentrations used to kill the Mycobacterium were higher than the concentration of the natural lassomycin (0.8 – 3 μg/ml).[2] The lassomycin and lassomycin-amide derivative synthesized by Lear (2016)[69] were inactive and those synthesized by Harris (2017)[21] were active at higher concentrations of 32 μg/ml. The results comparing the bactericidal activities of lassomycin and previously synthesized derivatives are summarized in Table 14 below.

Table 14 Comparing the activities obtained with regards to lassomycin and some of its derivatives, to date

Compound/ Analogue	**% Purity**	**% yield**	**Conditions/ factors**	**MIC/ (μg/ml)**	**Source**
Natural isolated peptide	100	nr*	Natural screening	0.8 -3 Active	Gavrish *et al.*[2]
Natural isolated peptide	nr	nr	Commercially sourced	> 53 Not active	P. Harris *et al.*[21]
Synthesized lassomycin	nr	nr	Chemical synthesis	> 100 Not active	S. Lear *et al.*[69]
Synthesized lassomycin	nr	14	Chemical synthesis	32 Active	P. Harris *et al.*[21]
Lassomycin amide	nr	nr	Chemical synthesis	> 100 Not active	S. Lear *et al.*[69]

Compound/ Analogue	% Purity	% yield	Conditions/ factors	MIC/ (µg/ml)	Source
Lassomycin amide	> 95	31	Chemical synthesis	32 Active	P. Harris *et al*.[21]
Lassomycin acid	> 95	45	Chemical synthesis	64 Not active	P. Harris *et al*.[21]

***nr** = not reported**

The biological activities of Pep_2_NN, Pep_2_NNA and Pep_Lys_NN were tested against the Mycobacterium and the results are discussed below..

4.1.1. Pep_2_NN, Pep_2_NNA_conf1 and Pep_2_NNA_conf2

Cytotoxicity studies of Pep_2_NN showed that toxicity increased with concentration and the data is summarized in Table 15. In a previous study by Gavrish *et al*., lassomycin showed low cytotoxity against human liver cells (HepG2 cells) at a half-maximal inhibitory concentration of 350 µg/ml., The toxicity screening for Pep_2_NN was done at Mintek-Advance Material Division as a dose-response study against Human T cells (MT4 cells) and the results are summarized in Table 13. The experimental procedure calculations were done at Mintek-Advance Material Division and a report of the study is shown in Figure 57 in the Appendix section.

Table 15 The relationship between the concentration of Pep_2_NN and toxicity

Entry	Concentration/ (µg/ml)	Toxicity (%)
1	100	58.54
2	50	55.93
3	25	45.57
4	12.5	35.50

Entry	Concentration/ (µg/ml)	Toxicity (%)
5	6.25	36.22
6	3.125	18.63
7	1.56	34.45

Pep_2_NN and Pep_2_NNA (Pep_2_NNA_conf1 and Pep_2_NNA_conf2) derivatives were tested against *M. tb* during an incubation period of two weeks. The activity of the derivatives was determined after a week of interacting with the Mycobacterium cell and also after 2 weeks. The results obtained after 7 days (first lag) showed that Pep_2_NN (9.87 µg/ml) had better activity than Pep_2_NNA_conf1 (39.5 µg/ml) and Pep_2_NN_conf2 (79.0 µg/ml).

The activity of Pep_2_NN was comparable to that of ethambutol which was used as a control. The incorporation of Asn in place of Asp in Pep_2_NN may have enhanced cell permeability as the amide functional groups have been reported to increase membrane permeability.[87] Furthermore the difference in the arrangement of amino residues within the cyclic ring of Pep_2_NN could have caused the knotting effect. The major cause of the knotting effect is the arrangement of the sterically demanding amino acid residues holding the C-terminal tail above and below the ring (Figure 21).

Compounds with lower MIC require low concentration to successfully kill the Mycobacterium. The Pep_2_NNA isomers behaved differently and Pep_2_NNA_conf2 had better activity during the first lag. Pep_2_NN and Pep_2_NNA_conf2 lost activity in the second week of bacterial incubation while that of Pep_2_NNA_conf1 decreased. The results are represented in Table 16 below.

Table 16 The biological activity results of Pep_2_NN and the Pep_2_NNA conformers. RIF (rifampicin), INH (isoniazid) and EMB (ethambutol) were used as control.

Entry	Compound	MIC_{99} (µg/ml) 7 days	MIC_{99} (µg/ml) 14 days
1	Pep_2_NNA_conf1	79.0	316
2	Pep_2_NNA_conf2	39.5	> 632

Entry	Compound	MIC_{99} (µg/ml) 7 days	MIC_{99} (µg/ml) 14 days
3	Pep_2_NN	9.87	> 632
4	RIF	0.008	
5	INH	0.054	
6	EMB	12.5	

The peptide derivatives had no restrictions in entering and killing the Mycobacterium during the first lag. Arginine was found to play an important role in binding to the ClpC1, however it was successfully replaced by lysine (Pep_2_NN and Pep_2_NNA isomers) as the derivatives were active against the Mycobacterium. These derivatives are also more active than the derivatives previously synthesized (Table 14).

The loss of activity of Pep_2_NN and Pep_2_NNA_conf2 during the second week may be attributed to the Mycobacterium getting stronger as it adapts to the environment. Interestingly, Pep_2_NNA_conf1 remained active (while Pep_2_NNA_conf2 lost activity) during the second week and this may be due to the structural shape of the isomers as they both have the same molecular mass. Pep_2_NNA_conf 1 was only 28% cyclized (72% was uncyclized) while Pep_2_NNA_conf2 and Pep_2_NN were 40% and > 95% cyclized, respectively. The presence of the uncyclized peptide may have played a role in keeping Pep_2_NNA_conf1 active. Pep_2_NN and Pep_2_NNA_conf2 behave similarly when compared to Pep_2_NNA_conf1 and therefore may have the same interaction with the protease and possibly due to a similar structural shape.

Pep_2_NN and Pep_2_NNA_conf2 have different sequences, therefore the arrangement of amino acids in the peptide sequence might not play a huge role, what matters could be the structural conformation.

4.1.2. Pep_Lys_NN

The bactericidal effect of Pep_Lys_NN was tested against various bacterial strains that included *E. coli*, *P. aeruginosa*, *S. aureus* and *B. subtilis* and the results are reported in Table

17. Pep_Lys_NN was active against the *B. subtilis* pathogen because it shares a similar caseinolytic protease to *M. tb* that is targeted by the lassomycin. *E. coli, P. aeruginosa* and *S. aureus* do not contain ClpC1 and were therefore not killed by the peptide. This is supported by the results obtained in a study by Gavrish, showing that *E. coli* and *S. aureus* (along with other organisms that do not share the ClpC1 enzyme) were not targeted by lassomycin.[2] This proves that lassomycin may be very selective in its target for the ClpC1. *B. subtilis* is found naturally in a human body but its caseinolytic protease and its AAA+ ATPases are non-essential for cell viability when compared to those found in the *M. tb*.[65] The bactericidal data for Pep_Lys_NN is shown in Table 17.

Table 17 Minimum Inhibition Concentration of Pep_Lys_NN against different organisms

		Minimum inhibitory concentration (µg/ml) for different organisms			
Compound	Starting concentration/ (µg/ml)	E.*coli* ATCC25922	*P. aeruginosa* ATCC 27853	*S. aureus* ATCC29913	*B. subtilis* ATCC 2002
Pep-Lys-NN	256	>256	>256	>256	256

Pep_Lys_NN, Pep_Lys_NNA and Pep_1_NN peptide derivatives were also tested against the *M. tb* using an Alamar blue assay; however they precipitated out in media. When the Alarmar blue dye was added to the samples, the color turned pink to indicate that the derivatives were inactive against the Mycobacterium (Figure 37). The Mycobacterium growth was milky and spread out, which was not expected. Therefore, the Alarmar blue assay may not be the best technique to test for the activity of the peptide against the Mycobacterium.

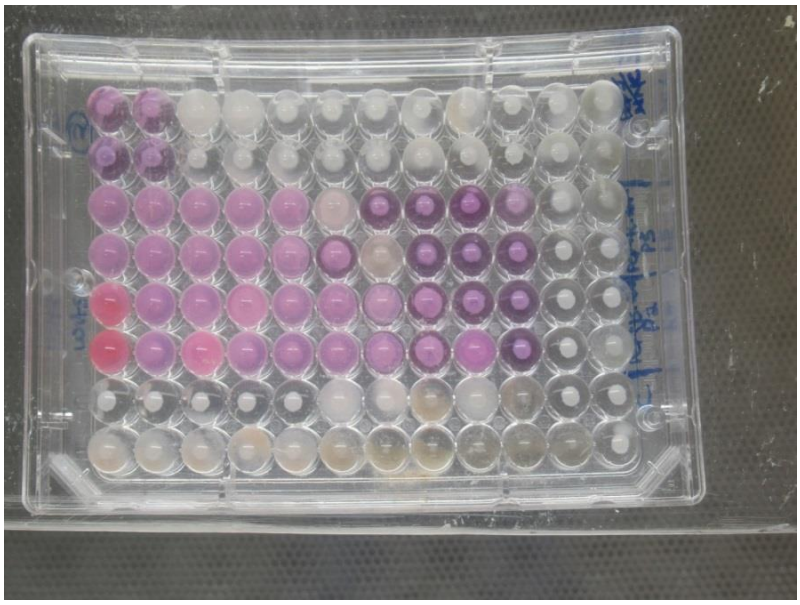


Figure 37 The Alarmar blue assays done on the peptide derivatives

CHAPTER 5

5.1 CONCLUSION AND FUTURE WORK

For all the peptide derivatives synthesized and discussed, the derivatives with the reverse sequence to the natural lassomycin peptide (-NN) seem to provide better results in terms of synthesis, purification and biological activity. Despite structural differences both groups (-NN and –NNA) show the ability to be active against *M. tb*.

The addition of the Cys amino acids to increase the lasso ring and replacing the lactam bond does not eliminate the peptide's ability to bind to the Mycobacterium and kill it. The ability of the derivatives to kill the Mycobacterium even in the presence of uncyclized peptide (Pep_2_NNA_conf1 and Pep_2_NNA_conf2) might suggest that more studies need to be done to understand the active conformation of the peptide and how it binds.

Replacing the Arg groups with the less basic Lys groups did not compromise the activity of the peptide (and might have elevated it) as one of the lysine- derivatives (Pep_2_NN) was able to kill the Mycobacterium with a concentration that is comparable to ethambutol.

The cationic peptide derivatives were successfully synthesized and one of the derivatives, Pep_Lys_NN was found to be active against the *B. subtilis* pathogen sharing a similar protease as the *M. tb*. Pep_Lys_NN shows a potential for selectivity against *M. tb* by being active against pathogens with a similar protease to the *M. tb.* This observation, supported by the study done by Gavrish *et al*[2], shows that lassomycin and its derivatives may have the ability to selectively target bacterial pathogens that have the ClpC1 ATPase. However, more work is needed to study the structure of the peptide and its derivatives.

The *N*- methylated amino acids were successfully incorporated into the peptide sequence; however, it was not successfully separated and purified. For future studies, modifications are to be done to improve the synthesis, as *N*-methylation plays an important role in making peptides stable against enzymatic degradation.

Comparing all the derivatives synthesized, it appears that the Pep_2_NN derivative gave better results from synthesis to biological testing. Therefore, the substitution of the arginine with the lysine residues has been a success. Future work involves 3D structure elucidation using NMR

spectroscopy to understand the activity of Pep_2_NN, after which further derivatives will be synthesized.

CHAPTER 6

EXPERIMENTAL PROCEDURE

6.1 Materials and Instrumentation

Fmoc protected amino acids, N,N,N′,N′-Tetramethyl-O-(1H-benzotriazol-1-yl)uronium hexafluorophosphate (HBTU), Hexafluorophosphate Azabenzotriazole Tetramethyl Uronium (HATU), Hydroxybenzotriazole (HOBt), Rink amide MBHA, Diisopropylethylamine (DIPEA), piperidine, Triisopropylsilane (TIS), formic acid, trifluoroacetic acid (TFA), Iodine, ascorbic acid, dichloromethane (DCM) which was dried upon distillation over calcium hydride, Dimethylformamide (DMF), methanol, acetonitrile, hexane, dimethyl sulfoxide (DMSO) and ether, Bromoacetic acid, diethyl ether, N,N'-Diisopropylcarbodiimide (DIC), thionyl chloride, chloroform ($CHCl_3$), 1,2-Ethanedithiol (EDT), acetic acid (AcOH), aluminium trichloride ($AlCl_3$), sodium hydrogen carbonate ($NaHCO_3$), magnesium sulphate ($MgSO_4$), triethylsilane, hexane, ethyl acetate, paraformaldehyde, *p*-toluenesulfonic acid, toluene and acetone. The chemicals were purchased from Dld Scientific, Sigma Aldrich and Radchem

6.2 Instrumentation

Synthesis:

Some of the peptide derivatives were synthesized automatically, using the automated Protein Technologies, Inc. PS-3TM Peptide Synthesizer.

Purification and analytical analysis:

All peptide derivatives synthesized were subjected to purification using semi-preparative HPLC which was carried out on an Agilent 1260 Infinity semi-preparative instrument via the reverse phase chromatography. A Phenomenex Kinetex XB-C18 column (5 µm, 100 Å, 250 mm × 21.2 mm) was used to separate the compounds with a flow rate of 15 ml/min. The compounds were detected at wavelengths of 215 nm and 254 nm. For the mobile phase, a two-buffer system consisting of 0.1 % formic acid/H_2O (v/v) (Buffer A) and 0.1 % formic acid/acetonitrile (v/v) (Buffer B) was utilized. The formic acid was used as an ion pairing agent.

The peptide derivatives were eluted using a gradient method of 5 – 95 % Buffer B in 10 min, unless stated otherwise.

A Thermo Scientific Dionex Ultimate 3000 UHPLC instrument coupled to a Bruker Compact Q-TOF mass spectrometer was used to analyse the results and determine purity. The compounds were separated using a Phenomenex C18 column (5 μm, 100 Å, 250 mm × 21.2 mm) and mass spectrometry analysis was done using a positive mode electrospray ionization source (ESI).

The melting points of the *N*-methylated Fmoc- amino acids were carried out on a Stuart SMP10 instrument and NMR spectra were acquired on a Bruker 300 MHz spectrometer to obtain the ^{1}H and ^{13}C Nuclear Magnetic Resonance (NMR) data, at room temperature. The NMR data was processed and analyzed using the MestreNova Software. The samples analyzed were dissolved in deuterated chloroform solvent.

6.3. Synthesis of the peptide derivatives

6.3.1 Synthesis of Pep_2_NNA

Automated peptide synthesis:

Pep_2_NNA was synthesized on a rink amide resin (0.100 g, 0.4 mmols/g) via the Fmoc solid phase peptide synthetic strategy. The resin was added into a PS-3TM Peptide Synthesizer reaction vessel. Each amino acid on the peptide sequence (0.2 M, 1.2 mmols) was weighed into a vial containing HBTU (0.19 M, 0.430 g). A stock solution of DIPEA (1 M, 500 ml) in DMF was prepared and used for coupling.

The process of coupling:

The Fmoc- protected rink amide resin was de-protected using 20 % piperidine in DMF (v/v) for 20 minutes and the resin was then washed with DMF (6 x 6 ml). To couple the amino acids, DIPEA (1 M, 6 ml) and HBTU were shaken together with the first amino acid (Fmoc-Ile-OH) in order to activate the OH group and make it into an active ester. The activated amino acid was then reacted with the rink amide resin. Nitrogen was gently bubbled to mix the reaction for 45 minutes.

To couple the second amino acid, 20% piperidine was used to deprotect the Fmoc-Ile-OH. HBTU and DIPEA were used to activate the OH of the newly entering amino acid (Fmoc-Asn(Trt)-OH) and the reaction was mixed for 45 minutes using nitrogen. In order to couple the other remaining amino acids, the same procedure was followed until the last amino acid, Fmoc-Cys(Trt)-OH (cysteine), was coupled.

Loading capacity:

A few resin beads (~10 mg) were removed from the reaction vessel after the coupling of the first amino acid and left to dry. A solution of 20% piperidine in DMF was added to the dried resin beads (~5 mg) and left to stand for 20 minutes. 100 µl of the solution was transferred into a tube containing 10 ml DMF.

A UV-vis spectrophotometer was set to zero using 2 ml of DMF (blank). A cuvet containing a sample solution was then placed in the sample cell and the absorbance was observed at the wavelength of 301 nm three times. This procedure was done in triplicate and the average loading capacity was then calculated to be 0.4 mmol/g.

Calculations:

Loading capacity = 101 (A) / 7.8 (w), where A is the absorbance (Abs) and w is the weight of the resin (mg), was used to determine the Loading capacity.

Table 18 Absorbances used to determine loading test of Pep_2_NNA

Entry No.	Mass/ mg	Absorbance/ (Abs)	Average Absorbance/ (Abs)
1	9.8	0.2954	0.2956
		0.2956	
		0.2958	
2	5.5	0.1822	0.1830
		0.1834	
		0.1835	

The loading capacity obtained for this derivative was found to be 0.4 mmol/g.

Cyclization:

The peptide was cyclized using a solution of iodine in DMF/H_2O (4:1), the mass of the peptide was determined using the weight of the resin and the loading capacity. The mass of the iodine used for cyclization was 0.102 g as determined by the calculations: Loading capacity x 10 equivalence x resin mass (0.100 g) x iodine Mr (253.81 g/mol) = 0.1015 g. To cyclize the peptide a disulfide bridge was formed through the cysteine-cysteine side chains. The iodine was added to 8 ml DMF and 2 ml H_2O and gently shaken with the resin for 40 minutes. The resin was then washed with DMF (2 x 10 ml), followed by 2% ascorbic acid in DMF until the golden brown color in the washing solvent was no longer observed, lastly the resin was thoroughly washed and dried with DCM.

Cleavage of the peptide from the resin linker and the permanent protecting groups:

The resin bound peptide was removed from the peptide synthesizer, thoroughly washed and dried with DCM; then transferred to a 50 ml tube containing a 94% TFA cleavage solution (with 2.5% EDT, 2.5% H_2O and 1% TIS), the mixture was shaken for 3 hours. The reaction mixture was then filtered and cold ether was then added to the supernatant. The product was obtained as a white precipitate after centrifuging and washing three times with cold ether. The crude product was then filtered to determine yield and was characterized using a mass spectrometer.

6.3.2 Synthesis of other peptide derivatives

6.3.2.1. Pep_2_NN, Pep_2_NNA, Pep_Lys_NN, Pep_Lys_NNA, Pep_1_NN and Pep_1_NNA

All the peptides were also synthesized in a similar manner, but manually. To ensure complete aminoacylations, scale up of the amino acids (0.20 M, 2.4 mmol) and the DIPEA (1 M, 12 ml) and HATU (0.19 M, 0.87 g) were used. The coupling reaction times for all peptide derivatives synthesized manually were decreased to 2 x 30 min. The iodine cyclization times were increased to 3 hours.

6.3.2.2 Pep_1_NN_Lys

A similar synthetic method as the one mentioned above was used with the addition of HOBt as an additive. Table 19 below summarizes the data obtained for the derivatives.

Table 19 with characterization data, found mass, yield and colour for lassomycin derivatives

Peptide derivative	Found mass (mg)	% Yield	Color
Pep_2_NN	13.8	18.28	Golden brown crystals
Pep_2_NNA_conf1	3.9	5.16	Golden brown crystals with black traces
Pep_2_NNA_conf2	6.5	8.61	Golden brown crystals with black traces
Pep_1_NN	12.3	16	Off white
Pep_1_NNA	119.6	26	Off white
Pep_Lys_NN	29.5	37.67	Off white
Pep_Lys_NNA	54.1	69.09	Light yellow crystals
Pep_1_NN_Lys	7.9	9.14	Off white
Pep_1_NNA_Lys	-	-	-

Table 20 LCMS results for Pep_1_NN and Pep_1_NNA lassomycin derivatives

Derivative	% Purity	Mass (mg)	% Yield	Calculated Mass	Found Mass
Pep_1_NN	> 95	12.3	15	2086.1346	1044.0720 $[M+2H]^{2+}$
Pep_1_NNA	92	119.6	28	2087.1186	1044.5733 $[M+2H]^{2+}$

Table 21 LCMS results for Pep_2_NN and Pep_2_NNA derivatives

Compound	Calculated mass	Observed mass [Molecular ion]	Retention time (min)	Purity (%)
Pep_2_NNA_ conf1	1975.0947 $C_{88}H_{150}N_{24}O_{23}S_2$ Cyclized	495.0276 $[M + 4H]^{4+}$	8.99	28
	1977.0904 $C_{88}H_{152}N_{24}O_{23}S_2$ Uncyclized	660.0388 $[M + 3H]^{3+}$	7.38	72
Pep_2_NNA_ conf2	1975.0947 $C_{88}H_{150}N_{24}O_{23}S_2$ Cyclized	659.7071 $[M + 3H]^{3+}$	9.04	40
	1977.0904 $C_{88}H_{152}N_{24}O_{23}S_2$ Uncyclized	989.5577 $[M + 2H]^{2+}$	7.53 & 8.57	60
Pep_2_NN	1974.1100 $C_{88}H_{152}N_{26}O_{21}S_2$ Cyclized	988.0602 $[M + 2H]^{2+}$	7.86	> 95

Table 22 LCMS results for cationic lassomycin derivatives

Compound	Calculated mass	Observed mass [Molecular ion]	Retention time (min)	Purity (%)
Pep_Lys_NN	2048.1693 $C_{89}H_{158}N_{30}O_{21}S_2$ Cyclized	1025.0980, $[M + 2H]^{2+}$	3.49	90
Pep_Lys_NNA	2049.1533 $C_{89}H_{157}N_{29}O_{22}S_2$ Cyclized	684.0569, $[M + 3H]^{3+}$	3.92	**
	2051.1689 $C_{89}H_{159}N_{29}O_{22}S_2$ Uncyclized	1026.5924 $[M + 2H]^{2+}$	3.40	**
Pep_1_NN_Lys	2159.1905 $C_{89}H_{158}N_{38}O_{21}S_2$ Cyclized	730.4135, $[3M + Methanol]^{+}$	4.70	56
	2161.2062 $C_{89}H_{160}N_{38}O_{21}S_2$ Uncyclized	1081.6120, $[M + 2H]^{2+}$	3.60	43

**** Problems were encounted with UV data**

Table 23 LCMS results for N-methylated lassomycin derivatives

Compound	**Calculated Mass**	**Observed Mass [Molecular ion]**	**Retention Time (min)**
N-methylated Pep_2_NN	2044.1889 $C_{93}H_{161}N_{25}O_{22}S_2$ Cyclized	1023.1012, $[M + 2H]^{2+}$	10.11
N-methylated Pep_2_NNA	2003.1060 $C_{90}H_{154}N_{24}O_{23}S_2$ Cyclized	1002.5714, $[M + 2H]^{2+}$	9.97

6.3.2.3 *N*-methylated Pep_2_NN and *N*-methylated Pep_2_NNA.

To synthesize these *N*-methylated peptides, *N*-methylated amino acids are synthesized and incorporated into the peptide sequences. Ethyl (hydroxyimino)cyanoacetate (OxymaPure) was used to couple the *N*-methylated amino acids.

Synthesis of *N*-methylated amino acids:

For the synthesis of the 5-oxazolidinones, Fmoc- protected amino acids (5 mM, 15 mmol) were mixed with paraformaldehyde (0.3 M, 3 g) and *p*- toluenesulfonic acid (0.3 M, 300 mg) in 100 ml toluene. The mixture was refluxed overnight in a Dean-Stark setup at a temperature of 110°C. Thin Layer Chromatography (TLC), ($CHCl_3$/MeOH/AcOH 97.05:2:0.5), was used to monitor the reaction until the starting materials were no longer detected. Upon cooling, the solution was washed with saturated sodium hydrogen carbonate ($NaHCO_3$) to remove the excess acid and then dried over anhydrous magnesium sulfate ($MgSO_4$). The mixture was then concentrated *in vacuo* to give the crude product. In some cases re-crystallization was used to

purify the products. The amino acids that were *N*-methylated are the non-polar commercially obtained Fmoc- protected Val, Leu and Ala amino acids. HPLC-MS was used to analyze the results. The Val oxazolidinone was observed as yellow crystals, while Val and Ala were white crystals.

To synthesize the *N*-methylated amino acids from the 5-oxazolidinone precursors, triethylsilane (2 equiv) was added to a solution containing the 5-oxazolidinone (1 equiv) and aluminium trichloride (2 equiv) in dry DCM. The reaction was stirred overnight at room temperature and TLC (Ethyl acetate/hexane 1:3) was used to monitor the reaction until the starting materials were no longer detected. The mixture was then washed with 1 M hydrochloric acid (HCl) and the organic layer, containing the final product, was dried over anhydrous $MgSO_4$. The product was then concentrated *in vacuo* and solidified upon cooling. The crude products were purified by re-crystallization and characterization analysis was done using NMR spectroscopic analysis.

_N_-methylated Leucine:

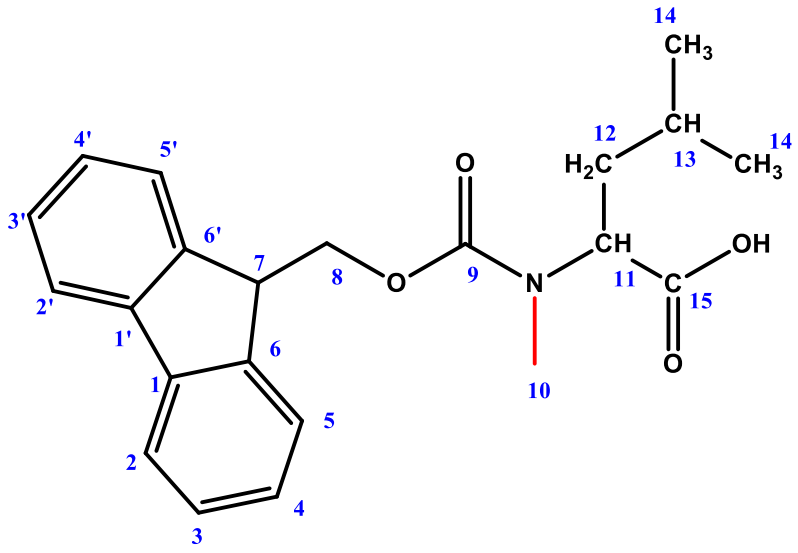


Figure 38 The structure of *N*-methylated Leucine

^{1}H NMR (300 MHz, $CDCl_3$) δ 10.14 (1H, s, OH), 7.76 (2H, m, J = 9.03 Hz, H2, H2'), 7.59 – 7. (2H, m, H5, H5'), 7.33 – 7.42 (4H, m, H3 ,H3'; H4, H4'), 4.94 (1H, t, J = 7.90, 7.90 Hz, H7), 4.46 (2H, d, J = 6.3Hz, H8), 4.27 (1H, t, J = 6.9 Hz, H11), 2.86 (3H, s, H10), 1.77 (1H, m, H13), 1.57 (2H, dd, J = 7.8, 4.9 Hz, H12), 0.94 (6H, m, , H14).

^{13}C NMR (300 MHz, $CDCl_3$) δ 170.0 (C-15); 157.3 (C-9); 148.9 (C-6); 147.7 (C-1); 127.94 (C-2); 127.97 (C-3); 125.0 (C-4); 120.3 (C-5); 67.8 (C-8); 56.9 (C-11); 47.2 (C-7), 37.2 (C-12), 30.3 (C-10); 24.9 (C-13) 21.3, (C-14)

***N*-methylated Valine:**

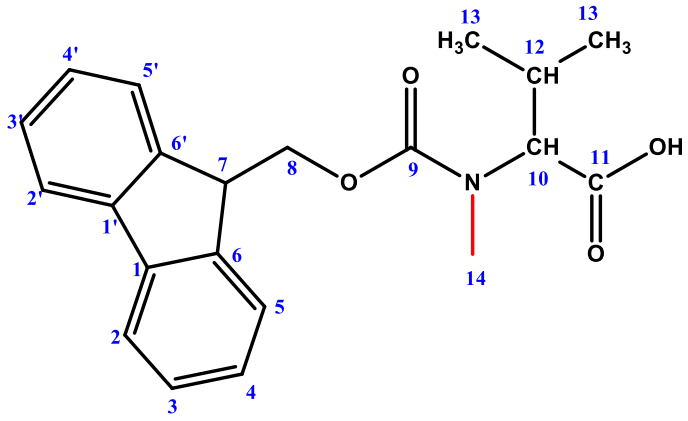


Figure 39 The structure of *N*-methylated Valine

^{1}H NMR (300 MHz, Chloroform-d) δ 7.76 (2H, d, J = 7.4 Hz, H2, H2'), 7.59 (2H, d, J = 5.0 Hz, H5, H5'), 7.24 – 7.44 (4H, m, H3, H3'; H4, H4'), 4.50 (2H, d, J = 6.7, 3.6Hz, H7), 4.28 (2H, d, *J* = 8.1 Hz, H8), 4.14 (H, d, J = 10.52, H10) 2.90 (3H, s, H14), 2.02 – 2.35 (1H, m, H12), 0.90 (6H, m, H13).

^{13}C NMR (300 MHz, $CDCl_3$) δ 143.8.0 (C-11); 141.4 (C-9); 127.7 (C-6); 127.1 (C-1); 124.9 (C-3); 180.0 (C-2); 76.58 (C-10); 67.9 (C-8); 47.3 (C-7); 27.4 (C-14); 19.7 (C-12)

N-methylated Alanine:

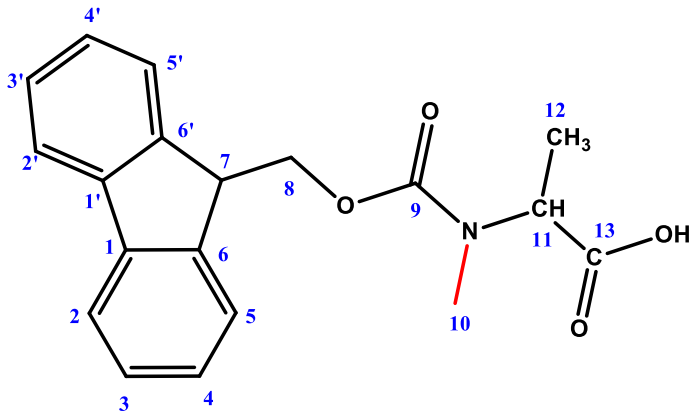


Figure 40 The structure of *N*-methylated Alanine

^{1}H NMR (300 MHz, $CDCl_3$) δ 8.68 (1H, s, OH), 7.76 (2H, d, *J* = 7.3 Hz, H2, H2'), 7.63 – 7.49 (2H, m, H5,H5'), 7.43 – 7.25 (4H, m, H3, H3'; H4, H4'), 4.91 (2H, d, *J* = 7.3 Hz, H8), 4.43 (1H, q, *J* = 17.5, 17.5, 10.4 Hz, H11), 4.26 (1H, dd, *J* = 14.3, 7.0 Hz, H7), 2.91 (3H, s, H10), 1.46 (3H, d, *J* = 7.3 Hz, H12).

^{13}C NMR (300 MHz, $CDCl_3$) δ 174.0 (C-13); 154.0 (C-9); 143.6 (C-6); 126.7 (C-3); 126.2 (C-2); 125.2 (C-4); 120.5 (C-5); 67.6 (C-8); 64.3 (C-11); 47.0 (C-7), 31.4 (C-10), 12.1 (C-12)

References

(1) World Health Organization. *Global Tuberculosis Report 2018*; 2018.

(2) Gavrish, E.; Sit, C. S.; Cao, S.; Kandror, O.; Spoering, A.; Peoples, A.; Ling, L.; Fetterman, A.; Hughes, D.; Bissell, A.; et al. Lassomycin ,a Ribosomally Synthesized Cyclic Peptide , Kills Mycobacterium Tuberculosis by Targeting the ATP-Dependent Protease ClpC1P1P2. *Chem. Biol.* **2014**, *21* (4), 509–518. https://doi.org/10.1016/j.chembiol.2014.01.014.

(3) Leung, C. C.; Chang, K. C.; Sun, H.-Y.; Daley, L. C. Mycobacterium Tuberculosis Complex http://www.antimicrobe.org/ms06.asp (accessed Dec 18, 2018).

(4) Wirth, T.; Hildebrand, F.; Allix-Béguec, C.; Wölbeling, F.; Kubica, T.; Kremer, K.; Van Soolingen, D.; Rüsch-Gerdes, S.; Locht, C.; Brisse, S.; et al. Origin, Spread and Demography of the Mycobacterium Tuberculosis Complex. *PLoS Pathog.* **2008**, *4* (9), e1000160. https://doi.org/10.1371/journal.ppat.1000160.

(5) Mostowy, S.; Inwald, J.; Gordon, S.; Martin, C.; Warren, R.; Kremer, K.; Cousins, D.; Behr, M. A. Revisiting the Evolution of Mycobacterium Bovis. *Society* **2005**, *187* (18), 6386–6395. https://doi.org/10.1128/JB.187.18.6386.

(6) Campen, R. L. PhD Thesis, Victoria University of Wellington, 2015.

(7) Rastogi, N.; Legrand, E.; Sola, C. The Mycobacteria: An Introduction to Nomenclature and Pathogenesis. *Rev. Sci. Tech.* **2001**, *20* (1), 21–54. https://doi.org/http://dx.doi.org/10.20506/rst.20.1.1265.

(8) Kaiser, G. 2.3C: The Acid-Fast Cell Wall https://bio.libretexts.org/Bookshelves/Microbiology/Book%3A_Microbiology_(Kaiser)/Unit_1%3A_Introduction_to_Microbiology_and_Prokaryotic_Cell_Anatomy/2%3A_The_Prokaryotic_Cell_-_Bacteria/2.3%3A_The_Peptidoglycan_Cell_Wall/2.3C%3A_The_Acid-Fast_Cell_Wall (accessed Feb 15, 2019).

(9) Hett, E. C.; Rubin, E. J. Bacterial Growth and Cell Division: A Mycobacterial Perspective. *Microbiol. Mol. Biol. Rev.* **2008**, *72* (1), 126–156.

https://doi.org/10.1128/MMBR.00028-07.

(10) Silhavy, T. J.; Kahne, D.; Walker, S. The Bacterial Cell Envelope. *Cold Spring Harb. Perspect. Biol.* **2010**, *2* (5), 1–16. https://doi.org/10.1101/cshperspect.a000414.

(11) Lowery, C. J.; Snelling, W. J.; Dooley, J. S. G.; Talip, B. A.; Sleator, R. D. An Update on Global Tuberculosis (TB). *Infect. Dis. Res. Treat.* **2013**, *6*, 39–50. https://doi.org/10.4137/idrt.s11263.

(12) Draper, P. The Walls of Mycobacterium Lepraemurium: Chemistry and Ultrastructure. *J. Gen. Microbiol.* **1971**, *69* (3), 313–324. https://doi.org/10.1099/00221287-69-3-313.

(13) Cook, G. M.; Berney, M.; Gebhard, S.; Heinemann, M.; Robert, A.; Danilchanka, O.; Niederweis, M. Physiology of Mycobacteria. *Adv. Microb. Physiol.* **2009**, *55*, 81–182. https://doi.org/10.1016/S0065-2911(09)05502-7.Physiology.

(14) Starck, J.; Kallenius, G.; Marklund, B.-I.; Andersson, D. I.; Thomas, A. Comparative Proteome Analysis of Mycobacterium Tuberculosis Grown under Aerobic and Anaerobic Conditions. *Microbiology* **2004**, *150*, 3821–3829. https://doi.org/10.1099/mic.0.27284-0.

(15) Reichlen, M. J.; Leistikow, R. L.; Scobey, M. S.; Born, S. E. M.; Voskuil, M. I. Anaerobic Mycobacterium Tuberculosis Cell Death Stems from Intracellular Acidification Mitigated by the DosR Regulon. *J. Bacteriol.* **2017**, *199* (23), 1–12. https://doi.org/10.1128/JB.00320-17.

(16) Centres for Diesease Control and Prevention. Transmission and pathogenesis of tuberculosis. https://www.cdc.gov/tb/education/corecurr/pdf/chapter2.pdf (accessed Jun 18, 2019).

(17) Mallozi, J. Tuberculosis: An Airborne Disease. *UN Chron.* **1998**, *5* (2), 73.

(18) Lee, J. Y. Diagnosis and Treatment of Extrapulmonary Tuberculosis. *Tuberculosis and Respiratory Diseases*. April 2015, pp 47–55. https://doi.org/10.4046/trd.2015.78.2.47.

(19) Semenya, S. S.; Maroyi, A. Medicinal Plants Used for the Treatment of Tuberculosis by Bapedi Traditional Healers in Three Districts of the Limpopo Province, South Africa. *Afr. J. Tradit. Complement. Altern. Med.* **2013**, *10* (2), 316–323.

https://doi.org/10.4314/ajtcam.v10i2.17.

(20) Mohajan, H. K. Tuberculosis Is a Fatal Disease Among Some Developing Countries of the World. *Am. J. Infect. Dis. Microbiol.* **2015**, *3* (1), 18–31. https://doi.org/10.12691/ajidm-3-1-4.

(21) Harris, P. W. R.; Cook, G. M.; Leung, I. K. H.; Brimble, M. A. An Efficient Chemical Synthesis of Lassomycin Enabled by an On-Resin Lactamisation-Off-Resin Methanolysis Strategy and Preparation of Chemical Variants. *Aust. J. Chem.* **2017**, *70* (2), 172–183. https://doi.org/10.1071/CH16499.

(22) Murray, J. F. A Century of Tuberculosis. *Am. J. Respir. Crit. Care Med.* **2004**, *169*, 1181–1186. https://doi.org/10.1164/rccm.200402-140OE.

(23) Badri, M.; Wilson, D.; Wood, R. Effect of Highly Active Antiretroviral Therapy on Incidence of Tuberculosis in South Africa: A Cohort Study. *Lancet* **2002**, *359* (9323), 2059–2064. https://doi.org/10.1016/S0140-6736(02)08904-3.

(24) de Olalla, P. G.; Orcau, A.; Fina, L.; Moreno, A.; del Baño, L.; Caylà, J. A.; Millet, J.-P. Factors That Influence Current Tuberculosis Epidemiology. *Eur. Spine J.* **2012**, *22* (S4), 539–548. https://doi.org/10.1007/s00586-012-2334-8.

(25) Fitch, L. E. PhD Thesis, Boston University, 2015.

(26) Parish, T. Targeting Mycobacterial Proteolytic Complexes with Natural Products. *Chem. Biol.* **2014**, *21* (4), 437–438. https://doi.org/10.1016/j.chembiol.2014.04.002.

(27) Lee, H.; Suh, J. W. Anti-Tuberculosis Lead Molecules from Natural Products Targeting Mycobacterium Tuberculosis ClpC1. *Journal of Industrial Microbiology and Biotechnology*. Springer Berlin Heidelberg 2016, pp 205–212. https://doi.org/10.1007/s10295-015-1709-3.

(28) Gandhi, N. R.; Moll, A.; Sturm, A. W.; Pawinski, R.; Govender, T.; Lalloo, U.; Zeller, K.; Andrews, J. Extensively Drug-Resistant Tuberculosis as a Cause of Death in Patients Co-Infected with Tuberculosis and HIV in a Rural Area of South Africa. *Lancet* **2006**, *119*, 1575–1580. https://doi.org/10.1016/S0140-6736(06)69573-1.

(29) Thapa, G.; Pant, N. D.; Khatiwada, S.; Shrestha, B. Drug Susceptibility Patterns of the

Mycobacterium Tuberculosis Isolated from Previously Treated and New Cases of Pulmonary Tuberculosis at German-Nepal Tuberculosis Project Laboratory , Kathmandu ,. *Antimicrob. Resist. Infect. Control* **2016**, 1–7. https://doi.org/10.1186/s13756-016-0129-0.

(30) (The Government of the Hong Kong Special Administrative Region), https://www.info.gov.hk/tb_chest/contents/c121.htm (accessed May 23, 2019).

(31) Caño-Muñiz, S.; Anthony, R.; Niemann, S.; Alffenaar, J. C. New Approaches and Therapeutic Options for Mycobacterium Tuberculosis in a Dormant State. *Clin. Microbiol. Rev.* **2017**, *31* (1), 1–13. https://doi.org/10.1128/CMR.00060-17.

(32) Barberis, I.; Bragazzi, N. L.; Galluzzo, L.; Martini, M. The History of Tuberculosis: From the First Historical Records to the Isolation of Koch's Bacillus. *J. Prev. Med. Hyg.* **2017**, *58* (1), E9–E12.

(33) Jena, L.; Nayak, T.; Deshmukh, S.; Wankhade, G.; Waghmare, P.; Harinath, B. C. Isoniazid with Multiple Mode of Action on Various Mycobacterial Enzymes Resulting in Drug Resistance. *J. Infect. Dis. Ther.* **2016**, *4* (5). https://doi.org/10.4172/2332-0877.1000297.

(34) Zink, A. R.; Sola, C.; Reischl, U.; Grabner, W.; Rastogi, N.; Wolf, H.; Nerlich, A. G. Characterization of Mycobacterium Tuberculosis Complex DNAs from Egyptian Mummies by Spoligotyping. *Am. Soc. Microbiol.* **2003**, *41* (1), 359–367. https://doi.org/10.1128/JCM.41.1.359.

(35) Good, M.; Bakker, D.; Duignan, A.; Collins, D. M. The History of In Vivo Tuberculin Testing in Bovines: Tuberculosis, a "One Health" Issue. *Front. Vet. Sci.* **2018**, *5* (59). https://doi.org/10.3389/fvets.2018.00059.

(36) Johnson, L. F.; Dorrington, R. E.; Moolla, H. HIV Epidemic Drivers in South Africa: A Model-Based Evaluation of Factors Accounting for Inter-Provincial Differences in HIV Prevalence and Incidence Trends. *South. Afr. J. HIV Med.* **2017**, *18* (1), 1–9. https://doi.org/10.4102/sajhivmed.v18i1.695.

(37) World Health Organization. *Global Tuberculosis Report 2017: MDR/RR-TB Update*; 2017.

(38) (Worldometers). World Population Clock http://www.worldometers.info/world-population/ (accessed Dec 24, 2018).

(39) TBFACTS.ORG https://www.tbfacts.org/tb-statistics-south-africa/ (accessed May 29, 2019).

(40) Dye, C.; Lönnroth, K.; Jaramillo, E.; Williams, B. G.; Raviglione, M. Trends in Tuberculosis Incidence and Their Determinants in 134 Countries. *Bull. World Health Organ.* **2009**, *87* (9), 683–691. https://doi.org/10.2471/BLT.08.058453.

(41) Walzl, G.; Mcnerney, R.; Plessis, N.; Bates, M.; Mchugh, T. D.; Chegou, N. N.; Zumla, A. Series Tuberculosis 2 Tuberculosis: Advances and Challenges in Development of New Diagnostics and Biomarkers. *Lancet Infect. Dis.* **2018**, *3099* (18), 1–12. https://doi.org/10.1016/S1473-3099(18)30111-7.

(42) Yon Ju Ryu, M. D. Diagnosis of Pulmonary Tuberculosis: Recent Advances. *J. Indian Med. Assoc.* **2013**, *111 (5)*, 332–336. https://doi.org/10.4046/trd.2015.78.2.64.

(43) Eddabra, R.; Ait Benhassou, H. Rapid Molecular Assays for Detection of Tuberculosis. *Pneumonia* **2018**, *10* (1), 4. https://doi.org/10.1186/s41479-018-0049-2.

(44) (Medical device exhibition), http://www.medicalexpo.com/prod/bd/product-71022-622517.html (accessed Mar 12, 2019).

(45) Couriel, J. Assessment of the Child with Recurrent Chest Infections. *Br. Med. Bull.* **2002**, *61* (1), 115–132. https://doi.org/10.1093/bmb/61.1.115.

(46) Getahun, H.; Sculier, D.; Sismanidis, C.; Grzemska, M.; Raviglione, M. Prevention, Diagnosis, and Treatment of Tuberculosis in Children and Nothers: Evidence for Action for Maternal, Neonatal, and Child Health Services. *J. Infect. Dis.* **2012**, *205* (SUPPL. 2). https://doi.org/10.1093/infdis/jis009.

(47) Santosa, G. Diagnosis of Pulmonary Tuberculosis in Children. *Paediatr. Indones.* **2017**, *15* (11–12), 286. https://doi.org/10.14238/pi15.11-12.1975.286-96.

(48) Kwan, B. C. H.; Yu, Y.; Goldberg, H. A Case of Tuberculosis in a Pregnant Woman and Review of Current Literature. *Obstet. Med.* **2010**, *3* (4), 161–163. https://doi.org/10.1258/om.2010.100008.

(49) Patrick, G. L. *An Introduction to Medicinal Chemistry*, 5th ed.; Oxford University Press, 2013.

(50) Yadav, K.; Prakash, S. Tuberculosis: An Airborne Disease. *Glob. J. Microbiol. Res.* **1998**, *5* (5), 225–243.

(51) (Bacille de Calmette-Guérin, or BCG Vaccine for Tuberculosis), http://activehistory.ca/2015/03/bacille-de-calmette-guerin-or-bcg-vaccine-for-tuberculosis/ (accessed Mar 12, 2019).

(52) (Optional Vaccines for Infants in India), http://www.babycareforyou.com/2014/03/.

(53) Smith, I. Mycobacterium Tuberculosis Pathogenesis and Molecular Determinants of Virulence. *Clin. Microbiol. Rev.* **2003**, *16* (3), 463–496. https://doi.org/10.1128/CMR.16.3.463.

(54) Kwiatkowska, B.; Maslinska, M.; Przygodzka, M.; Dmowska-Chalaba, J.; Dabrowska, J.; Sikorska-Siudek, K. Immune System as a New Therapeutic Target for Antibiotics. *Adv. Biosci. Biotechnol.* **2013**, *04* (04), 91–101. https://doi.org/10.4236/abb.2013.44A013.

(55) Xavier, A. S.; Lakshmanan, M. Delamanid: A New Armor in Combating Drug-Resistant Tuberculosis. *J. Pharmacol. Pharmacother.* **2014**, *5* (3), 222–224. https://doi.org/10.4103/0976.

(56) Rana, F. Rifampicin- An Overview. *Int. J. Res. Pharm. Chem.* **2013**, *3* (1), 83–87.

(57) Nath, H.; Ryoo, S. First– and Second–Line Drugs and Drug Resistance. In *Tuberculosis - Current Issues in Diagnosis and Management*; InTech, 2013. https://doi.org/10.5772/54960.

(58) Anastasia S. Kolyva; Karakousis, P. C. Old and New TB Drugs: Mechanisms of Action and Resistance. In *Understanding Tuberculosis - New Approaches to Fighting Against Drug Resistance*; InTech, 2012. https://doi.org/10.5772/30992.

(59) (National Institute of Allergy and Infectious Diseases), https://www.niaid.nih.gov/diseases-conditions/tbdrugs (accessed May 29, 2019).

(60) Arbex, M. A.; Varella, M. de C. L.; Siqueira, H. R. de; Mello, F. A. F. de. Antituberculosis Drugs: Drug Interactions, Adverse Rffects, and Use in Special Situations. *J. Bras. Pneumol.* **2010**, *36* (5), 641–656. https://doi.org/10.1590/s1806-37132010000500017.

(61) WHO Guideline. Ethambutol Efficacy and Toxicity : Literature Review and Recommendations for Daily and Intermittent Dosage in Children. *WHO Bull.* **2006**, 1–76.

(62) Momekov, G.; Ferdinandov, D.; Voynikov, Y.; Stavrakov, G. Pyrazinamide – Pharmaceutical, Biochemical and Pharmacological Properties and Reappraisal of Its Role in the Chemotherapy of Tuberculosis. *Int. J. Pharm. Sci.* **2014**, *61* (May), 38–66.

(63) Malik, I. T.; Brötz-Oesterhelt, H. Conformational Control of the Bacterial Clp Protease by Natural Product Antibiotics. *Nat. Prod. Rep.* **2017**, *34* (7), 815–831. https://doi.org/10.1039/C6NP00125D.

(64) Lupoli, T. J.; Vaubourgeix, J.; Burns-Huang, K.; Gold, B. Targeting the Proteostasis Network for Mycobacterial Drug Discovery. *ACS Infect. Dis.* **2018**, *4* (4), 478–498. https://doi.org/10.1021/acsinfecdis.7b00231.

(65) Culp, E.; Wright, G. D. Bacterial Proteases, Untapped Antimicrobial Drug Targets. *Journal of Antibiotics*. Nature Publishing Group April 30, 2017, pp 366–377. https://doi.org/10.1038/ja.2016.138.

(66) Zhang, S.; Chen, J.; Shi, W.; Cui, P.; Zhang, J.; Cho, S.; Zhang, W.; Zhang, Y. Mutation in ClpC1 Encoding an ATP-Dependent ATPase Involved in Protein Degradation Is Associated with Pyrazinamide Resistance in Mycobacterium Tuberculosis. *Emerg. Microbes Infect.* **2017**, *6* (1), 1–2. https://doi.org/10.1038/emi.2017.1.

(67) Nhieu, A. J. PhD Thesis, University of Toronto, 2012.

(68) Schmitt, E. K.; Riwanto, M.; Sambandamurthy, V.; Roggo, S.; Miault, C.; Zwingelstein, C.; Krastel, P.; Noble, C.; Beer, D.; Rao, S. P. S.; et al. The Natural Product Cyclomarin Kills Mycobacterium Tuberculosis by Targeting the ClpC1 Subunit of the Caseinolytic Protease. *Angew. Chemie Int. Ed.* **2011**, *50* (26), 5889–5891. https://doi.org/10.1002/anie.201101740.

(69) Lear, S.; Munshi, T.; Hudson, A. S.; Hatton, C.; Clardy, J.; Mosely, J. A.; Bull, T. J.; Sit, C. S.; Cobb, S. L. Total Chemical Synthesis of Lassomycin and Lassomycin-Amide. *Org. Biomol. Chem.* **2016**, *14* (19), 4534–4541. https://doi.org/10.1039/C6OB00631K.

(70) Alessandra, V. R.; Souza, B. M. De; Marcia, P.; Cabrera, S.; Dias, N. B.; Gomes, P. C.; Ruggiero, J.; Stabeli, R. G.; Palma, M. S. The EEffects of the C-Terminal Amidation of Mastoparans on Their Biological Actions and Interactions with Membrane-Mimetic Systems. *Biochim. Biophisica Acta* **2014**, *1838* (10), 2357–2368. https://doi.org/10.1016/j.bbamem.2014.06.012.

(71) Vijayadas, K. N.; Nair, R. V; Gawade, R. L.; Kotmale, A. S.; Prabhakaran, P.; Gonnade, R. G.; Puranik, V. G.; Rajamohanan, P. R.; Sanjayan, G. J. Ester vs. Amide on Folding: A Case Study with a 2-Residue Synthetic Peptide. *Org. Biomol. Chem.* **2013**, *11* (48), 8348–8356. https://doi.org/10.1039/c3ob41967c.

(72) N. Jisha, V.; B. Smitha, R.; Pradeep, S.; Sreedevi, S.; N. Unni, K.; Sajith, S.; Priji, P.; Sarath Josh, M.; Benjamin, S. Versatility of Microbial Proteases. *Adv. Enzym. Res.* **2013**, *01* (03), 39–51. https://doi.org/10.4236/aer.2013.13005.

(73) Mogemark, M. PhD Thesis, Umeå University, 2005.

(74) Pedersen, S. L.; Tofteng, A. P.; Malik, L.; Jensen, K. J. Microwave Heating in Solid-Phase Peptide Synthesis. *Chem. Soc. Rev.* **2012**, *41* (5), 1826–1844. https://doi.org/10.1039/c1cs15214a.

(75) Isidro-Llobet, A.; Álvarez, M.; Albericio, F. Amino Acid-Protecting Groups. *Chem. Rev.* **2009**, *109* (6), 2455–2504. https://doi.org/10.1021/cr800323s.

(76) Palomo, J. M. Solid-Phase Peptide Synthesis: An Overview Focused on the Preparation of Biologically Relevant Peptides. *RSC Adv.* **2014**, *4*, 32658–32672. https://doi.org/10.1039/C4RA02458C.

(77) Kamber, B.; Hartmann, A.; Eisler, K.; Riniker, B.; Rink, H.; Sieber, P.; Rittel, W. The Ssynthesis of Cystine Peptides by Iodine Oxidation of S-Tritylcysteine and S-Acetamidomethylcycsteine Peptides. *Chem. Informationsd.* **1980**, *11* (36), 899–915. https://doi.org/10.1002/chin.198036312.

(78) Elsaid, K. PhD Thesis, University of Rhode Island, 2001.

(79) Busick, A. PhD Thesis, University of Arkansas, 2011.

(80) Luna, O.; Gomez, J.; Cárdenas, C.; Albericio, F.; Marshall, S.; Guzmán, F. Deprotection Reagents in Fmoc Solid Phase Peptide Synthesis: Moving Away from Piperidine? *Molecules* **2016**, *21* (11), 1542. https://doi.org/10.3390/molecules21111542.

(81) Torre, B. G. De; Marcos, M. A.; Eritja, R.; Albericio, F. "Solid-Phase Peptide Synthesis Using N. **2002**, *338*, 331–338.

(82) Bacsa, B.; Horváti, K.; Bõsze, S.; Andreae, F.; Kappe, C. O. Solid-Phase Synthesis of Difficult Peptide Sequences at Elevated Temperatures: A Critical Comparison of Microwave and Conventional Heating Technologies. *J. Org. Chem.* **2008**, *73* (19), 7532–7542. https://doi.org/10.1021/jo8013897.

(83) Varray, S.; Werbitzky, O.; Zeiter, T. On-Resin Peptide Cyclization. US 7,994,280 B2, 2011.

(84) Teixidó, M.; Albericio, F.; Giralt, E. Solid-Phase Synthesis and Characterization of N-Methyl-Rich Peptides. *J. Pept. Res.* **2008**, *65* (2), 153–166. https://doi.org/10.1111/j.1399-3011.2004.00213.x.

(85) Zhang, S.; Govender, T.; Norström, T.; Arvidsson, P. I. An Improved Synthesis of Fmoc- N -Methyl-α-Amino Acids. *J. Org. Chem.* **2005**, *70* (17), 6918–6920. https://doi.org/10.1021/jo050916u.

(86) Wade, J. D.; Bedford, J.; Sheppard, R. C.; Tregear, G. W. DBU as an N - Alpha-Deprotecting Reagent for the Fluorenylmethoxycarbonyl Group in Continuous Flow Solid-Phase Peptide Synthesis. *Pept. Res.* **1991**, *4* (3), 194–199. https://doi.org/10.1214/10-AOAS335.

(87) Walensky, L. D.; Bird, G. H. Hydrocarbon-Stapled Peptides: Principles, Practice, and Progress. *J. Med. Chem.* **2014**, *57* (15), 6275–6288. https://doi.org/10.1021/jm4011675.

Appendix:

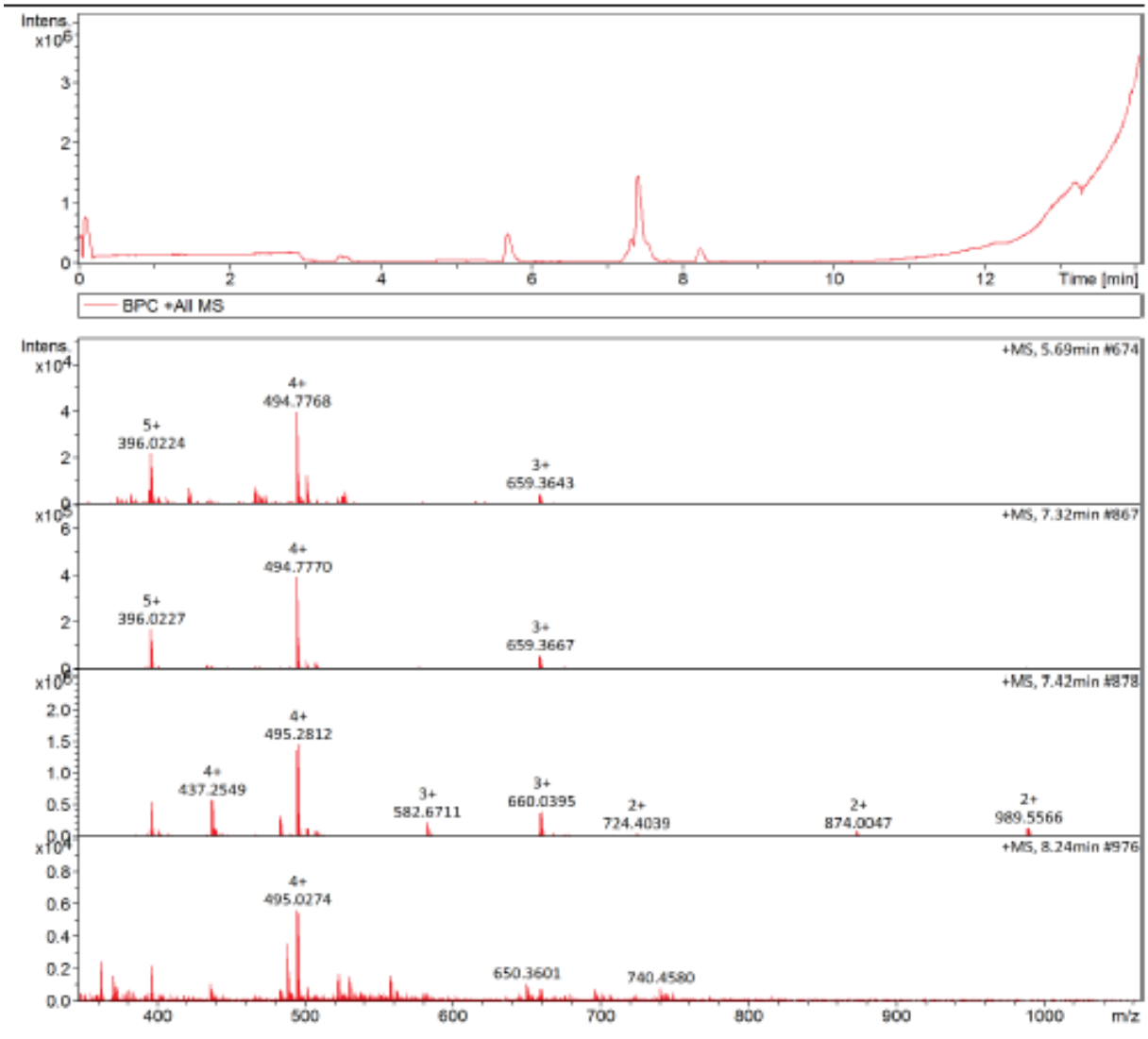
.

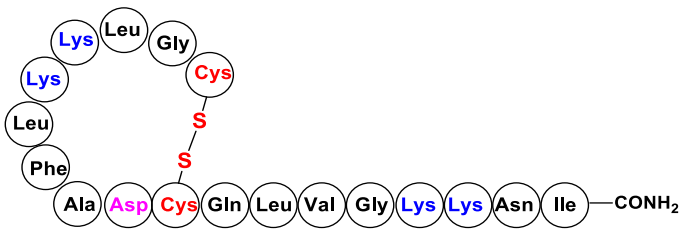
Analysis Info

Analysis Name	D:\Data\Runs\Ntombi\Pep2nna_05\Prep_HPLC\Pep-2-nna-05-P1(purer)_RE1_01_6757.d	Acquisition Date	11/30/2017 7:37:34 AM
Method	Wits HPLC Mid MS 100-3000 pos.m	Operator	Refilwe Moepya
Sample Name	Pep-2-nna-05-P1(purer)	Instrument	compact 8255754.20116
Comment			

Acquisition Parameter

Source Type	ESI	Ion Polarity	Positive	Set Nebulizer	1.8 Bar
Focus	Not active	Set Capillary	4500 V	Set Dry Heater	220 °C
Scan Begin	100 m/z	Set End Plate Offset	-500 V	Set Dry Gas	9.0 l/min
Scan End	3000 m/z	Set Charging Voltage	2000 V	Set Divert Valve	Waste
		Set Corona	0 nA	Set APCI Heater	0 °C





Pep_2_NNA

Figure 41 LC-MS of Pep_2_NNA_Conf1

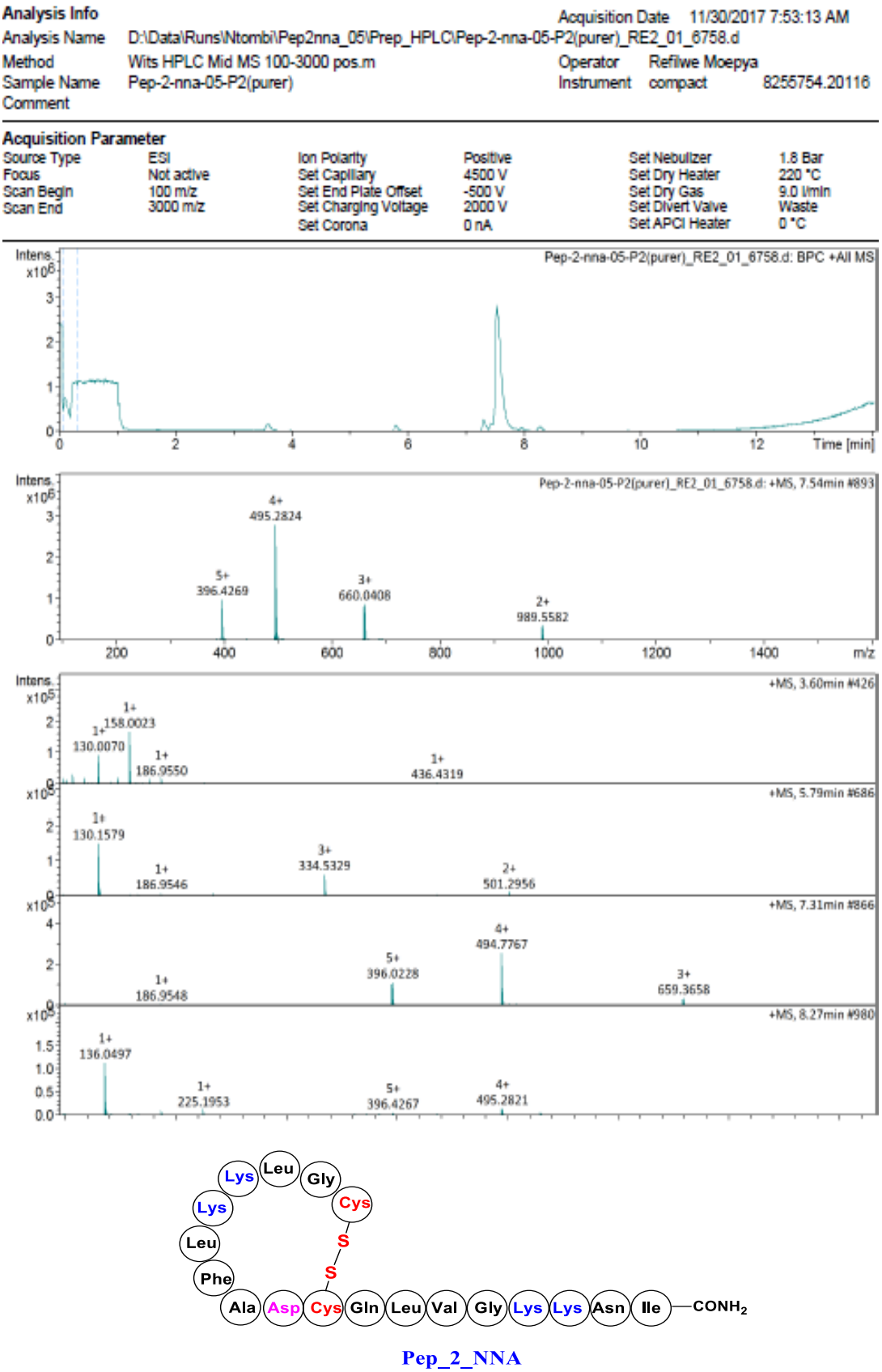


Figure 42 LC-MS of Pep_2_NNA_Conf2

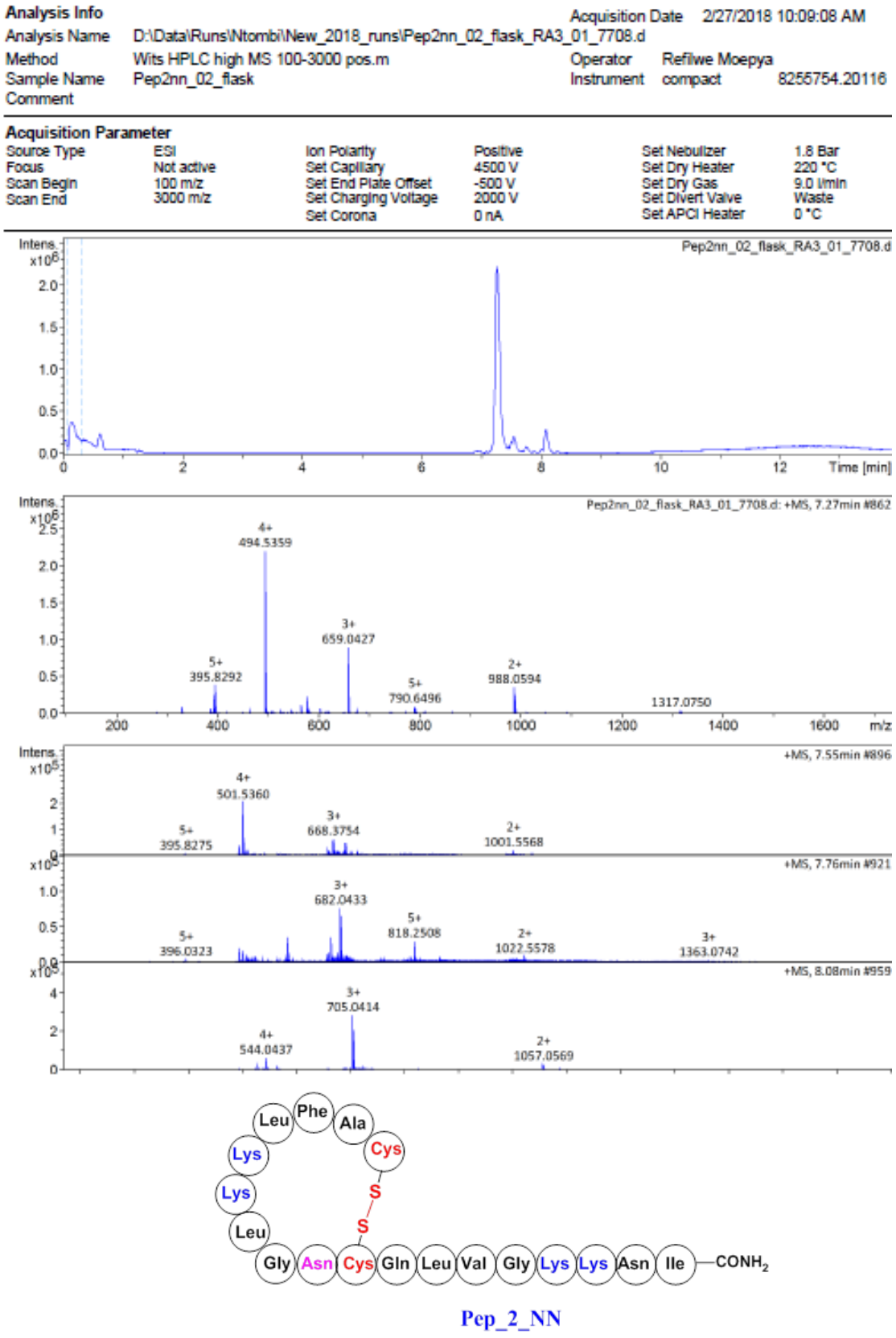
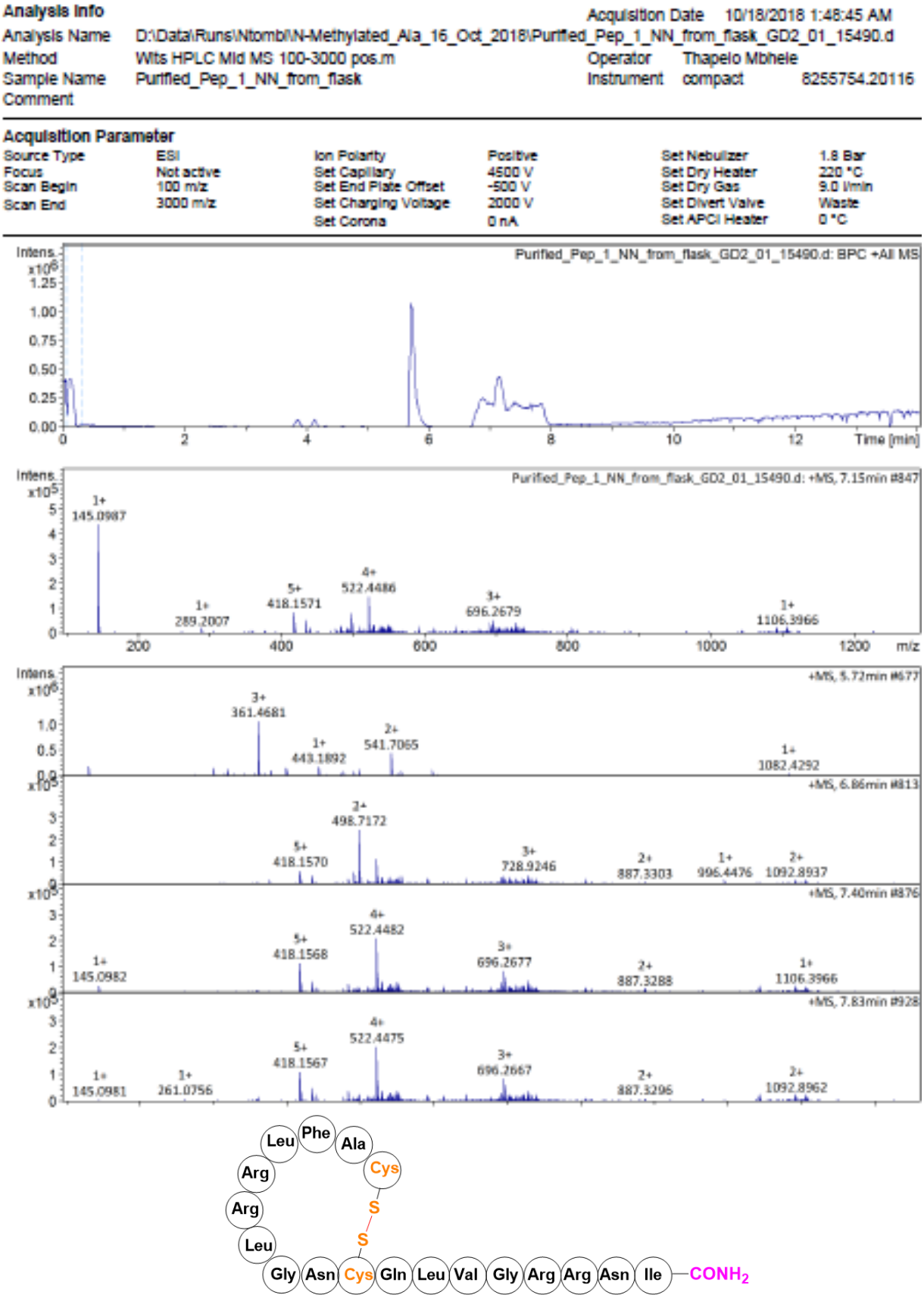


Figure 43 LC-MS of Pep_2_NN



Pep_1_NN

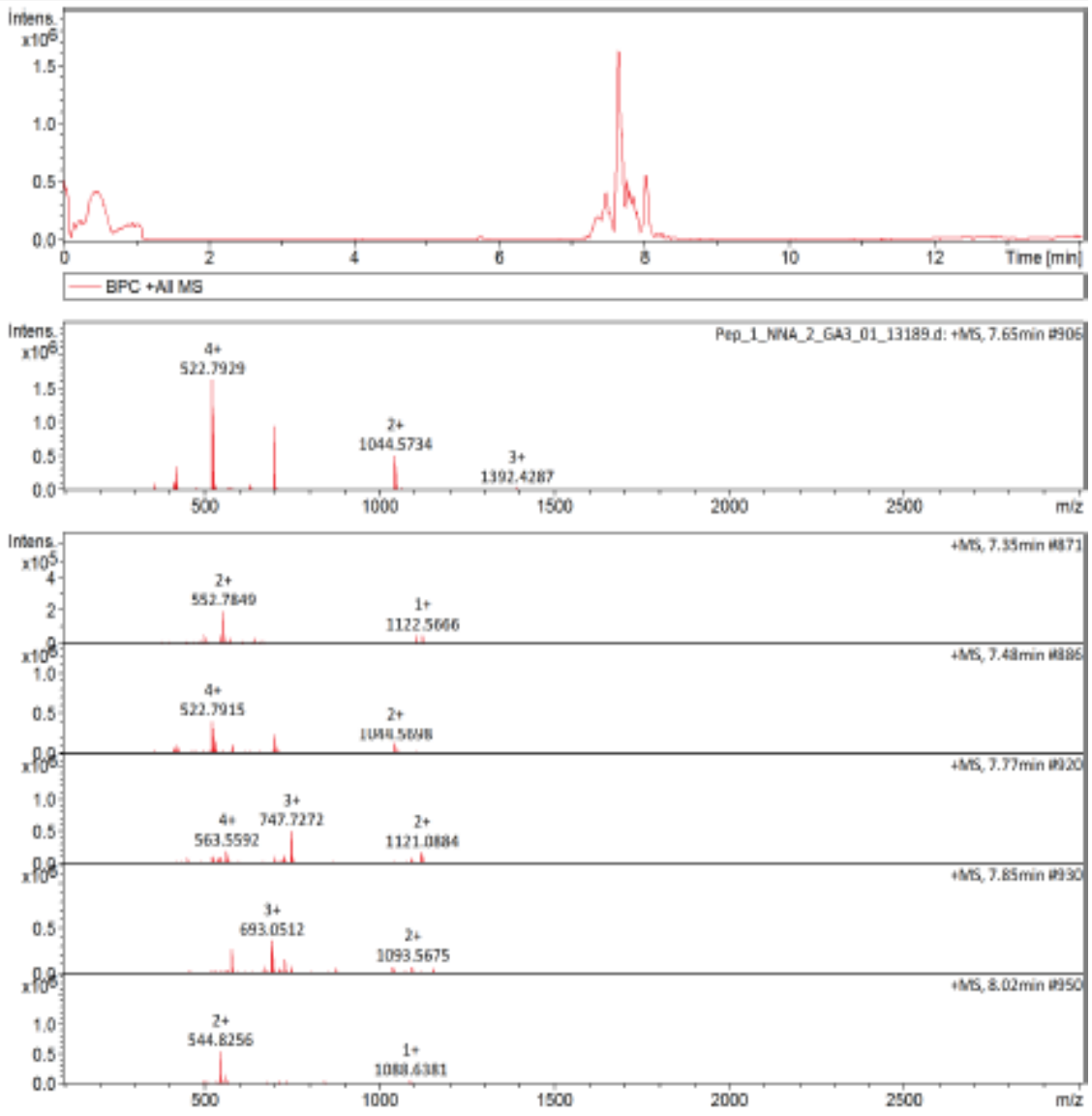
Figure 44 LC-MS of Pep_1_NN

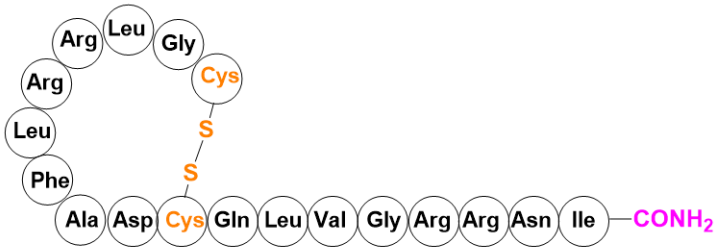
Analysis Info

Analysis Name	D:\Data\Runs\Ntombi\31_Aug_2018\Pep_1_NNA_2_GA3_01_13189.d	Acquisition Date	8/31/2018 1:59:33 PM
Method	Wits HPLC high MS 100-3000 pos.m	Operator	Thapelo Mbhele
Sample Name	Pep_1_NNA_2	Instrument	compact 8255754.20116
Comment			

Acquisition Parameter

Source Type	ESI	Ion Polarity	Positive	Set Nebulizer	1.8 Bar
Focus	Not active	Set Capillary	4500 V	Set Dry Heater	220 °C
Scan Begin	100 m/z	Set End Plate Offset	-500 V	Set Dry Gas	9.0 l/min
Scan End	3000 m/z	Set Charging Voltage	2000 V	Set Divert Valve	Waste
		Set Corona	0 nA	Set APCI Heater	0 °C





Pep_1_NNA

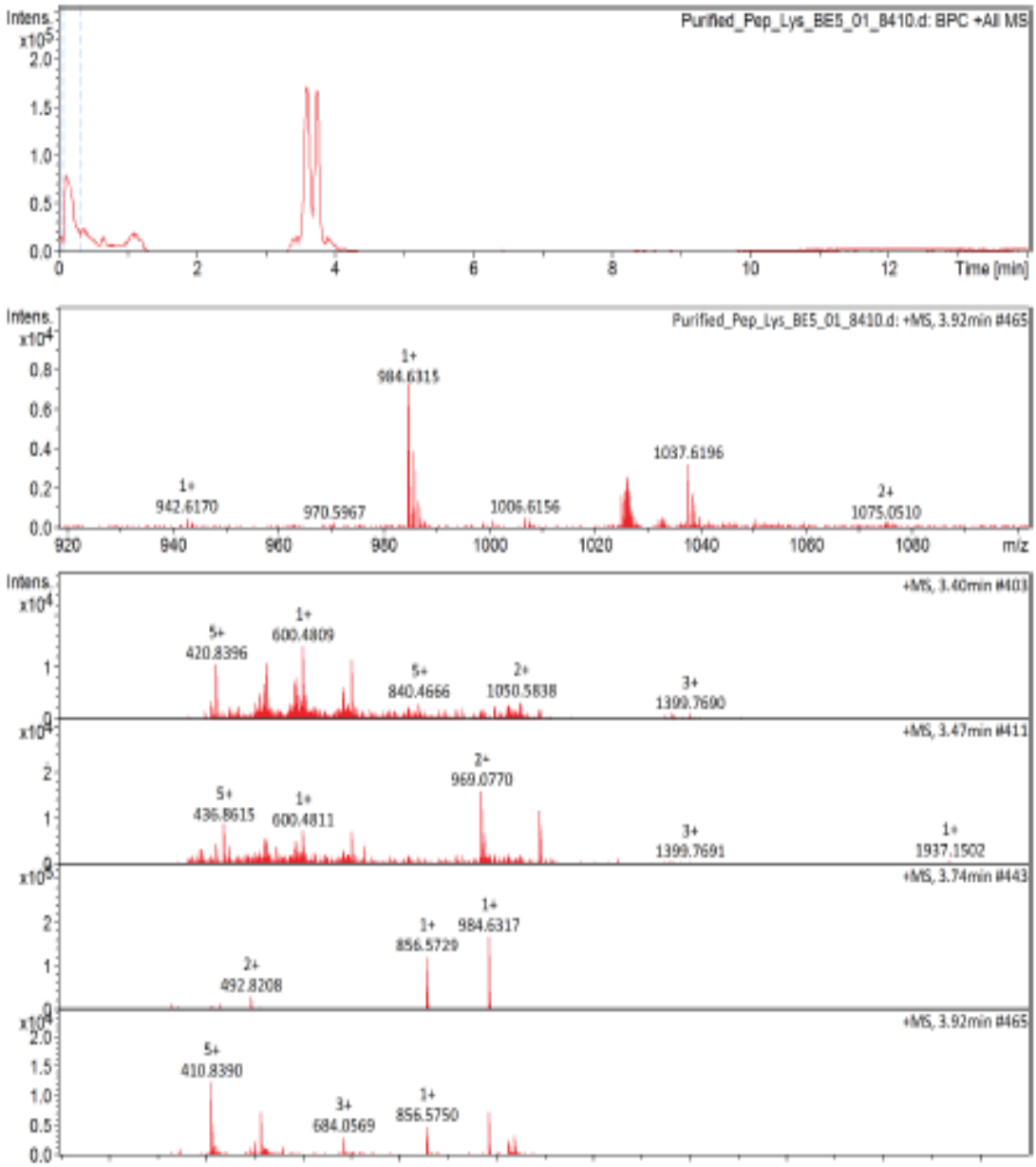
Figure 45 LC-MS Pep_1_NNA

Analysis Info

Analysis Name	D:\Data\Runs\Ntombi\New_2018_runs\Purified_Pep_Lys_BE5_01_8410.d	Acquisition Date	3/11/2018 9:09:40 PM
Method	Wits HPLC high MS 100-3000 pos.m	Operator	Refilwe Moepya
Sample Name	Purified_Pep_Lys	Instrument	compact 8255754.20116
Comment			

Acquisition Parameter

Source Type	ESI	Ion Polarity	Positive	Set Nebulizer	1.8 Bar
Focus	Not active	Set Capillary	4500 V	Set Dry Heater	220 °C
Scan Begin	100 m/z	Set End Plate Offset	-500 V	Set Dry Gas	9.0 l/min
Scan End	3000 m/z	Set Charging Voltage	2000 V	Set Divert Valve	Waste
		Set Corona	0 nA	Set APCI Heater	0 °C



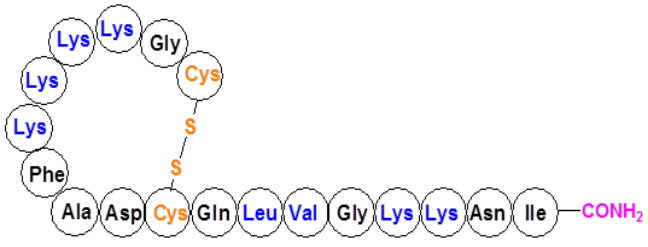


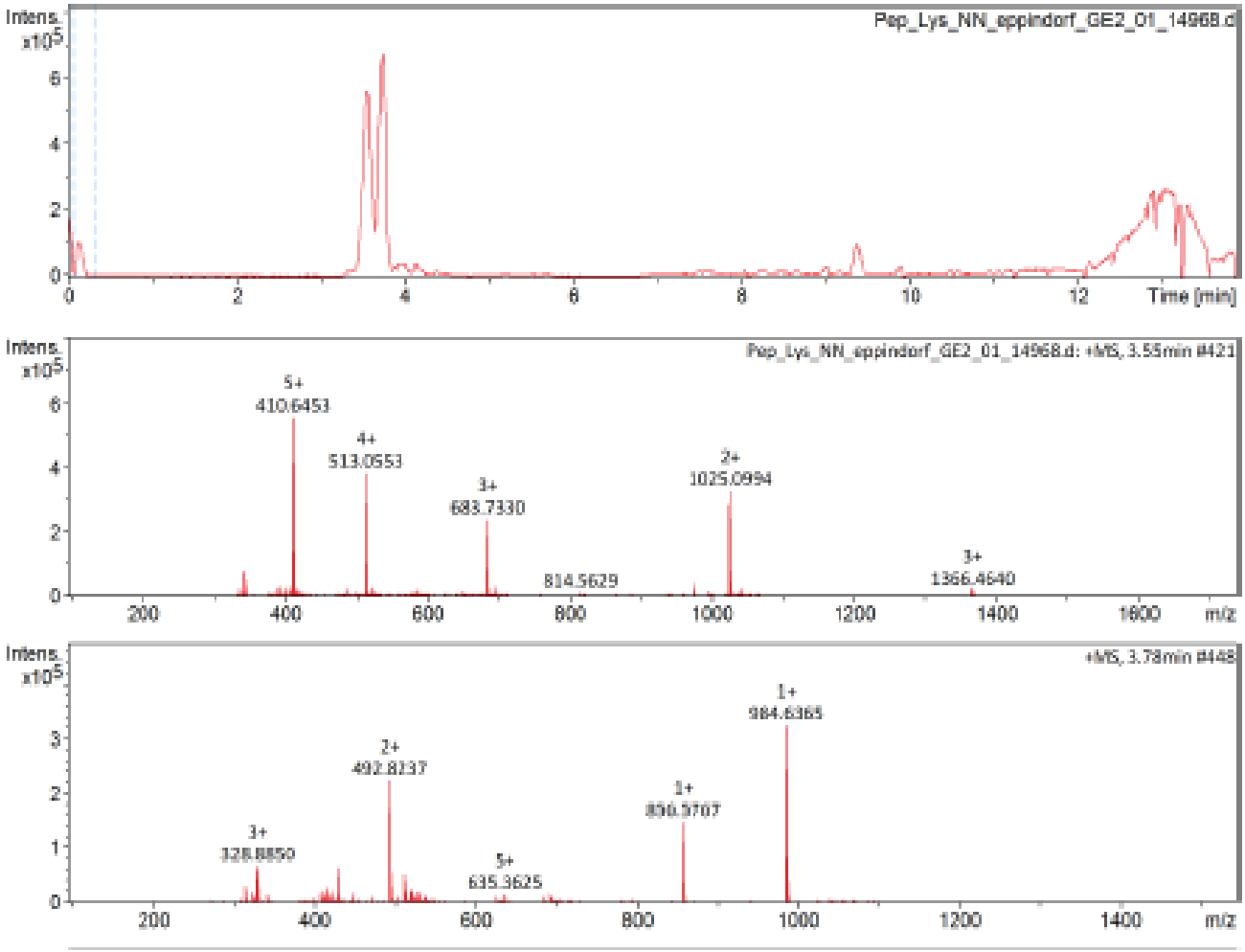
Figure 46 LC-MS of Pep_Lys_NNA

Analysis Info

Analysis Name	D:\Data\Runs\Ntombi\09_Oct_2018_samples_4_testing\Pep_Lys_NN_eppindorf_GE2_01_14968.d	Acquisition Date	10/9/2018 7:12:53 PM
Method	Wits HPLC high MS 100-3000 pos.m	Operator	Thapelo Mbhele
Sample Name	Pep_Lys_NN_eppindorf	Instrument	compact 8255754.20116
Comment			

Acquisition Parameter

Source Type	ESI	Ion Polarity	Positive	Set Nebulizer	1.8 Bar
Focus	Not active	Set Capillary	4500 V	Set Dry Heater	220 °C
Scan Begin	100 m/z	Set End Plate Offset	-500 V	Set Dry Gas	9.0 l/min
Scan End	3000 m/z	Set Charging Voltage	2000 V	Set Divert Valve	Waste
		Set Corona	0 nA	Set APCI Heater	0 °C



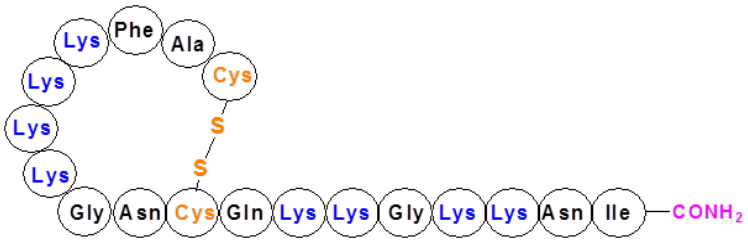


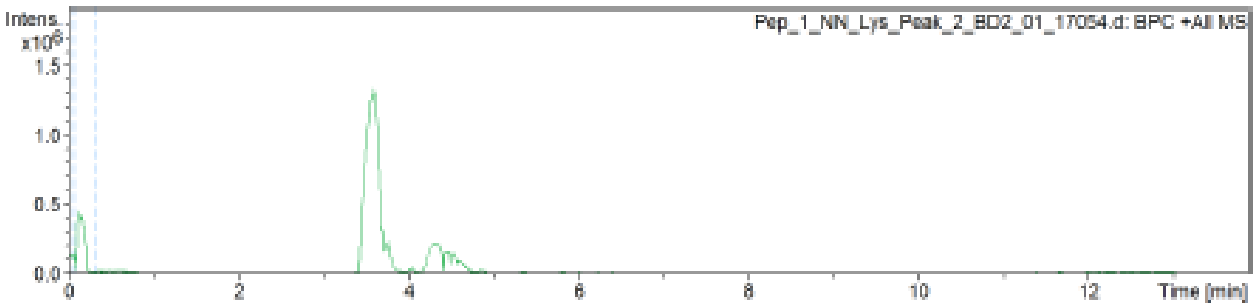
Figure 47 LC-MS of Pep_Lys_NN

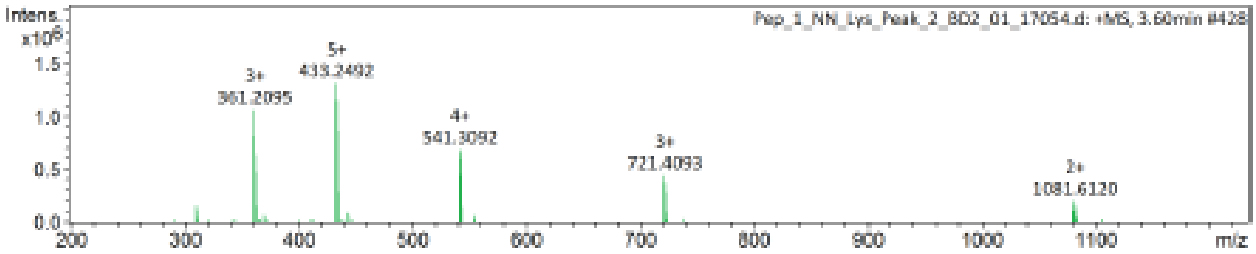
Analysis Info

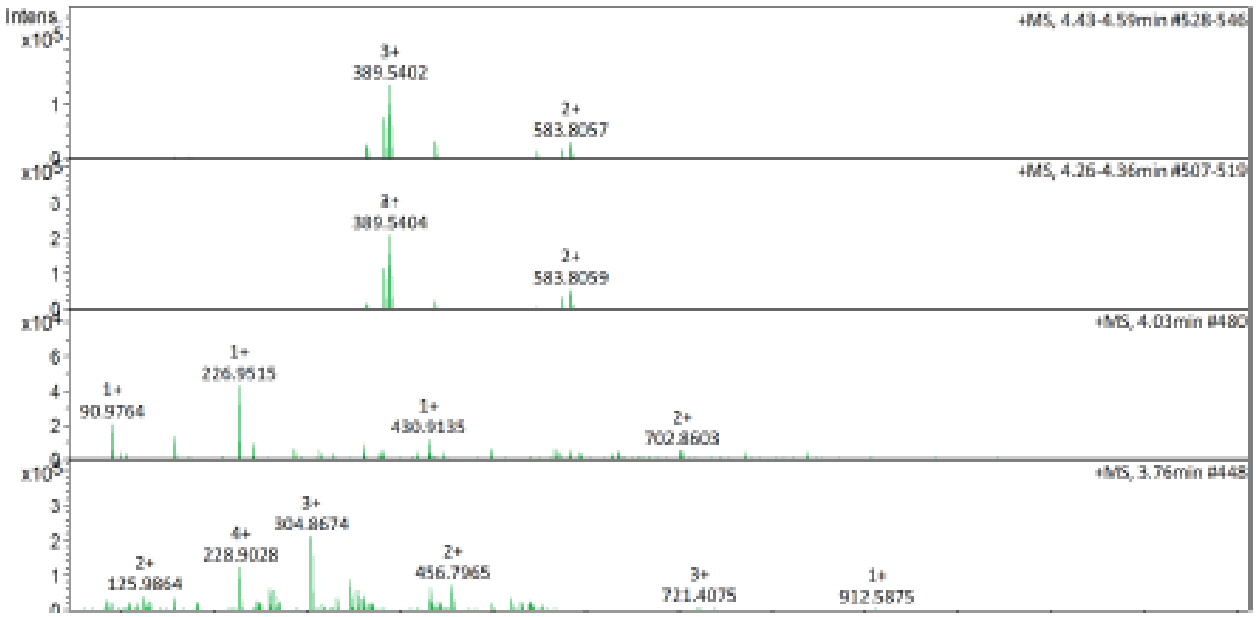
Analysis Name	D:\Data\Runs\Ntombi\Pep_1_NN_Lys\Pep_1_NN_Lys_Peak_2_BD2_01_17054.d	Acquisition Date	11/14/2018 11:57:08 AM
Method	Wits HPLC Std MS 50-1300 pos.m	Operator	Thapelo Mbhele
Sample Name	Pep_1_NN_Lys_Peak_2	Instrument	compact 8255754.20116
Comment			

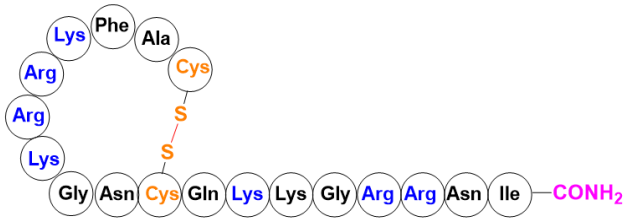
Acquisition Parameter

Source Type	ESI	Ion Polarity	Positive	Set Nebulizer	1.8 Bar
Focus	Not active	Set Capillary	4500 V	Set Dry Heater	220 °C
Scan Begin	50 m/z	Set End Plate Offset	-500 V	Set Dry Gas	9.0 l/min
Scan End	1300 m/z	Set Charging Voltage	2000 V	Set Divert Valve	Waste
		Set Corona	0 nA	Set APCI Heater	0 °C









Pep_1_NN_Lys

Figure 48 LC-MS of Pep_1_NN_Lys

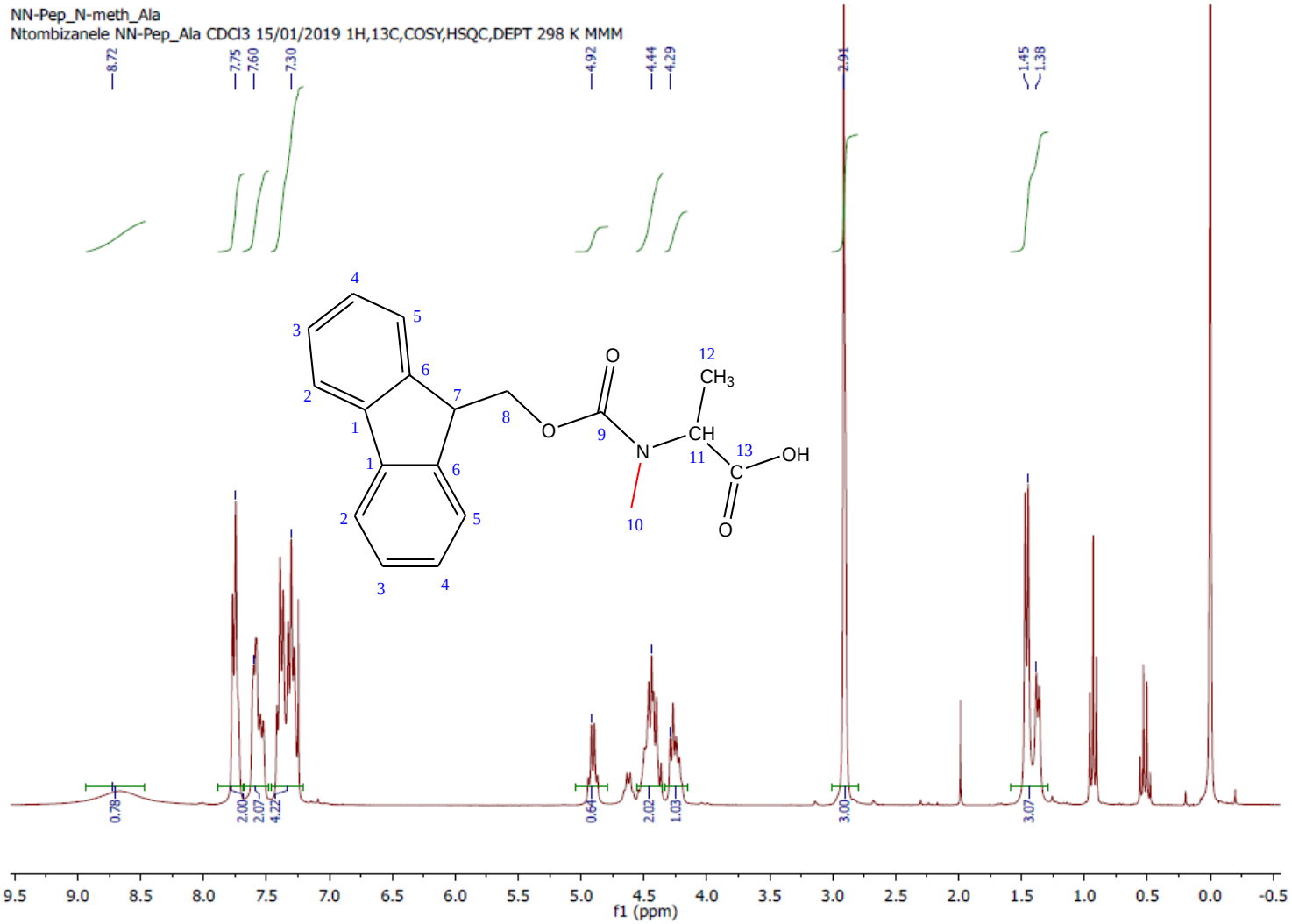


Figure 49 ^{1}H NMR of *N*-methylated Fmoc-alanine

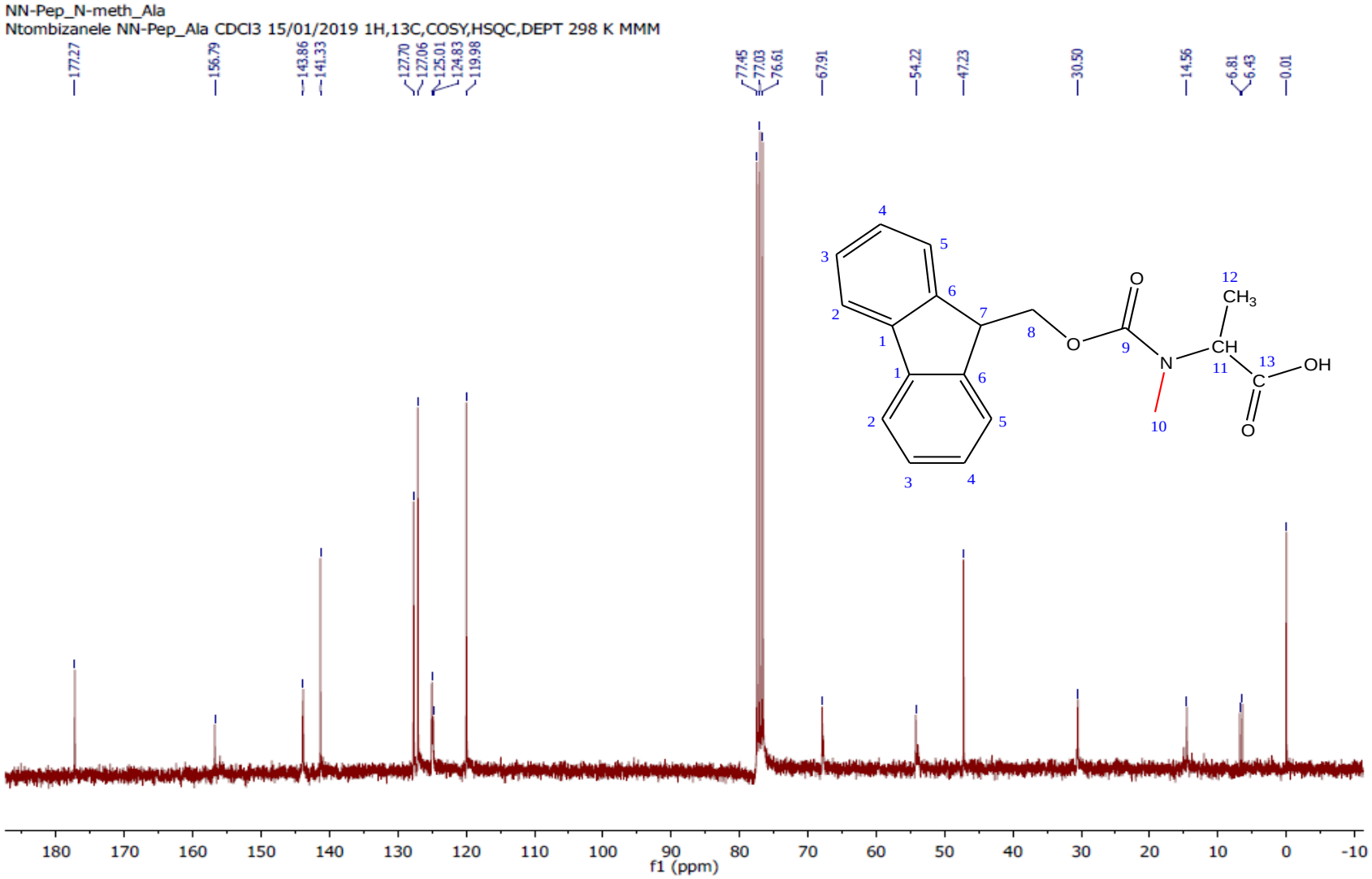


Figure 50 ^{13}C NMR of *N*-methylated Fmoc-alanine

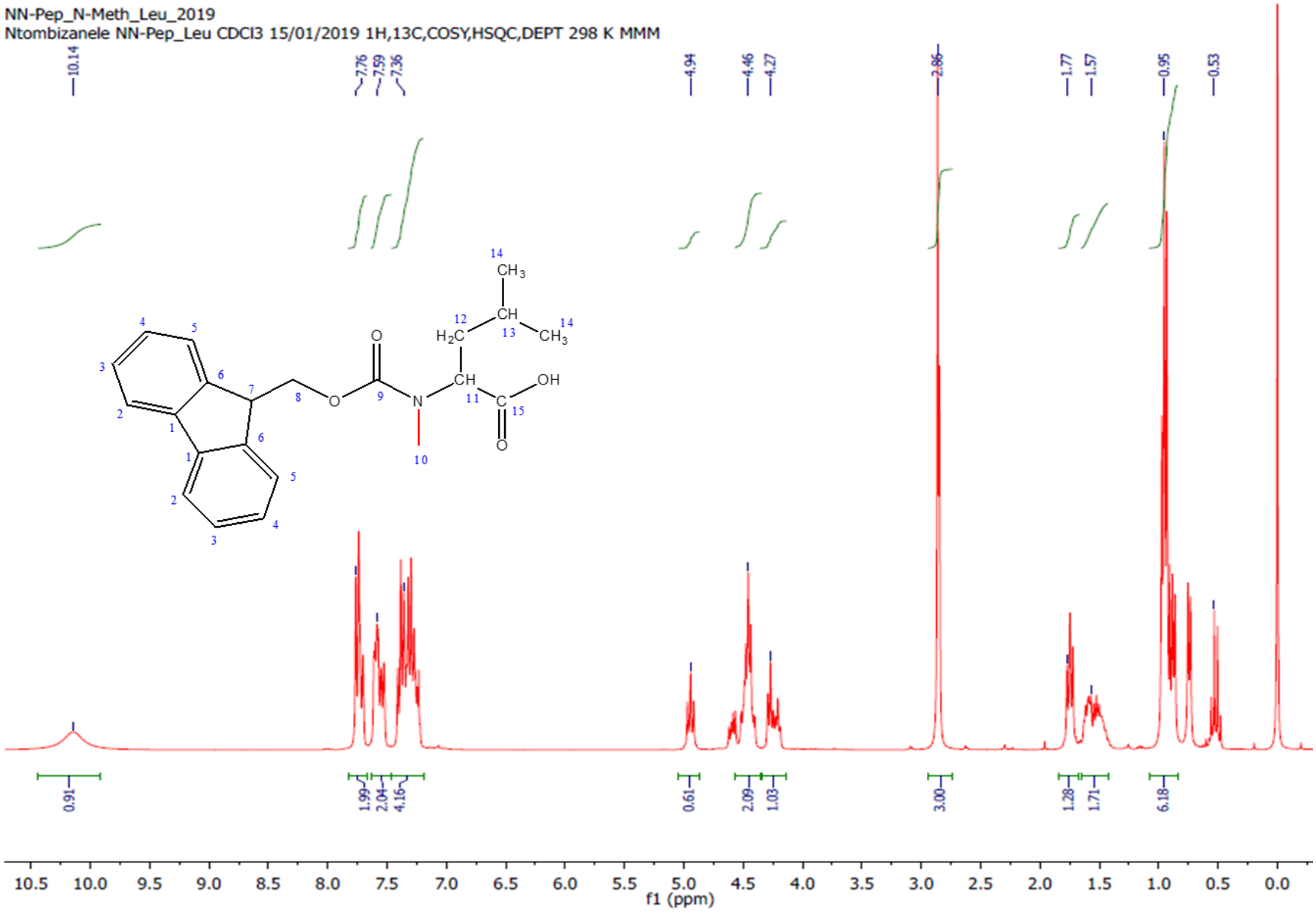


Figure 51 ^{1}H NMR spectrum of N-methylated Fmoc-Leucine

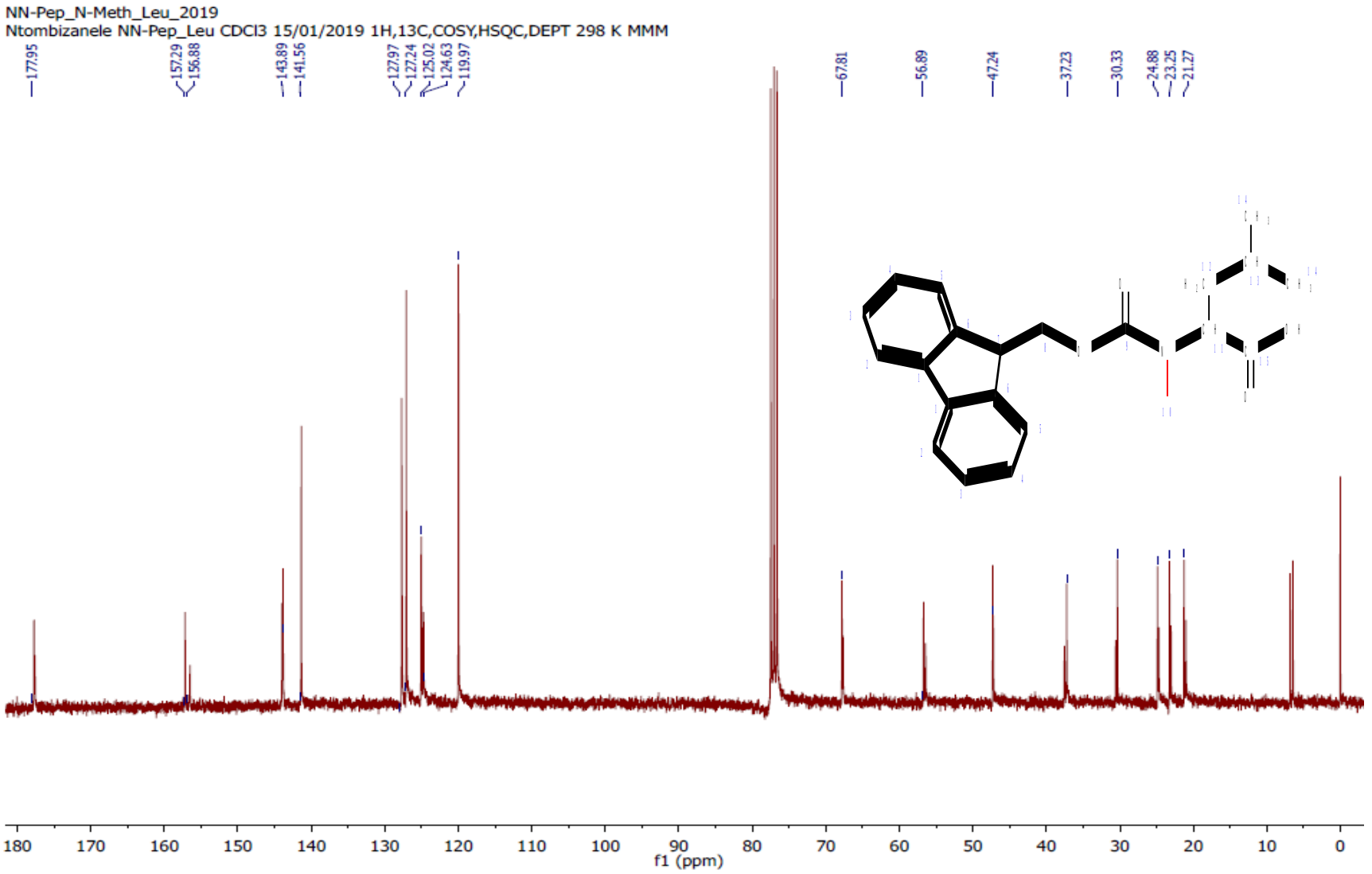


Figure 52 ^{13}C NMR spectrum of N-methylated Fmoc-Leucine

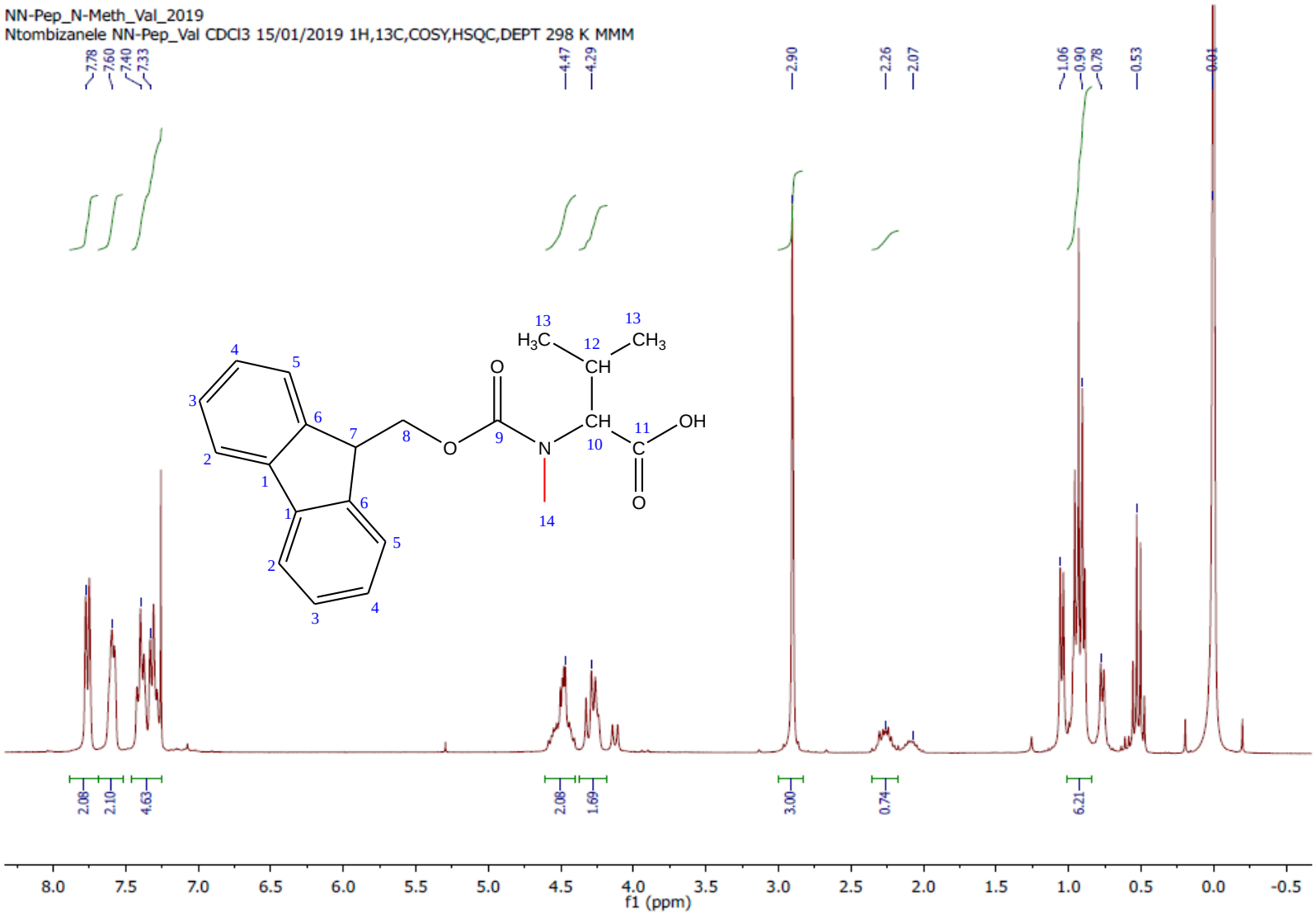


Figure 53 ^{1}H NMR spectrum of *N*-methylated Fmoc- Valine

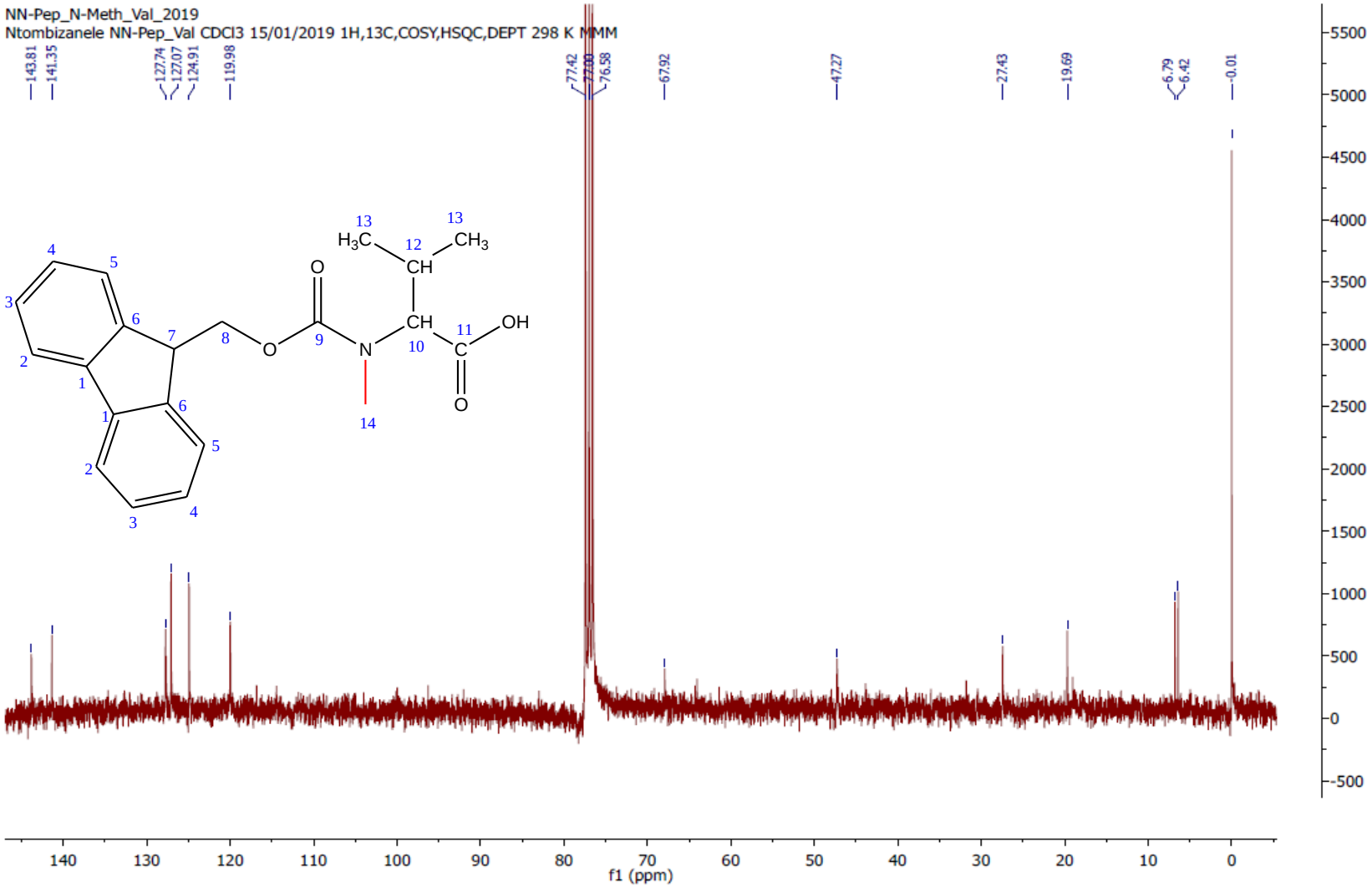


Figure 54 ^{13}C NMR spectrum of N-methylated Fmoc-Valine

Analysis Info

Analysis Name	D:\Data\Runs\Ntombi\N methylated peptide\N_methylated_Pep_2_NNA_Vial_54_GE4_01_19134.d	Acquisition Date	1/22/2019 11:59:01 AM
Method	HPLC Mid 50-1300 low temp_reduced_voltage.m	Operator	Thapelo Mbhele
Sample Name	N_methylated_Pep_2_NNA_Vial_54	Instrument	compact 8255754.20116
Comment			

Acquisition Parameter

Source Type	ESI	Ion Polarity	Positive	Set Nebulizer	1.8 Bar
Focus	Not active	Set Capillary	4500 V	Set Dry Heater	180 °C
Scan Begin	100 m/z	Set End Plate Offset	-500 V	Set Dry Gas	9.0 l/min
Scan End	3000 m/z	Set Charging Voltage	2000 V	Set Divert Valve	Waste
		Set Corona	0 nA	Set APCI Heater	0 °C

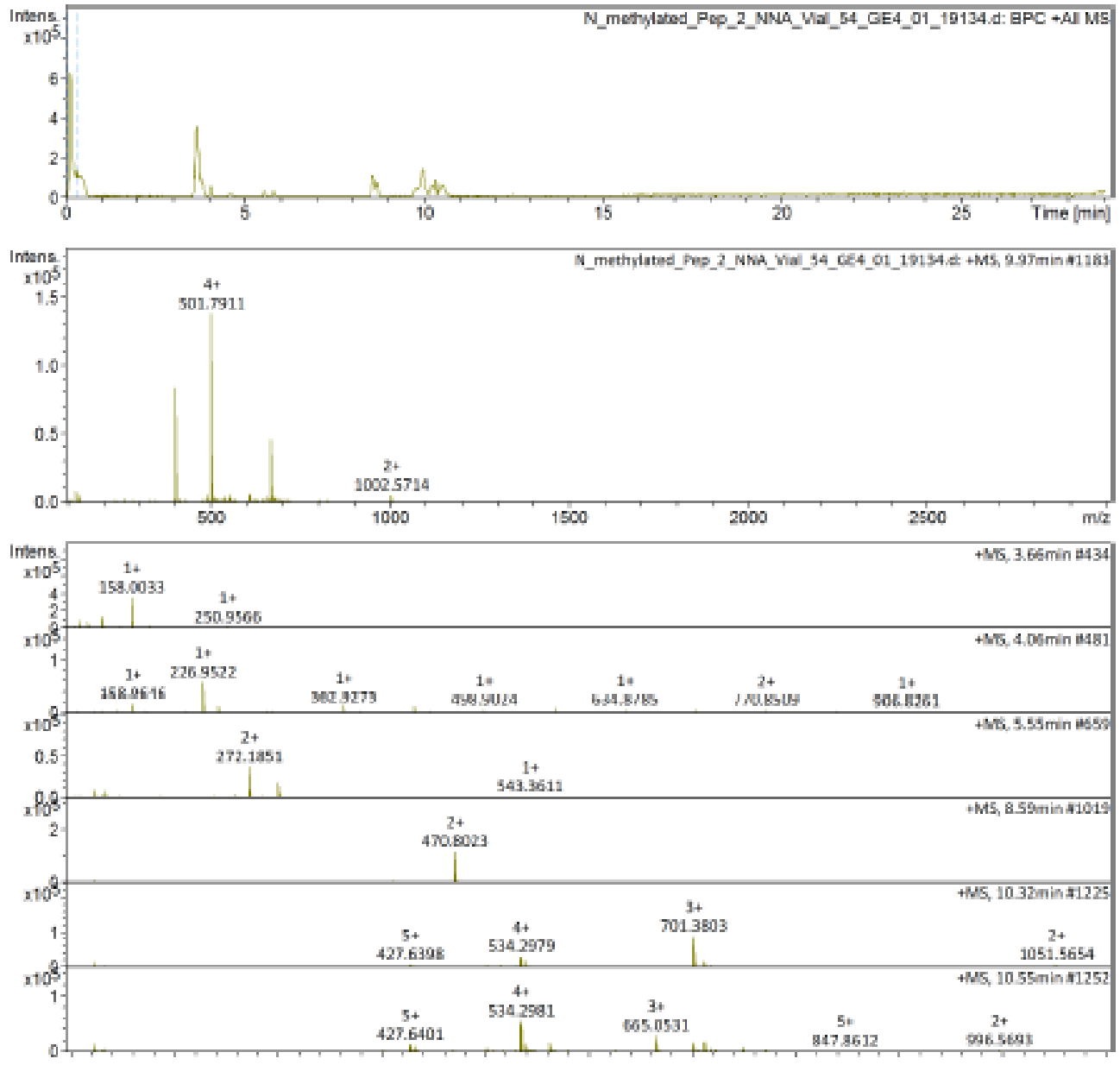


Figure 55 LC-MS of *N*-methylated Pep_2_NN

Analysis Info

Analysis Name	D:\Data\Runs\Ntombi\N methylated peptide\N-meth_Pep_2_NN_Peak1_no2_BD2_01_18775.d	Acquisition Date	1/14/2019 9:59:13 PM
Method	HPLC Mid 50-1300 low temp_reduced_voltage.m	Operator	Thapelo Mbhele
Sample Name	N-meth_Pep_2_NN_Peak1_no2	Instrument	compact 8255754.20116
Comment			

Acquisition Parameter

Source Type	ESI	Ion Polarity	Positive	Set Nebulizer	1.8 Bar
Focus	Not active	Set Capillary	4500 V	Set Dry Heater	180 °C
Scan Begin	100 m/z	Set End Plate Offset	-500 V	Set Dry Gas	9.0 l/min
Scan End	3000 m/z	Set Charging Voltage	2000 V	Set Divert Valve	Waste
		Set Corona	0 nA	Set APCI Heater	0 °C

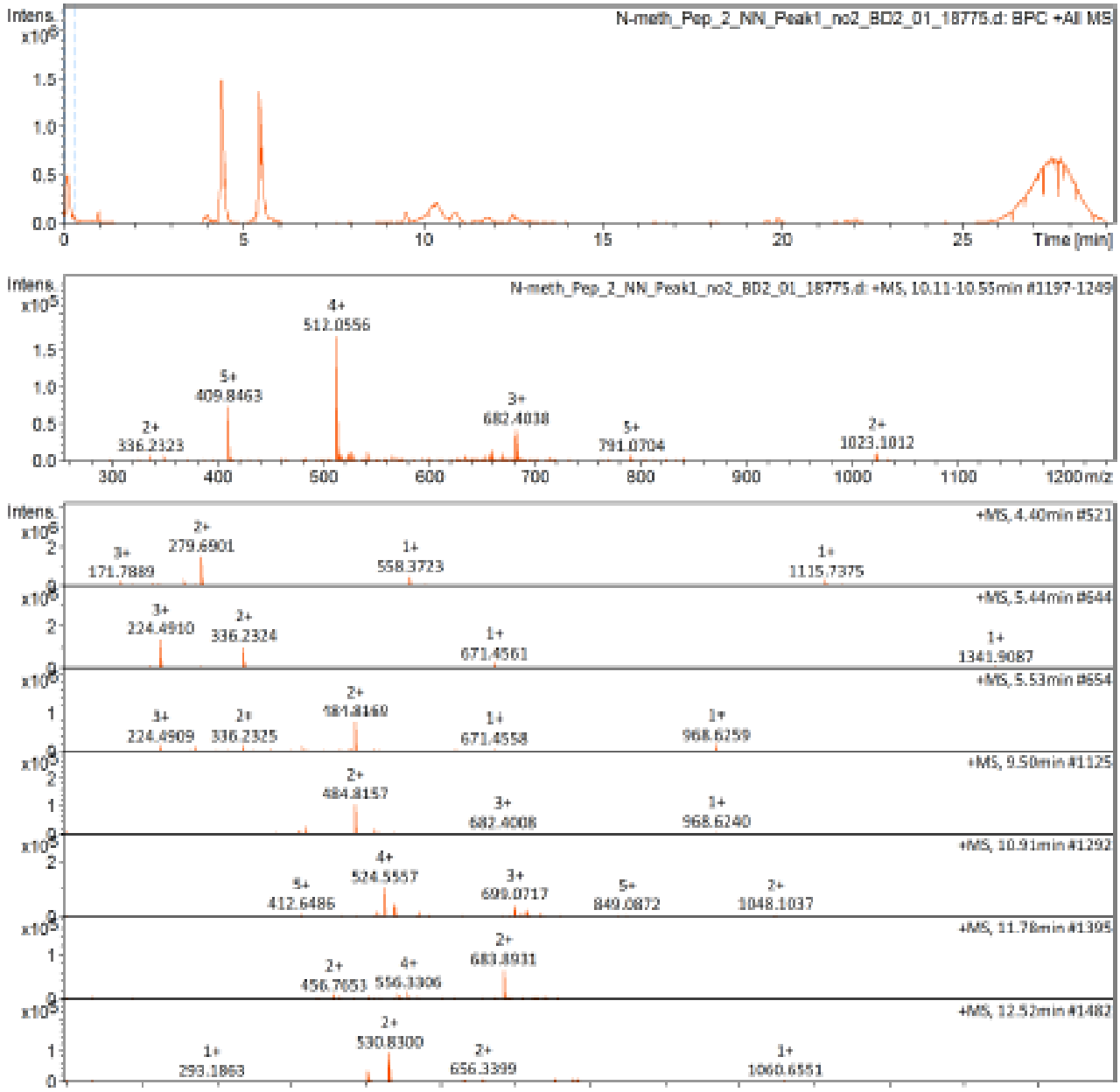


Figure 56 LC-MS of *N*-Methylated Pep_2_NN

BACKGROUND	University of the Witwatersrand sent 10 samples for testing on the cytotoxic assays developed and optimized in-house. Screening was conducted at 20 µl and 100 µl for the 8 peptides and at dose responses for the two peptides (Pep KM and Pep 2) as requested by the client.

PROCEDURE	**EXPERIMENTS CARRIED OUT ON THE SAMPLES:** **1. Cytotoxicity evaluation in the HIV growth supporting human T cell-line, MT4 (Human T cell leukaemia).** **1.1 Cytotoxicity assay** Number of samples evaluated for single concentration(s): 8 Compound concentration: 20 µl and 100 µl Number of samples for dose response: 2 (Pep KM & Pep 2) Compound concentration (100 µg/ml to 6.25 µg/ml) Control compound: Auranofin (Biomol International, LP) Number of replicates: n = 6 Endpoint method: Absorbance Validation parameters: No compound control: Below 0.3 AU Cell control: Above 1.0 AU
	EXPERIMENTAL PROCEDURE **(i) Cellular Toxicity** The day of cytotoxicity testing, cells were counted and seeded at 1 x 10^6 cells per ml. A total of 100 µl of cells were added to each well of a 96 well cell culture plate for testing. The plate was placed into the incubator to equilibrate to 37°C and 5 % CO_2. During this time, test compounds were made up in 10% RPMI solution in the desired concentration. A total of 100 µl compound was added to wells containing cells and mixed to ensure the solution was homogeneous with the cells. The plate was placed into the 37°C incubator for 5 days. On the 5th day 10 µl of MTS was added and mixed. The plates were then incubated for a further four hours, and read at 450 nm (xMARK™, Bio-Rad, USA.).

Figure 57 Experimental procedure for Pep_Lys_NN cytotoxicity studies against Human T cell (MT4) obtained from Mintek-Advance Material Division